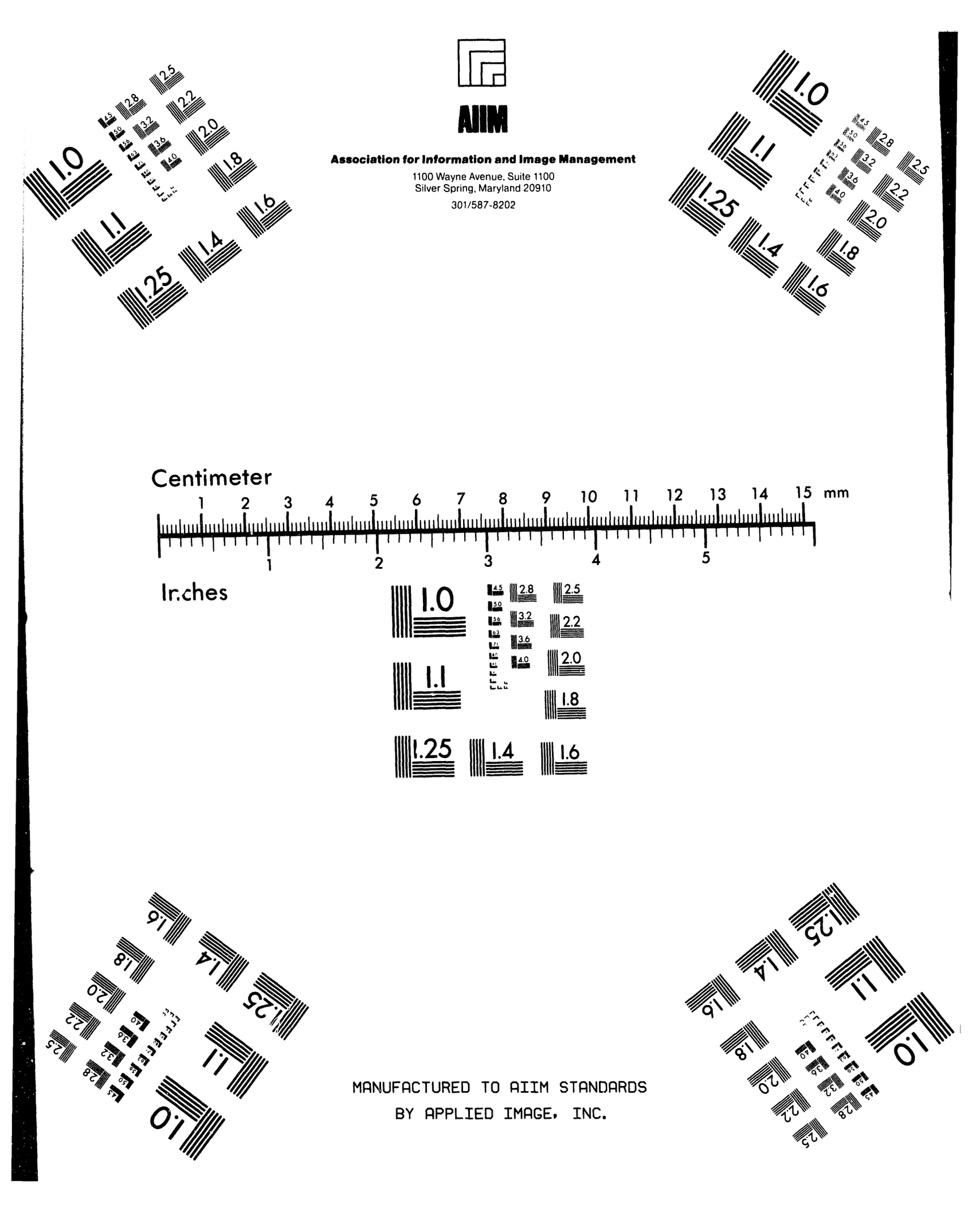
AIIM
Association for Information and Image Management
1100 Wayne Avenue, Suite 1100
Silver Spring, Maryland 20910
301/587-8202
Centimeter
Inches
MANUFACTURED TO AIIM STANDARDS
BY APPLIED IMAGE, INC.

1 of 1

LBL-35710
UC-414

Z' Phenomenology: Constraints from Low-Energy Measurements, and Detailed Study at TeV-Scale Lepton and Hadron Colliders

Matthew Harold Austern
Ph.D. Thesis

Physics Department
University of California

and

Physics Division
Lawrence Berkeley Laboratory
University of California
Berkeley, CA 94720

May 1994

This work was supported by the Director, Office of Energy Research, Office of High Energy and Nuclear Physics, Division of High Energy Physics of the U.S. Department of Energy under Contract No. DE-AC03-76SF00098.

May 20, 1994

LBL-35710
UCB-PTH-94/14

Z' Phenomenology: Constraints from low-energy measurements, and detailed study at TeV-scale lepton and hadron colliders *

Matthew Harold Austern
Theoretical Physics Group
Lawrence Berkeley Laboratory
University of California
Berkeley, California 94720

Abstract

In this dissertation, I discuss the phenomenology of new massive neutral gauge bosons, or Z' bosons, concentrating on experimental tests by which the properties of a Z' boson could be determined.

In Chapter I, I briefly review the Standard Model of elementary particle physics, and discuss the motivation for extending it. I review some of the extensions to the Standard Model that predict the existence of Z' bosons, and present a general, model-independent parameterization of the Z''s properties, as well as a simpler parameterization that applies to the most important class of models. In Chapter II, I discuss present-day limits on the existence of Z' bosons, both from direct searches, and from indirect higher-order tests.

*This work was supported by the Director, Office of Energy Research, Office of High Energy and Nuclear Physics, Division of High Energy Physics of the U.S. Department of Energy under Contract DE-AC03-76SF00098.

In Chapter III, I discuss the production and discovery of a Z' at a future hadron collider, such as the CERN Large Hadron Collider (LHC). Discovery of a Z' at the LHC may be possible if its mass is less than 5 TeV. I also discuss the experimental tests of its properties that could be performed at such a collider, emphasizing the measurement of leptonic asymmetries.

Finally, in Chapter IV, I discuss the experimental tests that could be performed at an e^+e^- collider with $\sqrt{s} = M_{Z'}$. I include several higher-order effects, such as initial-state radiation and beamstrahlung, whose inclusion is necessary for a realistic description of the experimental environment at a very high energy e^+e^- collider.

The combination of leptonic and hadronic experiments permits the measurement of all of the parameters discussed in Chapter I.

Contents

List of Figures

List of Tables

Acknowledgements

First and foremost I wish to thank my advisor, Robert N. Cahn, without whose help and prodding this dissertation would scarcely have been begun, let alone completed. Bob has been involved with this work at every stage, from first suggesting it to proofreading drafts of this manuscript.

Many other individuals in the LBL Theory Group have helped me with this research on occasions too numerous to mention. In particular, though, I would like to acknowledge Ian Hinchliffe for assisting me with his Monte Carlo program PAPAGENO and with many other aspects of perturbative QCD; Mary K. Gaillard for suggesting the line of inquiry that eventually became Chapter IV of this thesis; Dave Jackson both for help with beamstrahlung and for a close reading of this thesis; and Steve Johnson for persuading me that writing a dissertation in less than a month wasn't quite as idiotic an idea as it sounded.

Most of the work in Section 3.4 was done in collaboration with Bob, and also with my fellow student and friend Jeff Anderson. This work was first suggested to us by Eric Carlson.

Finally, I wish to thank my parents, for their support and also for encouraging my interest in physics in the first place, and Bethany Grenald for putting up with me while I was writing this, for being there (at least in spirit) when I needed her, and for keeping me from going *too* crazy.

Chapter 1

Introduction

1.1 The Standard Model

All known experimental results in elementary particle physics are described by, or at least are consistent with, the so-called "Standard Model," a non-abelian gauge theory [1] based on the gauge group $\mathrm{SU}(3) \times \mathrm{SU}(2) \times \mathrm{U}(1)$, or G_{321}. To establish notation, I discuss the main features of the Standard Model.

Every gauge theory necessarily possesses one massless spin-1 field for each generator of the gauge group. For the Standard Model, these twelve gauge bosons are the eight gluons G_i, (corresponding to the generators of SU(3)), the three W bosons, W_1, W_2, and W_3 (corresponding to the generators of SU(2)), and the B boson (corresponding to the generator of U(1)). The gluons mediate the strong interaction, while the W and B bosons mediate the electromagnetic and weak interactions.

In addition to the gauge bosons, which are the minimal particle content of any gauge theory, the most general renormalizable gauge theory [2] may also contain spin-0 and spin-$\frac{1}{2}$ fields. The Lagrangian for the most general gauge theory based on G_{321} may be written

$$\mathcal{L} = \mathcal{L}_k + \mathcal{L}_s + \mathcal{L}_f + \mathcal{L}_Y, \tag{1.1}$$

where $\mathcal{L}_k$ contains the gauge bosons' kinetic energy terms, $\mathcal{L}_f$ contains the fermions' kinetic energy term, $\mathcal{L}_s$ contains the scalars' mass term, kinetic energy term, and self-interactions, and $\mathcal{L}_Y$, the Yukawa sector, contains interactions between the fermions and the scalars. Because the scalars' and fermions' kinetic energy terms involve the covariant derivative D^μ, given in Eq. (1.6), their kinetic energy terms imply interactions between the gauge bosons and the scalars and fermions. Explicitly, the terms in Eq. (1.1) are

$$\mathcal{L}_k = -\tfrac{1}{4} B^{\mu\nu} B_{\mu\nu} - \tfrac{1}{4} W_i^{\mu\nu} W_{\mu\nu,i} - \tfrac{1}{4} G_i^{\mu\nu} G_{\mu\nu,i}, \tag{1.2}$$

$$\mathcal{L}_s = (D^\mu \Phi)^\dagger (D_\mu \Phi) - V(\Phi), \tag{1.3}$$

$$\mathcal{L}_f = \bar{\Psi} (i \not{D}) \Psi, \tag{1.4}$$

$$\mathcal{L}_Y = H(\Psi, \bar{\Psi}, \Phi), \tag{1.5}$$

where $V(\Phi)$ contains all scalar interactions of quartic and lower order that are invariant under G_{321}, and $H(\Psi, \Phi)$ contains all interactions that are linear in Ψ, $\bar{\Psi}$, and Φ, and that

Table 1.1: Particle content, and SU(3), SU(2), and U(1) quantum number assignments, for the first generation of fermions. The Higgs boson, Φ, is not part of any of the three generations, and is listed here only for convenience.

Particle	SU(3) multiplet	SU(2) multiplet	Y
Q_L	triplet	doublet	1/3
L_L	singlet	doublet	-1
u_R	triplet	singlet	4/3
d_R	triplet	singlet	$-2/3$
e_R	singlet	singlet	-2
Φ	singlet	doublet	1

are invariant under Lorentz transformations and under G_{321}. The quantities $\mathcal{F}^{\mu\nu}$, $W_i^{\mu\nu}$, and $G_i^{\mu\nu}$ are the gauge bosons' field strength tensors, and D^μ, the covariant derivative, is given by

$$D^\mu = \partial^\mu + ig_s I_i G_i^\mu + igT_i W_i^\mu + ig'\frac{Y}{2}B^\mu. \tag{1.6}$$

The constants g_s, g, and g' are, respectively, the coupling constants of SU(3), SU(2), and U(1), and I_i, T_i, and $Y/2$ are a representation of the gauge group's generators. To specify the theory fully, it suffices to choose some specific representation, that is, to choose the quantum numbers of the fermion and scalar states.

In the Standard Model [3], these states consist of a single complex scalar that transforms as a singlet under SU(3) and a doublet under SU(2), and three "generations," each of which consists of 15 massless fermions arranged into singlets and triplets of SU(3) and singlets and doublets of SU(2). This decomposition into irreducible representations of SU(2) and SU(3) specifies I and T completely, but Y is still an arbitrary diagonal matrix, subject only to the condition that every particle i in an SU(2) or SU(3) multiplet must have the same value of Y_i. The Standard Model quantum number assignments are summarized in Table 1.1. The symbol Q_L in Table 1.1 refers to the left-handed up and down quarks, and L_L refers to the left-handed electron and electron neutrino. The right-handed up quark, down quark, and electron are u_R, d_R, and and e_R. The scalar doublet can be written explicitly as

$$\Phi = \begin{pmatrix} \phi^+ \\ \phi^0 \end{pmatrix}, \tag{1.7}$$

where both ϕ^+ and ϕ^0 are complex scalar fields.

Given these particle assignments, it is possible to write down the most general form for the functions V and H that appear in Eqs. (1.3) and (1.5). The scalar and Yukawa sectors of the theory are

$$\mathcal{L}_s = (D^\mu\Phi)^\dagger (D_\mu\Phi) + \mu^2\Phi^\dagger\Phi - \tfrac{1}{2}\lambda\left(\Phi^\dagger\Phi\right)^2, \text{ and} \tag{1.8}$$

$$\mathcal{L}_Y = -h_e\bar{e}_R\Phi^\dagger L_L - h_d\bar{d}_R\Phi^\dagger Q_L - h_u\bar{u}_R\Phi_c^\dagger Q_L + \text{h.c.}, \tag{1.9}$$

where μ is a constant with dimensions of mass, and λ, h_e, h_d, and h_u are dimensionless constants. The field Φ_c is the charge conjugate of Φ, defined as

$$\Phi_c = i\sigma_2\Phi^*, \tag{1.10}$$

where σ_2 is one of the familiar Pauli matrices. As in Table 1.1, Eq. (1.9) contains the couplings only for a single generation of fermions. The generalization to the full three generations of the Standard Model is straightforward.

Eq. (1.1) describes a world where all gauge bosons and fermions are massless; this is not the world we live in. The Standard Model exhibits spontaneous symmetry breaking [4]. That is, although the fundamental Lagrangian is invariant under the gauge group G_{321}, the ground state of the theory is not. Specifically, the scalar potential, Eq. (1.8), is minimized not for $\phi = 0$, but for $|\Phi|^2 = v^2$, with $v^2 \equiv \frac{\mu^2}{\lambda}$. The true vacuum, by definition, is the state of minimum energy, so Φ must have a nonzero vacuum expectation value, with $|\langle\Phi\rangle|^2 = v^2$. The ground state, then, is not invariant under G_{321}. Forming a perturbative expansion about this ground state yields an effective Lagrangian that is not invariant under G_{321}, but merely under $\mathrm{SU(3)} \times \mathrm{U(1)}_{EM}$. The factor $\mathrm{U(1)}_{EM}$ is not the U(1) factor of G_{321}; it is generated by a linear combination of that group's generator and the diagonal generator of SU(2), and it is the gauge group of electromagnetism.

Straightforward but laborious algebra yields the Lagrangian

$$\begin{aligned}
\mathcal{L} = &- \tfrac{1}{2}\left(\partial_\mu W_\nu^+ - \partial_\nu W_\mu^+\right)\left(\partial^\mu W^{-\nu} - \partial^\nu W^{-\mu}\right) - \frac{1}{\xi}\left(\partial^\mu W_\mu^+\right)\left(\partial^\mu W_\mu^-\right) \\
&+ \tfrac{1}{4}g^2v^2W^+\cdot W^- - \tfrac{1}{4}\left(\partial_\mu Z_\nu - \partial_\nu Z_\mu\right)^2 - \frac{1}{2\xi}\left(\partial^\mu Z_\mu\right)^2 + \frac{1}{8}\left(\frac{e}{sc}\right)^2 v^2Z^2 \\
&- \tfrac{1}{4}\left(\partial_\mu A_\nu - \partial_\nu A_\mu\right)^2 - \frac{1}{2\xi}\left(\partial^\mu A_\mu\right)^2 - \tfrac{1}{4}\left(\partial_\mu G_\nu^a - \partial_\nu G_\mu^a\right)\left(\partial^\mu G^{\nu,a} - \partial^\nu G^{\mu,a}\right) \\
&- \frac{1}{2\xi}\left(\partial^\mu G_\mu^a\right)^2 + \tfrac{1}{2}\partial^\mu h\partial_\mu h - \tfrac{1}{2}\lambda v^2h^2 + \tfrac{1}{2}\partial^\mu\phi^0\partial_\mu\phi^0 - \frac{1}{8}\left(\frac{e}{sc}\right)^2\xi v^2\phi^{0\,2} \\
&+ \partial^\mu\phi^+\partial_\mu\phi^- - \tfrac{1}{4}g^2\xi v^2\phi^+\phi^- - \tfrac{1}{2}g^2\left[\left(W^+\cdot W^-\right)^2 - (W^+)^2(W^-)^2\right] \\
&- e^2\left[A^2(W^+\cdot W^-) - (A\cdot W^+)(A\cdot W^-)\right] \\
&- c^2g^2\left[Z^2(W^+\cdot W^-) - (Z\cdot W^+)(Z\cdot W^-)\right] \\
&- ecg\left[2(A\cdot Z)(W^+\cdot W^-) - (A\cdot W^+)(Z\cdot W^-) - (Z\cdot W^+)(A\cdot W^-)\right] \\
&+ ie\left[\partial^\mu A^\nu W_\mu^- W_\nu^+ + \partial^\mu W^{-\nu}W_\mu^+A_\nu + \partial^\mu W^{+\nu}A_\mu W_\nu^-\right] + \text{h.c.} \\
&+ icg\left[\partial^\mu Z^\nu W_\mu^- W_\nu^+ + \partial^\mu W^{-\nu}W_\mu^+Z_\nu + \partial^\mu W^{+\nu}Z_\mu W_\nu^-\right] + \text{h.c.} \\
&- \tfrac{1}{4}g_s^2(G^a\cdot G^c)(G^b\cdot G^d)f^{abe}f^{cde} - \tfrac{1}{2}g_s\left(\partial_\mu G_\nu^c - \partial_\nu G_\mu^c\right)G^{\mu,a}G^{\nu,b}f^{abc} \\
&- \frac{\lambda v}{2}h^3 - \frac{\lambda}{8}h^4 - \frac{\lambda v}{2}h\phi^{0\,2} - \frac{\lambda}{8}\phi^{0\,4} - \frac{\lambda}{4}h^2\phi^{0\,2} - v\lambda h\phi^+\phi^- - \tfrac{1}{2}\lambda h^2\phi^+\phi^- \\
&- \tfrac{1}{2}\lambda\phi^{0\,2}\phi^+\phi^- - \tfrac{1}{2}\lambda\left(\phi^+\phi^-\right)^2 + \left(ieA^\mu\phi^+\partial_\mu\phi^- + \text{h.c.}\right) \\
&+ \left(\frac{i}{2}\frac{e}{sc}(1-2s^2)Z^\mu\phi^+\partial_\mu\phi^- + \text{h.c.}\right) + \frac{e}{2sc}Z^\mu\left(\phi^0\partial_\mu h - h\partial_\mu\phi^0\right)
\end{aligned} \tag{1.11}$$

$$
\begin{aligned}
&+ \left[\frac{i}{2}gW^{+\mu}\left(h\partial_\mu\phi^- - \phi^-\partial_\mu h\right) + \tfrac{1}{2}gW^{+\mu}\left(\phi^-\partial_\mu\phi^0 - \phi^0\partial_\mu\phi^-\right) + \text{h.c.}\right] \\
&+ \left(\frac{e}{2sc}\right)^2 v\,hZ^2 + \tfrac{1}{2}g^2 vhW^+\cdot W^- + \left(\frac{e^2}{s}\frac{v}{2}\phi^- W^+\cdot A + \text{h.c.}\right) \\
&- \left(\frac{e^2}{c}\frac{v}{2}\phi^- W^+\cdot Z + \text{h.c.}\right) + \tfrac{1}{4}g^2h^2W^+\cdot W^- + \frac{1}{8}\left(\frac{e}{sc}\right)^2 h^2Z^2 \\
&+ \tfrac{1}{4}g^2\phi^{0\,2}W^+\cdot W^- + \frac{1}{8}\left(\frac{e}{sc}\right)^2\phi^{0\,2}Z^2 + e^2\phi^+\phi^-A^2 + \tfrac{1}{2}g^2\phi^+\phi^-W^+\cdot W^- \\
&+ \left(\frac{e}{2sc}\right)^2(1-2s^2)^2\phi^+\phi^-Z^2 + \frac{e^2}{sc}(1-2s^2)\phi^+\phi^-A\cdot Z \\
&+ \left[\frac{e^2}{2s}h\phi^-W^+\cdot A - \frac{e^2}{2c}h\phi^-W^+\cdot Z + i\frac{e^2}{2s}\phi^0\phi^-W^+\cdot A - i\frac{e^2}{2c}\phi^0\phi^-W^+\cdot Z + \text{h.c.}\right] \\
&+ \partial_\mu\bar\eta_+\partial^\mu\eta_+ - \tfrac{1}{4}g^2\xi v^2\bar\eta_+\eta_+ + \partial_\mu\bar\eta_-\partial^\mu\eta_- - \tfrac{1}{4}g^2\xi v^2\bar\eta_-\eta_- + \partial_\mu\bar\eta_z\partial^\mu\eta_z \\
&+ \partial_\mu\bar\eta^a\partial^\mu\eta^a - ig_s f^{abc}\partial_\mu\bar\eta^a G^{\mu,b}\eta^c \\
&- \left(\frac{e}{2sc}\right)^2\xi v^2\bar\eta_z\eta_z + \partial_\mu\bar\eta_\gamma\partial^\mu\eta_\gamma + ie\left(\partial_\mu\bar\eta_+\eta_+ - \partial_\mu\bar\eta_-\eta_-\right)A^\mu \\
&+ e\left(i\partial_\mu\bar\eta_\gamma\eta_- W^{+\mu} - i\partial_\mu\bar\eta_+\eta_\gamma W^{+\mu} + \text{h.c.}\right) + igc\left(\partial_\mu\bar\eta_+\eta_+ - \partial_\mu\bar\eta_-\eta_-\right)Z^\mu \\
&+ gc\left(i\partial_\mu\bar\eta_z\eta_- W^{+\mu} - i\partial_\mu\bar\eta_+\eta_z W^{+\mu} + \text{h.c.}\right) - \frac{g^2\xi v}{4}\left(h\bar\eta_+\eta_+ + h\bar\eta_-\eta_-\right) \\
&- \left(\frac{e}{2sc}\right)^2\xi v\,h\bar\eta_z\eta_z + \frac{ig^2\xi v}{4}\left(\phi^0\bar\eta_-\eta_- - \phi^0\bar\eta_+\eta_+\right) - \frac{eg\xi v}{2}\left(\phi^+\bar\eta_+\eta_\gamma + \phi^-\bar\eta_-\eta_\gamma\right) \\
&- \frac{e^2\xi v}{4s^2c}(1-2s^2)\left(\phi^+\bar\eta_+\eta_z + \phi^-\bar\eta_-\eta_z\right) + \frac{e^2\xi v}{4s^2c}\left(\phi^+\bar\eta_z\eta_- + \phi^-\bar\eta_z\eta_+\right) \\
&+ \bar\nu\left(i\partial\!\!\!/\right)\nu + \bar e\left(i\partial\!\!\!/ - m_e\right)e + \bar u\left(i\partial\!\!\!/ - m_u\right)u + \bar d\left(i\partial\!\!\!/ - m_d\right)d \\
&- \frac{m_e}{v}\bar eeh - \frac{m_u}{v}\bar uuh - \frac{m_d}{v}\bar ddh \\
&- i\frac{m_e}{v}\bar e\gamma_5 e\phi^0 - i\frac{m_d}{v}\bar d\gamma_5 d\phi^0 + i\frac{m_u}{v}\bar u\gamma_5 u\phi^0 - \sqrt{2}\frac{m_e}{v}\left(\bar e\frac{1-\gamma_5}{2}\nu\phi^- + \text{h.c.}\right) \\
&- \frac{\sqrt{2}}{v}\left[\bar d\left(\frac{m_u+m_d}{2} + \frac{m_u-m_d}{2}\gamma_5\right)u\phi^- + \text{h.c.}\right] \\
&- \frac{g}{\sqrt{2}}\left(\bar\nu W\!\!\!/^+\frac{1-\gamma_5}{2}e + \bar u W\!\!\!/^+\frac{1-\gamma_5}{2}d + \text{h.c.}\right) + g_s\bar u G\!\!\!/^a\frac{\lambda^a}{2}u + g_s\bar d G\!\!\!/^a\frac{\lambda^a}{2}d \\
&+ e\,\bar e A\!\!\!/ e + \frac{1}{3}e\bar d A\!\!\!/ d - \frac{2}{3}e\bar u A\!\!\!/ u - \tfrac{1}{4}\frac{e}{sc}\bar\nu Z\!\!\!/(1-\gamma_5)\nu + \tfrac{1}{4}\frac{e}{sc}\bar e Z\!\!\!/\left(1-4s^2-\gamma_5\right)e \\
&- \tfrac{1}{4}\frac{e}{sc}\bar u Z\!\!\!/\left(1-\frac{8}{3}s^2-\gamma_5\right)u + \tfrac{1}{4}\frac{e}{sc}\bar d Z\!\!\!/\left(1-\frac{4}{3}s^2-\gamma_5\right)d,
\end{aligned}
$$

where A and Z, the photon and the Z boson, are linear combinations of the W_3 and the B; ξ is an arbitrary real dimensionless parameter that determines a particular gauge; $\frac{1}{2}\lambda^a$ are the Gell-Mann SU(3) matrices and f^{abc} the SU(3) structure constants; ϕ^+, ϕ^-, and ϕ^0 are unphysical Goldstone bosons resulting from the symmetry breaking; and η_+, η_-, η_γ, η_z, and η_a are the unphysical Faddeev-Popov ghosts that arise [5] from the quantization

of a non-abelian gauge theory in a covariant gauge.

The parameters e, s, and c that appear in Eq. (1.11) are combinations of parameters that appear in the unbroken Lagrangian. Specifically, s and c are abbreviations, respectively, for $\sin\theta_w$ and $\cos\theta_w$, and

$$\tan\theta_w \equiv \frac{g'}{g}, \tag{1.12}$$

$$e \equiv \frac{gg'}{\sqrt{g^2+g'^2}} = g\sin\theta_w = g'\cos\theta_w. \tag{1.13}$$

Similarly, the particle masses are defined in terms of the parameters of Eqs. (1.8) and (1.9). The mass of a fermion f is given by

$$m_f = h_f v. \tag{1.14}$$

The masses of the W and Z bosons, and of the Higgs boson, are

$$M_W^2 = \tfrac{1}{4}g^2v^2 \tag{1.15}$$

$$M_Z^2 = \tfrac{1}{4}\frac{g^2v^2}{c^2} = \tfrac{1}{4}\left(\frac{e}{sc}\right)^2 v^2 \tag{1.16}$$

$$m_H^2 = \lambda v^2. \tag{1.17}$$

The vacuum expectation value v is directly related to the Fermi constant, the effective strength of low-energy weak interactions, which is defined as

$$\frac{G_F}{\sqrt{2}} = \frac{g^2}{8M_W^2}. \tag{1.18}$$

Experimentally, $v = 246$ GeV.

The photon and the Z, which arise from the requirement that the mass matrix of physical fields be diagonal, are defined by

$$A^\mu \equiv \sin\theta_w W_3^\mu + \cos\theta_w B^\mu \tag{1.19}$$

$$Z^\mu \equiv \cos\theta_w W_3^\mu - \sin\theta_w B^\mu. \tag{1.20}$$

Eq. (1.11) is rather formidable, but, fortunately, much of the complexity can be made to disappear. The gauge-fixing parameter ξ is arbitrary; for tree-level calculations it is convenient to work in the so-called unitary gauge, where $\xi \to \infty$ [6]. In this limit, the unphysical Goldstone bosons become infinitely massive and decouple from any physical processes. The Faddeev-Popov ghosts do not appear at all until the one-loop level, so, for tree-level calculations in unitary gauge, it is possible to ignore all terms in Eq. (1.11) that involve either ghosts or Goldstone bosons.

An abbreviated version of the Standard Model Lagrangian, suitable for tree-level calculations in unitary gauge, is

$$
\begin{aligned}
\mathcal{L} = & -\tfrac{1}{2}\left(\partial_\mu W^+_\nu - \partial_\nu W^+_\mu\right)\left(\partial^\mu W^{-\nu} - \partial^\nu W^{-\mu}\right) \\
& + \tfrac{1}{4}g^2v^2W^+\cdot W^- - \tfrac{1}{4}\left(\partial_\mu Z_\nu - \partial_\nu Z_\mu\right)^2 + \frac{1}{8}\left(\frac{e}{sc}\right)^2 v^2Z^2 \\
& - \tfrac{1}{4}\left(\partial_\mu A_\nu - \partial_\nu A_\mu\right)^2 - \tfrac{1}{4}\left(\partial_\mu G^a_\nu - \partial_\nu G^a_\mu\right)\left(\partial^\mu G^{\nu,a} - \partial^\nu G^{\mu,a}\right) \\
& + \tfrac{1}{2}\partial^\mu h\partial_\mu h - \tfrac{1}{2}\lambda v^2h^2 - \tfrac{1}{2}g^2\left[\left(W^+\cdot W^-\right)^2 - (W^+)^2(W^-)^2\right] \\
& - e^2\left[A^2(W^+\cdot W^-) - (A\cdot W^+)(A\cdot W^-)\right] \\
& - c^2g^2\left[Z^2(W^+\cdot W^-) - (Z\cdot W^+)(Z\cdot W^-)\right] \\
& - ecg\left[2(A\cdot Z)(W^+\cdot W^-) - (A\cdot W^+)(Z\cdot W^-) - (Z\cdot W^+)(A\cdot W^-)\right] \\
& + ie\left[\partial^\mu A^\nu W^-_\mu W^+_\nu + \partial^\mu W^{-\nu}W^+_\mu A_\nu + \partial^\mu W^{+\nu}A_\mu W^-_\nu\right] + \text{h.c.} \\
& + icg\left[\partial^\mu Z^\nu W^-_\mu W^+_\nu + \partial^\mu W^{-\nu}W^+_\mu Z_\nu + \partial^\mu W^{+\nu}Z_\mu W^-_\nu\right] + \text{h.c.} \\
& - \tfrac{1}{4}g_s^2(G^a\cdot G^c)(G^b\cdot G^d)f^{abe}f^{cde} - \tfrac{1}{2}g_s\left(\partial_\mu G^c_\nu - \partial_\nu G^c_\mu\right)G^{\mu,a}G^{\nu,b}f^{abc} \\
& - \frac{\lambda v}{2}h^3 - \frac{\lambda}{8}h^4 + \left(\frac{e}{2sc}\right)^2 v\,hZ^2 + \tfrac{1}{2}g^2vhW^+\cdot W^- + \tfrac{1}{4}g^2h^2W^+\cdot W^- \\
& + \frac{1}{8}\left(\frac{e}{sc}\right)^2 h^2Z^2 - \frac{m_e}{v}\bar{e}eh - \frac{m_u}{v}\bar{u}uh - \frac{m_d}{v}\bar{d}dh \\
& + \bar{\nu}\left(i\partial\!\!\!/\right)\nu + \bar{e}\left(i\partial\!\!\!/ - m_e\right)e + \bar{u}\left(i\partial\!\!\!/ - m_u\right)u + \bar{d}\left(i\partial\!\!\!/ - m_d\right)d \\
& - \frac{g}{\sqrt{2}}\left(\bar{\nu}W\!\!\!/^+\frac{1-\gamma_5}{2}e + \bar{u}W\!\!\!/^+\frac{1-\gamma_5}{2}d + \text{h.c.}\right) + g_s\bar{u}G\!\!\!/^a\frac{\lambda^a}{2}u + g_s\bar{d}G\!\!\!/^a\frac{\lambda^a}{2}d \\
& + e\,\bar{e}A\!\!\!/e + \frac{1}{3}e\bar{d}A\!\!\!/d - \frac{2}{3}e\bar{u}A\!\!\!/u - \tfrac{1}{4}\frac{e}{sc}\bar{\nu}Z\!\!\!/(1-\gamma_5)\nu + \tfrac{1}{4}\frac{e}{sc}\bar{e}Z\!\!\!/\left(1-4s^2-\gamma_5\right)e \\
& - \tfrac{1}{4}\frac{e}{sc}\bar{u}Z\!\!\!/\left(1-\frac{8}{3}s^2-\gamma_5\right)u + \tfrac{1}{4}\frac{e}{sc}\bar{d}Z\!\!\!/\left(1-\frac{4}{3}s^2-\gamma_5\right)d.
\end{aligned}
\tag{1.21}
$$

The generalization to three generations, rather than one, is straightforward. The only important change is in $\mathcal{L}_Y$, which becomes

$$
\mathcal{L}_Y = -\bar{E}_R H_E \Phi^\dagger L_L - \bar{D}_R H_D \Phi^\dagger Q_L - \bar{U}_R H_U \Phi_c^\dagger Q_L + \text{h.c.}, \tag{1.22}
$$

where E, D, U, L, and Q now refer to column vectors rather than to individual fields, and H_E, H_D, and H_U are arbitrary complex 3×3 matrices of coupling constants. After symmetry breaking the fermions acquire mass, and, by definition, the mass matrices of physical particles must be diagonal.

The lepton mass matrix can be diagonalized simply by making physically irrelevant field redefinitions. Diagonalizing the quark mass matrix, however, leads to off-diagonal terms in the couplings of quarks to the $W^\pm$ boson. That is, the charged-current interaction of quarks becomes

$$
\mathcal{L}_{cc} = \frac{g}{\sqrt{2}}\bar{U}W\!\!\!/^+\frac{1-\gamma_5}{2}VD + \text{h.c.}, \tag{1.23}
$$

where V is a unitary 3×3 matrix, the Kobayashi-Maskawa [7] mixing matrix. The Kobayashi-Maskawa matrix is roughly diagonal: Each quark couples most strongly to its partner in the same generation. Some off-diagonal terms, however, most notably that connecting the s and u quarks, are substantial. Additionally, there is no *a priori* reason to expect that the elements of the Kobayashi-Maskawa matrix should all be real. The most general Kobayashi-Maskawa matrix, up to physically irrelevant field redefinitions, can be parameterized by three real angles and one complex phase factor.

At present, using experimental data and the unitarity constraint, the 90% confidence limits on the magnitudes of the Kobayashi-Maskawa matrix elements are [8]

$$|V_{ij}| = \begin{pmatrix} 0.9747 \text{ to } 0.9759 & 0.218 \text{ to } 0.224 & 0.002 \text{ to } 0.007 \\ 0.218 \text{ to } 0.224 & 0.9735 \text{ to } 0.9751 & 0.032 \text{ to } 0.054 \\ 0.003 \text{ to } 0.018 & 0.030 \text{ to } 0.054 & 0.9985 \text{ to } 0.9995 \end{pmatrix}, \tag{1.24}$$

where the matrix elements are labelled

$$\begin{pmatrix} V_{ud} & V_{us} & V_{ub} \\ V_{cd} & V_{cs} & V_{cb} \\ V_{td} & V_{ts} & V_{tb} \end{pmatrix}. \tag{1.25}$$

The phase has not been measured. A non-zero value would explain the experimental observation of CP violation in the K meson system.

Many physical quantities, in particular those involving low-energy properties of hadrons, have not yet been calculated from first principles. The problem is simply that Eq. (1.11) describes the interactions of quarks, rather than the interactions of hadrons, and the necessary computational techniques for obtaining quantitative low-energy predictions about hadrons do not yet exist. Preliminary results from such methods as lattice gauge theory [9] and chiral perturbation theory [10], however, suggest that the flaw is indeed in our calculational ability rather than in the theory.

All quantities for which both theoretical and experimental results are available exhibit agreement between the measured values and the values predicted by the Standard Model [11], and there is no indication of any experimental result that is inconsistent with Standard Model expectations.

1.2 Defects of the Standard Model

Despite the spectacular successes of the Standard Model, it is theoretically problematic in many ways, and it is unlikely that the Standard Model is actually a complete description of nature. Most of the unresolved issues can be grouped into three broad categories: Problems associated with the gauge bosons and with their couplings to fermions, Eq. (1.6), problems associated with the Yukawa sector, Eq. (1.22), and problems associated with the scalar sector, Eq. (1.8).

The most serious objection to the gauge sector of the Standard Model is its arbitrariness. The gauge group G_{321}, SU(3) $\times$ SU(2) $\times$ U(1), is not simple. The gauge theory associated with this group thus has three independent coupling constants, and the Standard Model provides no understanding of their relative magnitudes.

Even more arbitrary than the gauge group itself, however, is the representation of that group used by the Standard Model, *i.e.*, the matter content of the theory. The Standard Model provides no understanding of why fermions are replicated in three generations, and even within a single generation the gauge group's representation is very complicated: It is formed from many different irreducible representations. The hypercharge assignments, *i.e.*, the U(1) quantum numbers, are postulates of the theory, rather than predictions: U(1) is abelian, so there is no obvious reason why the U(1) quantum numbers should be, as they are (see Table 1.1), small integers or ratios of small integers. Although the requirement of anomaly cancellation [12] imposes a sum rule on the U(1) quantum numbers, there is still a great deal of freedom in their assignments. Finally, although it has been known for decades that weak charged currents couple only to left-handed fermions, the Standard Model provides no explanation for this asymmetry. It is simply postulated, in Table 1.1, that left-handed fermions are members of SU(2) doublets and right-handed fermions members of SU(2) singlets.

The mass matrices in Eq. (1.22), or in more physical terms, the fermion masses and the Kobayashi-Maskawa mixing matrix, are also simply free parameters of the theory: The Standard Model provides no explanation for any of the mass ratios or the mixing angles. Given that the ratio between the mass of the lightest massive fermion, the electron, and that of the heaviest fermion, the t quark [13], is more than 3×10^5, some explanation of these ratios is called for. Similarly, while the presence of a complex phase in the Kobayashi-Maskawa matrix can explain the existence of CP violation, it does not explain why CP is so nearly conserved in weak interactions; still less does it explain why CP violation in strong interactions is, if present at all, measured [14] to be suppressed at least nine orders of magnitude relative to the value that would naïvely be expected [15] due to nonperturbative topological effects.

To some extent, many of these objections are essentially aesthetic: Our preconceptions, which suggest that a fundamental theory must be simple, may be in error. The problems in the scalar sector are considerably more serious. The Standard Model relies on elementary scalars, the complex doublet Φ, to break $\mathrm{SU}(2) \times \mathrm{U}(1)$ symmetry. Theories with self-interacting elementary scalar fields, however, suffer from two inherent problems, known as "naturalness" and "triviality."

The problem of naturalness deals with the scalar's mass renormalization, which is quadratic in the high-energy cutoff. If an elementary scalar is much lighter than the cutoff, its mass is thus the difference of two very large numbers. This situation is not only unnatural, requiring an extraordinarily precise cancellation, but is also unstable under higher-order corrections.

Just as naturalness is related to the mass renormalization of scalar fields, so triviality is related to coupling constant renormalization. The simple one-loop β function for the scalar self-interaction given in Eq. (1.8) is

$$\mu \frac{d\lambda}{d\mu} = \frac{3}{4\pi^2}\lambda^2. \tag{1.26}$$

This has the solution

$$\lambda(\mu) = \frac{1}{\lambda^{-1}(\mu_0) - \frac{3}{4\pi^2}\ln\left(\frac{\mu}{\mu_0}\right)}, \tag{1.27}$$

which diverges at a finite energy scale. If this one-loop result is to be believed, then the only way for a scalar field theory to be valid for all energy scales is if the coupling constant vanishes exactly. In fact, more sophisticated analyses confirm the conclusions suggested by the one-loop calculation. There is now very strong evidence [16], although not yet a rigorous proof, to support the idea that the only self-consistent scalar field theory in four dimensions is the free theory.

This does not, of course, mean that theories involving scalar fields are inadmissible; it merely means that these theories cannot be valid at all energy scales, but must instead be regarded as effective field theories that describe interactions at energies less than some scale Λ, where Λ is less than the scale at which the scalar coupling constant would diverge. Or, put less abstractly, it means that scalars cannot be elementary particles but must have some substructure, and that the substructure will be revealed at distances of $\mathcal{O}(1/\Lambda)$.

The larger the scalar self-interaction λ is at low energies, the lower must be the energy scale Λ at which new physics appears. Since Eq. (1.17) relates λ to the mass of the Higgs boson, this is equivalent to saying that a heavy Higgs boson requires new physics at low energy scales. This argument can be made quantitative [17]: If the Higgs boson has a mass of 175 GeV or less, then the Standard Model may be valid for all energies less than the Plank mass, while a mass of 300 GeV or more implies that the upper limit of validity must be less than about 10^3 TeV.

While none of these arguments, including triviality, is conclusive, they suggest that the Standard Model is probably incomplete, and may, at some high energy scale Λ, be embedded in a more complete theory.

1.3 Extensions of the Standard Model

1.3.1 Expansion of the gauge group

Many different extensions of the Standard Model have been proposed in order to address one or more of the issues discussed in Section 1.2. Because of the general phenomenon in physics that problems are often alleviated by symmetries, many of these extensions involve introducing additional symmetries beyond the SU(3) $\times$ SU(2) $\times$ U(1) gauge symmetry of the Standard Model.

Such models include the Peccei-Quinn model [18], which explains the suppression of CP violation in strong interactions by postulating an additional global U(1) symmetry; horizontally symmetric models [19], which explain the patterns of fermion masses and mixing angles by introducing global or local symmetries between generations; technicolor models [20], which introduce a new set of fermions, with new gauge interactions, in order to break SU(2) $\times$ U(1) symmetry without the use of elementary scalars; and supersymmetry [21, 22], which introduces a symmetry relating bosons and fermions, and which

eliminates many of the technical problems associated with the renormalization of theories containing elementary scalars.

Gauge symmetries have a special status in field theory, so many extensions of the Standard Model involve expanding the gauge group from SU(3) × SU(2) × U(1), or G_{321}, to some larger group G which contains G_{321} as a subgroup. Since this larger gauge symmetry is not observed at low energies, spontaneous symmetry breaking must once again be invoked. Enlarging the gauge group implies the existence of new gauge bosons; the symmetry must be broken in a manner that leaves only the 12 gauge bosons of the Standard Model observable at low energies.

The group G_{321} is a Lie group of rank 4, meaning that its Cartan subalgebra is four-dimensional. In more physical terms, this means that the gauge theory based on G_{321} has four neutral gauge bosons, *i.e.*, gauge bosons whose interactions with fermions change none of the fermions' quantum numbers. These gauge bosons are the photon, the Z, and two of the gluons.

It is a general result that if G_1 and G_2 are Lie groups, and $G_1 \subset G_2$, then the rank of G_2 cannot be less than that of G_1. The group G, in which G_{321} is embedded, must then have a rank greater than or equal to four. If G is of rank greater than four, the gauge theory based on it will have additional neutral gauge bosons, which are generically known as Z' bosons.

It should be emphasized that Z' bosons are a generic feature of any theory that includes a gauge group of rank greater than four: They appear naturally in many different extensions of the Standard Model. Given that the Standard Model is almost certainly incomplete, it is thus very plausible that Z' bosons exist. This does not, of course, mean that they are observable: The mass of a Z' could well be at an experimentally inaccessible energy, such as the GUT scale. In many models, however, even models where the fundamental symmetry-breaking scale of G is very large, $M_{Z'}$ is essentially unconstrained and could lie in an experimentally accessible range. A Z' necessarily provides information about an expanded gauge sector; a low-mass Z' could well be the only direct experimental probe of an expanded gauge sector.

1.3.2 The left-right symmetric model

As shown in Table 1.1, the Standard Model assigns left-handed fermions to SU(2) doublets, and right-handed fermions to SU(2) singlets. It thus provides no explanation of parity violation, but simply postulates it. The left-right symmetric model [23, 24] postulates a second SU(2) symmetry that acts on right-handed particle states, so that the fundamental Lagrangian of the theory conserves parity. Parity violation is then explained by spontaneous symmetry breaking: If the symmetry breaking occurs in such a fashion so that the gauge bosons associated with the right-handed SU(2) are much more massive than those associated with the left-handed SU(2), low-energy weak interactions will violate parity.

The gauge group of the left-right symmetric model is $\mathrm{SU(3)} \times \mathrm{SU(2)}_L \times \mathrm{SU(2)}_R \times \mathrm{U(1)}$, and the quantum number assignments, instead of the Standard Model assignments of Table 1.1, take the somewhat more orderly form shown in Table 1.2. The symbols

Table 1.2: Left-right symmetric model particle content, and SU(3), $SU(2)_L$, $SU(2)_R$ and U(1) quantum number assignments, for the first generation of fermions. Note the presence of a right-handed neutrino, which is absent in the Standard Model.

Particle	SU(3)	$SU(2)_L$	$SU(2)_R$	U(1)
Q_L	3	2	1	1/3
L_L	1	2	1	−1
Q_R	3	1	2	1/3
L_R	1	1	2	−1

Q_L and L_L have the same meanings as in Table 1.1, while Q_R refers to a right-handed quark doublet, u_R and d_R, and L_R refers to a right-handed lepton doublet, e_R and ν_R. The right-handed neutrino, ν_R, has not been observed, and is not present in the Standard Model. Unlike the "hypercharge" of the Standard Model, the U(1) quantum number given in Table 1.2 has a simple physical interpretation: It is $B - L$, where B is a particle's baryon number and L is its lepton number. The gauge coupling constant of $SU(2)_R$ is taken to be the same as that of the familiar $SU(2)_L$.

The group $SU(3) \times SU(2)_L \times SU(2)_R \times U(1)$ has rank 5, so the left-right symmetric model has five neutral gauge bosons. Four of them, the photon, the Z, and two of the gluons, are the same as in the Standard Model, while the fifth is a Z'. The photon, Z, and Z' do not, however, simply correspond to the diagonal generators of U(1), $SU(2)_L$, and $SU(2)_R$. Just as the photon and Z of the Standard Model are linear combinations of the W_3 and the B, so the physical neutral gauge bosons of the left-right symmetric model are linear combinations of the neutral gauge group generators, the details of this mixing being determined by the symmetry breaking.

As in the Standard Model, symmetry breaking in the left-right symmetric model is accomplished by means of interacting scalar fields with a nonzero vacuum expectation value. The scalar sector of the left-right symmetric model, however, is much more complicated than that of the Standard Model. The simplest version of the left-right symmetric model contains three different complex scalar multiplets, one of which transforms as a triplet under $SU(2)_L$, one as a triplet under $SU(2)_R$, and one as a doublet under both $SU(2)_L$ and $SU(2)_R$; this is a total of 20 scalar degrees of freedom. The scalar fields of the left-right symmetric model, and their quantum numbers, are specified in Table 1.3.

The reason for including so many scalars is that the two scalar triplets, the Δ_L and Δ_R, are required to break the left-right invariance, while the doublet field, ϕ, plays roughly the same role as does the Higgs doublet Φ in the Standard Model: It breaks $SU(2) \times U(1)$ down to U(1). This general hierarchical scheme, where one mechanism is responsible for the symmetry breaking $G \to SU(3) \times SU(2) \times U(1)$ and another for $SU(3) \times SU(2) \times U(1) \to SU(3) \times U(1)$, is repeated in many different extensions of the Standard Model.

The most general renormalizable potential involving these scalar fields is quite complicated: It depends on 18 independent parameters [25], three of which are masses

Table 1.3: Scalar fields, and their quantum numbers, in the left-right symmetric model.

Particle	SU(3)	$SU(2)_L$	$SU(2)_R$	U(1)
Δ_L	1	3	1	2
Δ_R	1	1	3	2
ϕ	1	2	2	0

and the other 15 are coupling constants. The minima of this potential have not been investigated in full detail, but it has been shown [26] that there exists a range of value of these parameters such that the minimum takes the form

$$\langle \Delta_{R,L} \rangle = \begin{pmatrix} 0 \\ 0 \\ v_{R,L} \end{pmatrix} \tag{1.28}$$

$$\langle \phi \rangle = \begin{pmatrix} \kappa & 0 \\ 0 & \kappa' \end{pmatrix}, \tag{1.29}$$

with $v_L \ll \kappa \ll v_R$. In this model, $\kappa^2 + \kappa'^2$ sets the scale of M_W^2 and M_Z^3, as does v^2 in the Standard Model.

The mass matrix for the $W_{3,L}$, $W_{3,R}$, and B is [24]

$$[W_{3L}\, W_{3R}\, B] \begin{pmatrix} \frac{1}{2}g^2(\kappa^2+\kappa'^2+4v_L^2) & -\frac{1}{2}g^2(\kappa^2+\kappa'^2) & -2gg'v_L^2 \\ -\frac{1}{2}g^2(\kappa^2+\kappa'^2) & \frac{1}{2}g^2(\kappa^2+\kappa'^2+4v_R^2) & -2gg'v_R^2 \\ -2gg'v_L^2 & -2gg'v_R^2 & g'^2(v_L^2+v_R^2) \end{pmatrix} \begin{bmatrix} W_{3L} \\ W_{3R} \\ B \end{bmatrix}. \tag{1.30}$$

Although it is possible to diagonalize Eq. (1.30) exactly, the results are too complicated to be of much use. In the limit where v_R is very large, however, and Z-Z' mixing is negligible,

$$M_Z^2 \approx \frac{1}{2}\frac{g^2}{\cos^2\theta_w}(\kappa^2+\kappa'^2) \tag{1.31}$$

$$M_{Z'}^2 \approx 2(g^2+g'^2)v_R^2, \tag{1.32}$$

and the photon, as electromagnetic gauge symmetry demands, remains exactly massless.

Without knowledge of the parameters in the scalar potential, it is impossible to make a more quantitative prediction of $M_{Z'}/M_Z$ or of the mixing angle between the Z and the Z'.

Assuming that mixing between the Z and Z' is negligible, the Z' coupling to fermions is given by

$$\mathcal{L}_{int} = g_{Z'} Q_f \bar{f} \not{Z}' f, \tag{1.33}$$

where

$$g_{Z'} = \frac{g}{\sqrt{1-2\sin^2\theta_w}} \tag{1.34}$$

Table 1.4: Charges Q for the coupling of one generation of fermions to a Z' of the left-right symmetric model. The normalization of Q_f is defined by Eq. (1.33).

Left-handed states		Right-handed states	
Particle	Q	Particle	Q
e_L	$\frac{1}{2}\sin^2\theta_w$	e_R	$\sin^2\theta_w - \frac{1}{2}\cos^2\theta_w$
ν_L	$\frac{1}{2}\sin^2\theta_w$	ν_R	$\frac{1}{2}\cos^2\theta_w$
d_L	$-\frac{1}{6}\sin^2\theta_w$	d_R	$\frac{1}{3}\sin^2\theta_w - \frac{1}{2}\cos^2\theta_w$
u_L	$-\frac{1}{6}\sin^2\theta_w$	u_R	$-\frac{2}{3}\sin^2\theta_w + \frac{1}{2}\cos^2\theta_w$

and

$$Q_f = \sin^2\theta_w(T_{3L} - Q) + \cos^2\theta_w T_{3R}. \tag{1.35}$$

In Eq. (1.35), T_{3L} and T_{3R} refer, respectively, to the fermion's left-handed and right-handed isospin assignments, and Q refers to its electromagnetic charge. These couplings are given explicitly in Table 1.4.

1.3.3 Grand Unified Theories

Much of the complexity of the Standard Model stems from the fact that its gauge group, G_{321}, is not simple. Grand unified theories (GUTs) are models in which $G_{321} \subset G$, where G is a simple group. The symmetry group G breaks spontaneously to G_{321}.

In GUTs, all gauge interactions are characterized by a single coupling constant. This appears to be contradicted by experiment, since the coupling strengths of the strong, weak, and electromagnetic interactions are very different, but, in fact, the relative magnitudes of the three Standard Model gauge coupling constants are a strong argument for the plausibility of grand unification.

A simple one-loop calculation [27] yields the β functions of the three Standard Model gauge coupling constants:

$$\mu\frac{dg_i}{d\mu} = -\frac{b_i}{16\pi^2}g_i^3, \tag{1.36}$$

where, for N generations of fermions,

$$b_{SU(3)} = -\frac{4}{3}N + 11 \tag{1.37}$$

$$b_{SU(2)} = -\frac{4}{3}N + \frac{22}{3} - \frac{1}{6} \tag{1.38}$$

$$b_{U(1)} = -\frac{4}{3}N - \frac{1}{10}. \tag{1.39}$$

More careful calculations [28], which include two-loop diagrams and the effects of heavy-particle thresholds, do not modify these equations significantly [29]: These higher-order effects are small corrections.

Table 1.5: Assignment of a single generation of left-handed fermions to irreducible representations of SU(5). All 15 fermionic states can be assigned to two irreducible representations. The symbol f_L^c refers to the left-handed component of the charge conjugate of the fermion f.

Multiplet	Particle content
$\mathbf{5^*}$	$[\nu\ e\ d^c]_L$
$\mathbf{10}$	$[u\ d\ u^c\ e^c]_L$

Integrating these equations yields the values of the coupling constants at an energy scale μ in terms of their values at a scale μ_0:

$$\alpha_i^{-1}(\mu) = \frac{b_i}{2\pi} \ln\left(\frac{\mu}{\mu_0}\right) + \alpha_i^{-1}(\mu_0). \tag{1.40}$$

When the known low-energy values of the three Standard Model gauge coupling constants are inserted into Eq. (1.40), it turns out that although the coupling constants have very different values at low energies, their values at high energies ($\mu \sim 10^{15}$ GeV) become roughly equal. This is suggestive of the behavior predicted by a GUT, where, at some scale M_{GUT}, they would be exactly equal.

The smallest simple group that can contain G_{321} as a subgroup, and that has representations in which the Standard Model fermion representations can be embedded, is SU(5) [30]. The fifteen states of a single generation of fermions can be embedded in two irreducible representations of SU(5), a $\mathbf{5^*}$ and a $\mathbf{10}$: The decomposition of these irreducible representations of SU(5) into representations of SU(3) $\times$ SU(2) is

$$\mathbf{5^*} = (\mathbf{3^*}, \mathbf{1}) \oplus (\mathbf{1}, \mathbf{2}) \tag{1.41}$$

$$\mathbf{10} = (\mathbf{3^*}, \mathbf{1}) \oplus (\mathbf{3}, \mathbf{2}) \oplus (\mathbf{1}, \mathbf{1}). \tag{1.42}$$

The assignments of left-handed particles to SU(5) multiplets are shown in Table 1.5. Note that left-handed charge conjugate states, rather than right-handed states, are included in this table. This is because all particles in a gauge multiplet must transform the same way under Lorentz transformations, or, more succinctly, because gauge transformations and Lorentz transformations commute.

As is the case in the left-right symmetric model, the gauge symmetry must be broken in two stages. At energy scales large compared to the GUT scale, the gauge symmetry is SU(5); at energy scales small compared to the GUT scale, but large compared to the electroweak scale, the gauge symmetry is SU(3) $\times$ SU(2) $\times$ U(1); and at energies small compared to the electroweak scale, the gauge symmetry is SU(3) $\times$ U(1). Again, much as in the left-right symmetric model, this hierarchical symmetry breaking may be accomplished with a scalar sector consisting of two different species of scalars. In the case of SU(5), the minimal phenomenologically acceptable scalar sector consists of a **24** and a **5** of SU(5), where the **24** breaks SU(5), and the **5** breaks electroweak symmetry. The **5** contains the familiar Standard Model Higgs doublet Φ.

The group SU(5) is 24-dimensional, so SU(5) has 12 more gauge bosons than does the Standard Model. Its rank, however, is 4, so it has no additional neutral gauge

bosons. There are no other rank 4 groups that can contain SU(3) × SU(2) × U(1) as a subgroup: Every other extension of the Standard Model gauge group, and, in particular, every other GUT, has at least one Z'.

This fact is significant, because the minimal SU(5) model has been conclusively ruled out. There are two convincing arguments against minimal SU(5). First, SU(5) predicts an excessively fast decay rate for the proton. The 12 new gauge fields introduced by SU(5) are fractionally charged; their interactions with matter connect quarks to leptons, and these interactions lead to proton decay [31], suppressed by M_{GUT}^{-4}. Although there is some uncertainty about the calculation of the proton lifetime, due both to the uncertainty in M_{GUT} and to the difficulty of calculating low-energy hadronic matrix elements, the experimental 90% confidence limit [8] for the decay $p \to e^+\pi^0$ is $\tau_p/B > 9 \times 10^{32}$ yr, which is two orders of magnitude larger than the upper limit allowed by minimal SU(5).

Independently, minimal SU(5) is ruled out because in this model the three Standard Model coupling constants do not actually unify. The values of the Standard Model coupling constants at M_Z are now known precisely enough to make it clear that, although they approach a similar magnitude at very high energies when they are evolved upwards using Eq. (1.36), they never actually become equal. The electroweak coupling constants $\alpha_1(M_Z)$ and $\alpha_2(M_Z)$ are obtained by the LEP measurements of $\alpha_{EM}(M_Z)$ and $\sin^2\theta_W$, yielding [32]

$$\alpha_1(M_Z) = 0.016887 \pm 0.000040 \tag{1.43}$$

$$\alpha_2(M_Z) = 0.03322 \pm 0.00025, \tag{1.44}$$

and the strong coupling constant α_3 can be extracted from a variety of experiments; the Particle Data Group [8] reports a world average of $\alpha_3(M_Z) = 0.1134 \pm 0.0035$. Using these values, as shown in Fig. 1.1, coupling constant unification is ruled out by more than seven standard deviations [32].

This does not mean that grand unification must be abandoned altogether, but, rather, that grand unification is tenable only if the assumptions implicit in the application of Eq. (1.36) are abandoned. Using Eq. (1.36) to run the coupling constants from M_Z to M_{GUT} is only valid if there are no thresholds between those scales, *i.e.*, if there is no new physics until M_{GUT}. Grand unification is still possible if some new physics exists at intermediate energy scales.

In minimal SU(5), no such intermediate scales exist: SU(5) breaks directly to SU(3) × SU(2) × U(1). Suitable GUTs that do possess intermediate scales include supersymmetric SU(5), and GUTs based on gauge groups larger than SU(5). Larger gauge groups are worthy of consideration in any case: SU(5) still uses two different irreducible representations to accommodate each generation of fermions, while a larger group can accommodate them in a single irreducible representation.

Other than SU(5), the smallest candidate for a GUT gauge group is SO(10) [33]. All fermions of a single generation can be accommodated in a single 16-dimensional SO(10) multiplet. The decomposition of the **16** of SO(10) into SU(5) multiplets is

$$[\mathbf{16}]_{SO(10)} = \mathbf{5}^* + \mathbf{10} + \mathbf{1}, \tag{1.45}$$

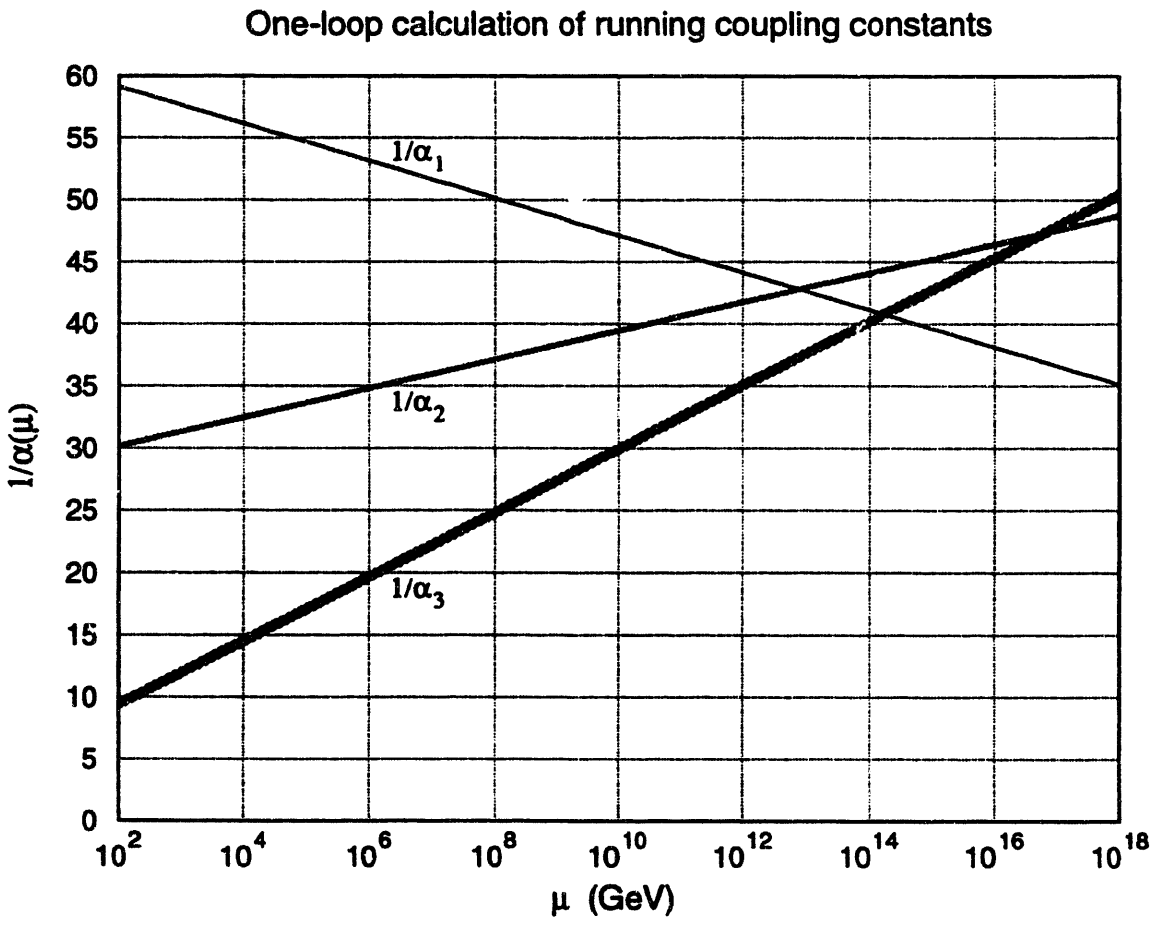

Figure 1.1: One-loop calculation of the running of the SU(3), SU(2), and U(1) gauge coupling constants. The three lines represent the central values of the coupling constants, and the shaded regions represent the one-σ errors. Note that the three coupling constants never actually become equal.

Table 1.6: Value of the charge Q for the coupling of an SO(10) Z', or Z_χ, to one generation of left-handed fermions. Note that the coupling is the same for all members of an SU(5) multiplet.

SU(5) multiplet	Particle	Q_L
10	e^+, d, u, u^c	$Q_L^{10} = -\frac{1}{2\sqrt{6}}$
5*	d^c, e^-, ν_e	$Q_L^{5^*} = \frac{3}{2\sqrt{6}}$

and, as discussed above, all known fermions of a single generation can be embedded in the 5* and the 10 of SU(5). The SU(5) singlet describes an additional fermion state, an electrically neutral fermion that transforms neither under $SU(3)_c$ nor under $SU(2)_L$. This state may be thought of as a right-handed neutrino.

The group SO(10) has rank 5, so the SO(10) GUT does predict the existence of a Z'. Also, since SO(10) has a larger rank than that of G_{321}, there are several ways in which it can be broken down to G_{321}. One symmetry-breaking scheme is that suggested by Eq. (1.45):

$$\begin{aligned} \mathrm{SO(10)} &\rightarrow \mathrm{SU(5)} \times \mathrm{U(1)} \\ &\rightarrow \mathrm{SU(3)} \times \mathrm{SU(2)} \times \mathrm{U(1)} \times \mathrm{U(1)} \\ &\rightarrow \mathrm{SU(3)} \times \mathrm{U(1)} \times \mathrm{U(1)}. \end{aligned} \tag{1.46}$$

The SO(10) gauge interactions, like those of the left-right symmetric model, conserve parity; in fact, it is possible to embed the left-right symmetric model in SO(10), via the breaking scheme

$$\begin{aligned} \mathrm{SO(10)} &\rightarrow \mathrm{SU(4)} \times \mathrm{SU(2)} \times \mathrm{SU(2)} \\ &\rightarrow \mathrm{SU(3)} \times \mathrm{SU(2)} \times \mathrm{SU(2)} \times \mathrm{U(1)} \\ &\rightarrow \mathrm{SU(3)} \times \mathrm{U(1)} \times \mathrm{U(1)}. \end{aligned} \tag{1.47}$$

The Z' in the symmetry-breaking scheme of Eq. (1.47) arises from the breaking of left-right symmetry, so its couplings are those described in Section 1.3.2. In the symmetry-breaking scheme of Eq. (1.46), however, the Z', conventionally called Z_χ, has a different set of couplings. The generator of the Z_χ commutes with the SU(5) generators, so the fermionic couplings of the Z_χ are the same for all fermions in an SU(5) multiplet. The coupling of the Z_χ to fermions is $g'Q$, where g' is the same as the U(1) gauge coupling constant in the Standard Model, and where Q is given in Table 1.6.

As is the case with the left-right symmetric model, each successive stage of symmetry-breaking in Eq. (1.46) or Eq. (1.47) involves a separate Higgs multiplet. In the case of the symmetry-breaking scheme of Eq. (1.46), the predicted mass of the Z_χ depends crucially on the structure of the Higgs sector: M_{Z_χ} may be of up to $\mathcal{O}(M_{GUT})$. For at least one choice of Higgs bosons, however [34], the Z_χ may have a mass as low as a few hundred GeV without any unnatural fine-tuning of parameters.

1.3.4 The E_6 model

Superstring theory suggests E_6 as a candidate GUT gauge group. Regardless of the status of superstrings, E_6 is a useful example of a model that predicts the existence of at least one Z'. If superstring theory is indeed a correct description of nature, this would imply that the Lagrangian of the theory should be supersymmetric, although the scale of supersymmetry breaking could conceivably be as high as M_{GUT} or even M_{Plank}. In any case, however, E_6 can be treated purely as a GUT, without including any effects of supersymmetry. For the purposes of understanding the gauge boson sector of E_6, the most important effect of supersymmetry would simply be a modification of the β function associated with the running of the gauge coupling constants.

The group E_6 has rank 6. There are many ways that it can break [35] down to the low-energy gauge group $SU(3) \times SU(2) \times U(1)$; the most common assumption is that it breaks according to the pattern

$$\begin{aligned} E_6 &\rightarrow SO(10) \times U(1)_\psi \\ &\rightarrow SU(5) \times U(1)_\chi \times U(1)_\psi \\ &\rightarrow SU(3) \times SU(2) \times U(1)_Y \times U(1)_\chi \times U(1)_\psi. \end{aligned} \tag{1.48}$$

The factor $U(1)_Y$ is the familiar hypercharge group, while $U(1)_\psi$ and $U(1)_\chi$ are additional symmetries. The $U(1)_\psi$ factor commutes with SO(10), so the couplings of the $U(1)_\psi$ are the same for all left-handed states. The couplings of the Z_χ are, as discussed in Section 1.3.3, the same for all particles in an SU(5) multiplet, but are different for the $\mathbf{5}^*$ and the **10** of SU(5).

In general, neither the Z_χ nor the Z_ψ will be a physical particle. A light Z' will be a linear combination of the generators of these two U(1) groups, which is typically parameterized [36] by the mixing angle α:

$$Z' = Z'_\psi \cos\alpha + Z'_\chi \sin\alpha. \tag{1.49}$$

In principle the Z' could mix with the Z, but this mixing is experimentally known to be small [37], and is expected to be negligible for $M_{Z'} \gg M_Z$.

A generation of fermions in E_6 forms a **27** representation, that is, it consists of 27 left-handed states related by a gauge symmetry, and another 27 right-handed states. Only fifteen left-handed fermionic states in each generation are known; E_6, then, predicts an additional twelve "exotic" fermions. In the breaking scheme of Eq. (1.48), the **27** of E_6 decomposes into irreducible representation of SO(10),

$$[\mathbf{27}]_{E_6} = \mathbf{16} + \mathbf{10} + \mathbf{1}. \tag{1.50}$$

The **16**, in turn, as discussed in Section 1.3.3, decomposes into irreducible representations of SU(5):

$$[\mathbf{16}]_{SO(10)} = \mathbf{5}^* + \mathbf{10} + \mathbf{1}, \tag{1.51}$$

and thus includes all of the known fermions and a right-handed neutrino. The **10** and the **1** of SO(10) are composed entirely of exotic fermions.

Table 1.7: Values of the charge Q for the coupling of one generation of left-handed fermions to an E_6 Z'. Note that the coupling is the same for all members of an SU(5) multiplet.

SU(5) multiplet	Particle	Q_L
10	e^+, d, u, u^c	$Q_L^{10} = \frac{1}{3}\left(\sqrt{\frac{5}{8}}\cos\alpha + \sqrt{\frac{3}{8}}\sin\alpha\right)$
$\mathbf{5^*}$	d^c, e^-, ν_e	$Q_L^{5^*} = \frac{1}{3}\left(\sqrt{\frac{5}{8}}\cos\alpha - \sqrt{\frac{27}{8}}\sin\alpha\right)$

Using the normalization conventions of Ref. [36], the coupling of a Z' to matter is

$$\mathcal{L}_{\rm int} = g_{Z'}\left(Q_L^f Z'_\mu \bar{f}_L \gamma^\mu f_L + Q_R^f Z'_\mu \bar{f}_R \gamma^\mu f_R\right), \tag{1.52}$$

where $g_{Z'}$ is the ordinary $U(1)_Y$ coupling constant, *i.e.*,

$$g_{Z'} = g' = \frac{e}{\cos\theta_W}. \tag{1.53}$$

Eq. (1.53) is exact only at the GUT scale: There are corrections when g' and $g_{Z'}$ are run down from the GUT scale to experimentally accessible energies. These corrections, however, are only logarithmic. In any case, calculating them requires knowledge of the physics between $M_{Z'}$ and $M_{\rm GUT}$, such as thresholds due to new fermions and to supersymmetry. Even in the context of the E_6 model, then, $g_{Z'}$ is best regarded as a quantity to be determined experimentally rather than as one for which there is a precise theoretical prediction.

In this E_6 model, the charge Q_L is a linear combination of the $U(1)_\psi$ and $U(1)_\chi$ charges. The normalization has been fixed by Eq. (1.53), and the charges for known fermions are given in Table 1.7. The right-handed charge Q_R is fixed by CPT invariance:

$$Q_R^f = -Q_L^{f^c}. \tag{1.54}$$

The width of the Z', if exotic fermions are too heavy to be produced and if the masses of all conventional fermions may be neglected, is

$$\Gamma_{Z'} = \frac{M_{Z'}}{2}\frac{g_{Z'}^2}{4\pi}\left[10(Q_L^{10})^2 + 5(Q_L^{5^*})^2\right]. \tag{1.55}$$

For a Z' of 1 TeV, this varies between 4 GeV and 10 GeV.

1.4 Parameterization of Z' properties

The fact that Z's are a generic feature of many models makes it plausible that they exist, but it also means that the mere observation of a Z' tells us very little about the physics that gives rise to it. Only by detailed study of its properties can the nature of the expanded gauge group that gives rise to it be determined. There is a large literature discussing tests that can distinguish one model from another, but, since the true physics

of an expanded gauge sector might not be that described by any of the currently popular models, it is desirable to have a model-independent parameterization of Z' properties.

Many models that predict the existence of a Z' boson, such as the E_6 model, also predict the existence of additional fermions that couple to the Z'. I assume, for the sake of simplicity, that all of these "exotic" fermions, if they exist, have a mass greater than $\frac{1}{2}M_{Z'}$. If any exotic fermions have a mass less than $\frac{1}{2}M_{Z'}$, this will have the effect of increasing the Z''s width and decreasing its branching ratio to ordinary fermions, thus decreasing its production cross section. This would make precision Z' studies more difficult, but, of course, by allowing direct study of new fermions, it would provide a great deal of additional information about the expanded gauge group. Assuming that this information will not be available, and that only the Z' will be accessible to study, is the conservative assumption.

I further assume universality, that is, that the Z' couples in the same way to each generation, and also the lack of flavor-changing neutral currents in the coupling of the Z' to ordinary fermions. Note that these three assumptions are not completely independent: Sufficiently light exotic fermions are likely to induce flavor-changing neutral currents [38].

The most general Z' consistent with this set of assumptions can be described by seven parameters. Two of these are the Z''s mass and its mixing to the ordinary Z, $M_{Z'}$ and θ_M, and the other five are coupling constants, which I will denote g_L, g_e, g_Q, g_u, and g_d. Because of $SU(2)_L$ invariance, the coupling to left-handed electrons and neutrinos must be the same, just as SU(3) invariance implies that the Z' must couple equally to the three quark colors. The coupling to left-handed electrons and neutrinos is denoted g_L. Similarly, g_Q is the coupling to left-handed quarks, and g_u, g_d, and g_e are the couplings to right-handed up quarks, down quarks, and electrons. The sign of the couplings is defined by the interaction Lagrangian

$$\mathcal{L}_{\rm int} = g_f \bar{f} \not{Z}' f. \tag{1.56}$$

Del Aguila, Cvetič, and Langacker [39] have proposed a different model-independent parameterization, introducing the four normalized couplings

$$\gamma_L^l \equiv \frac{g_L^2}{g_L^2 + g_e^2} \tag{1.57}$$

$$\gamma_L^q \equiv \frac{g_Q^2}{g_L^2 + g_e^2} \tag{1.58}$$

$$\tilde{U} \equiv \frac{g_u^2}{g_Q^2} \tag{1.59}$$

$$\tilde{D} \equiv \frac{g_d^2}{g_Q^2}, \tag{1.60}$$

and del Aguila and Cvetič [40] have proposed yet another parameterization,

$$P_V^l \equiv \frac{g_L + g_e}{g_L - g_e} \tag{1.61}$$

$$P_L^q \equiv \frac{g_Q}{g_L - g_e} \tag{1.62}$$

$$P_R^u \equiv \frac{g_u}{g_Q} \tag{1.63}$$

$$P_R^d \equiv \frac{g_d}{g_Q}. \tag{1.64}$$

These particular combinations of coupling constants are measured directly in certain experiments.

In fact, an important special case is even simpler: In many models, the couplings of the Z' are invariant not only under $SU(3)_c \times SU(2)_L$, but under SU(5). This is always true, in particular, for models in which at some energy scale the gauge group takes the form $G \times H$, where the Z' is one of the generators of H, $SU(5) \subseteq G$, and the Standard Model gauge group is contained in that SU(5).

Most of the Z' models commonly discussed in the literature, including the SO(10) model discussed in Section 1.3.3 and the E_6 model discussed in Section 1.3.4, are of this form. The only notable exceptions, in fact, are the left-right symmetric model discussed in Section 1.3.2, and the so-called sequential Z' model. The sequential model simply postulates a Z' whose couplings are identical to those of the Z; this model is completely unmotivated theoretically, and appears in the literature only because of its computational simplicity.

The special case of SU(5)-invariant couplings requires one additional assumption beyond those discussed above: Z' couplings are invariant under SU(5) only if mixing between the Z and the Z' is negligible. In fact, however, this assumption is already known to be true: As discussed in more detail in Section 2.2.1, experiments at LEP already constrain θ_M to be very small [37]. Except in the case of precision studies, such as rare decay modes of the Z', it is valid to neglect mixing.

All known elementary fermions in a single generation can be assigned to two irreducible representations of SU(5): ν_L, e_L, and d_L^c are assigned to a $\mathbf{5}^*$, and u_L, d_L, u_L^c, and e_L^c to a **10**. Instead of five independent coupling constants, then, a theory of this form only has two, g_{5^*} and g_{10}. The couplings of such a Z' to fermions take the form

$$\begin{aligned} g_L &= g_{5^*} \\ g_Q &= g_{10} \\ g_e &= -g_{10} \\ g_u &= -g_{10} \\ g_d &= -g_{5^*}. \end{aligned} \tag{1.65}$$

For most purposes, a different parameterization of the SU(5)-invariant couplings is more convenient:

$$\begin{aligned} g_{5^*} &= \tilde{g} \sin\beta \\ g_{10} &= \tilde{g} \cos\beta. \end{aligned} \tag{1.66}$$

Different models correspond to different values of β. The Z'_ψ and Z'_χ of E_6 [36], for example, correspond respectively to $\beta = \pi/4$ and $\beta = -\tan^{-1}(3)$.

A measurement of Z' couplings, in this language, means a measurement of a physically observable quantity that depends on $\tilde{\mathbf{g}}$ and β. Note that a quantity that depends only on the magnitudes of the couplings, not the signs, must have periodicity π or less.

This general class of SU(5)-invariant models is no less predictive than is the E_6 model: Both describe all ratios of coupling constants in terms of a single parameter. Although the E_6 model is seemingly more predictive in that it specifies the Z' coupling constant $g_{Z'}$ in terms of the U(1) coupling constant g', that, as discussed in Section 1.3.4, is an illusion: The precise value of $g_{Z'}$ can be predicted only by making assumptions about physics at energy scales between M_Z and $M_{\rm GUT}$.

The width $\Gamma_{Z'}$ is not an independent parameter of the theory. The partial width for Z' decay into a fermion-antifermion pair is

$$\Gamma_f = \frac{M_{Z'}}{24\pi}\sqrt{1-4\frac{m_f^2}{M_{Z'}^2}}\left[\left(1-\frac{m_f^2}{M_{Z'}^2}\right)\left((g_L^f)^2+(g_R^f)^2\right)+\frac{m_f^2}{M_{Z'}^2}6g_L^f g_R^f\right], \tag{1.67}$$

where g_L^f and g_R^f are the fermion's left-handed and right-handed couplings to the Z'. In the case of quarks, this must be multiplied by a color factor of 3, for the three quark colors, times a small enhancement factor due to final-state QCD interactions.

The only fermion whose mass cannot be neglected is, of course, the top quark. For $M_{Z'} = 500$ GeV and $m_t = 175$ GeV [13], the corrections due to nonzero m_t depend on the relative sign and magnitude of g_L^t and g_R^t, but are typically at least 10%.

Assuming that the Z' only decays into known fermions, and assuming $M_{Z'} > 2m_t$, the width of the Z' is

$$\begin{aligned}\Gamma_{Z'} = \frac{M_{Z'}}{8\pi}\Bigg[&2g_L^2 \;+\; g_e^2+3g_d^2+g_Q^2\left(5+(1-x)\sqrt{1-4x}\right) \\ &+\; g_u^2\left(2+(1-x)\sqrt{1-4x}\right)+6x\sqrt{1-4x}\,g_Q g_u\Bigg],\end{aligned} \tag{1.68}$$

where $x \equiv m_t^2/M_{Z'}^2$. In the case of a Z' with SU(5)-invariant couplings, this simplifies to

$$\Gamma_{Z'} = \frac{M_{Z'}\tilde{\mathbf{g}}^2}{8\pi}\left[5+\cos^2\beta\left(3+2(1-x)\sqrt{1-4x}-6x\sqrt{1-4x}\right)\right]. \tag{1.69}$$

This expression is graphed in Fig. 1.2, setting the Z' coupling constant $\tilde{\mathbf{g}}$ equal to the Standard Model U(1) coupling g'. This normalization is solely for convenience: In most realistic models, it is considerably smaller. In most models, $\Gamma_{Z'}/M_{Z'} \sim 1\%$. As is seen in this graph, the corrections from a finite top mass can be substantial if $M_{Z'}$ is sufficiently small.

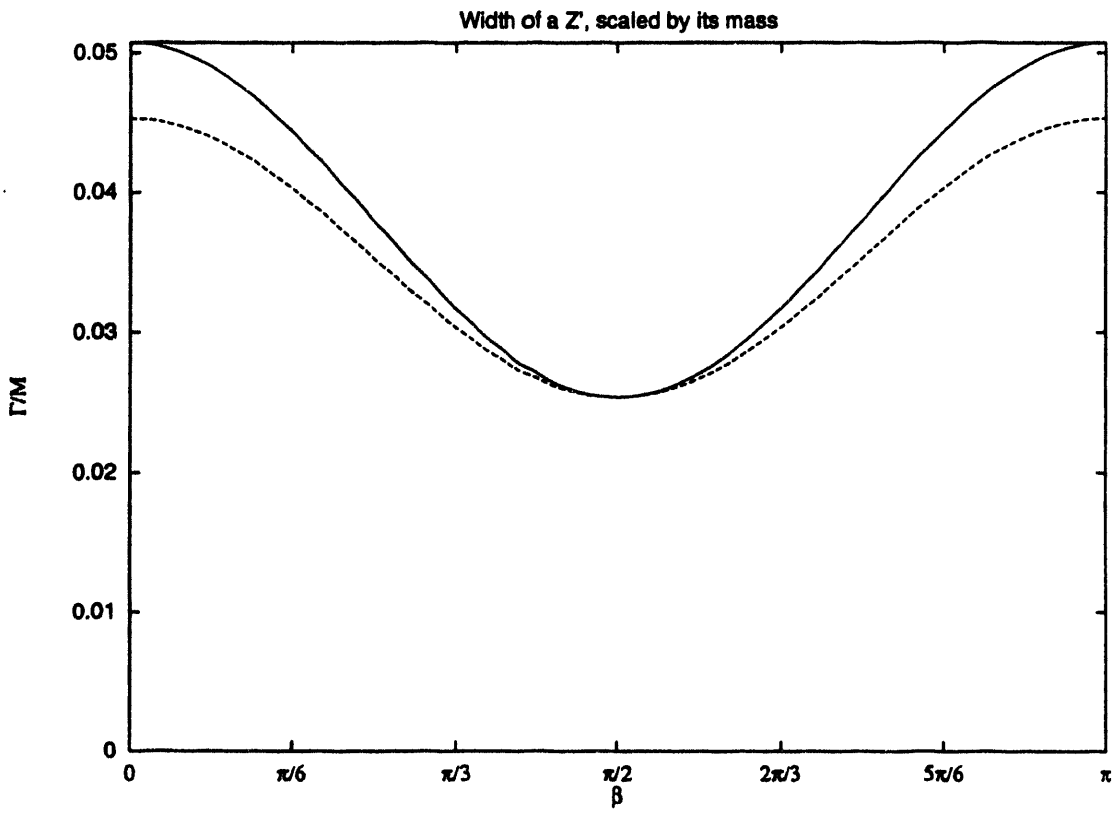

Figure 1.2: Graph of Eq. (1.69), $\Gamma_{Z'}/M_{Z'}$ for a Z' with SU(5)-invariant couplings. The coupling constant, $\tilde{g}$, is taken to be equal to the U(1) coupling constant g' of the Standard Model. The angle β determines the Z''s relative coupling strength to the SU(5) 5^* and **10** multiplets. The solid line is for $m_t^2/M_{Z'}^2$ negligible, and the dashed line is for $m_t^2/M_{Z'}^2 = 0.1$.

Chapter 2

Present-day limits on the existence of a Z'

Limits on the existence of a Z' may be divided into two categories: Limits from direct search, and limits from indirect arguments. Direct search limits arise from the failure to observe a Z' resonance in high-energy collisions, whereas indirect search limits arise from a diverse collection of effects where the existence of a Z' would affect physical observables even if the Z' were too massive to be produced on-shell.

Both direct and indirect searches lead to model-dependent constraints. Although the direct and indirect limits on $M_{Z'}$ are similar, the ranges of parameter space excluded by the two methods are different, and the two methods are complementary.

2.1 Direct search limits

At present, the most stringent direct search limits for new gauge bosons are those obtained by the CDF Collaboration [41] at the Fermilab Tevatron.

CDF's search limit is based on the non-observation of the reaction $p\bar{p} \rightarrow Z' \rightarrow l^+l^-$, where l^+l^- is either an electron or a muon pair. The actual quantity whose value is bounded, then, isn't $M_{Z'}$ but rather $\sigma(p\bar{p} \rightarrow Z')B(l^+l^-)$. In any particular model, $\sigma(p\bar{p})$ and $B(l^+l^-)$ can both be obtained as functions of $M_{Z'}$, and, by comparison with this prediction, the experimental upper bound on Z' production can be turned into a model-dependent lower bound on $M_{Z'}$.

For both the e^+e^- and the $\mu^+\mu^-$ modes, CDF required a candidate event to consist of an opposite sign dilepton pair, both members of which have high transverse momentum ($p_\perp > 25$ GeV for electrons, $p_\perp > 20$ GeV for muons). One member of each pair was required to be central ($|\eta| < 0.6$ for muons, $|\eta| < 1.1$ for electrons) the other only to lie within the central tracking chamber ($|\eta| < 1.4$). For both channels, the dilepton invariant mass was required to be greater than 40 GeV. The total sample, after all cuts, consists of 148 $\mu^+\mu^-$ events, none of which has $M_{\mu\mu} > 155$ GeV, and 1244 e^+e^- events, none of which has $M_{ee} > 320$ GeV.

The limit on $\sigma(Z')B(l^+l^-)$ is obtained by fitting the observed invariant mass

distribution to a distribution that includes both Drell-Yan production and Z' decay, taking into account trigger efficiencies and geometric acceptances. This limit is mass-dependent, mainly because the kinematics of Z' production and decay depends on $M_{Z'}$: Higher mass Z's tend to be produced more centrally, and their decay products tend to have higher $p_\perp$, so it is more likely that such events would pass CDF's cuts. The upper bound on σB (95% confidence limit) ranges from 0.8 pb for a 250 GeV Z' to 0.2 pb for a 600 GeV Z'.

CDF obtains a model-dependent lower bound on $M_{Z'}$ simply by finding the lowest value of $M_{Z'}$ for which the predicted value of σB is less than the experimental upper limit. For the model where the Z''s couplings are equal to those of the Standard Model Z, this limit is $M_{Z'} > 495$ GeV (95% confidence limit). This model, however, is poorly motivated theoretically. For more plausible models, such as those based on a broken E_6 symmetry, the limits are on the order of 350 GeV.

Similar upper limits for σB have been reported by D0 [42], UA1 [43], and UA2 [44]. CDF's limit is the most stringent.

CDF has also studied the dijet channel [45], and found no statistically significant excess over QCD expectations for M_{jj} up to 930 GeV. CDF does not report an upper limit on $\sigma(p\bar{p} \to Z' \to q\bar{q})$ based on this measurement, or a lower limit on $M_{Z'}$, but it is possible to obtain such limits [46]. These limits are similar to, but somewhat weaker than, those obtained in the dilepton channel. The difference is partly because dijet mass resolution is worse than dilepton mass resolution, and partly because of uncertainties in the calculation of QCD background. This limit is nevertheless valuable because the dilepton search limits apply only to models where the Z' couples to both quarks and leptons, while the dijet search applies also to models where the Z' couples only to quarks.

2.2 Indirect search limits

2.2.1 Measurements at M_Z

In the case of the left-right symmetric model, Section 1.3.2 shows that the Z and the Z' mix—that is, that the neutral gauge boson associated with the new generator of the gauge group, and the neutral gauge boson associated with SU(2) × U(1), are not mass eigenstates of the theory. In fact, this phenomenon is general. There is no symmetry forbidding mixing, so a general analysis of Z' models must include it.

If Z_0 is the massive gauge boson of SU(2) × U(1) and Z_0' is the new massive gauge boson, their mass matrix is, in general,

$$\begin{bmatrix} Z_0 & Z_0' \end{bmatrix} \begin{pmatrix} M_{Z_0}^2 & M_{Z'Z}^2 \\ M_{Z'Z}^2 & M_{Z_0'}^2 \end{pmatrix} \begin{bmatrix} Z_0 \\ Z_0' \end{bmatrix}. \tag{2.1}$$

The physical Z and Z', however, are (by definition) mass eigenstates, with the diagonal mass matrix

$$\begin{bmatrix} Z & Z' \end{bmatrix} \begin{pmatrix} M_Z^2 & 0 \\ 0 & M_{Z'}^2 \end{pmatrix} \begin{bmatrix} Z \\ Z' \end{bmatrix}. \tag{2.2}$$

The states (Z, Z') and (Z_0, Z_0') are related by

$$Z = \cos\theta_M Z_0 + \sin\theta_M Z_0' \tag{2.3}$$

$$Z' = -\sin\theta_M Z_0 + \cos\theta_M Z_0', \tag{2.4}$$

where the mixing angle, θ_M, is determined in terms of of $M_{Z_0}^2/M_{Z_0'}^2$ and $M_{Z'Z}^2/M_{Z_0}^2$. More conveniently, it can be expressed in terms of $M_Z^2/M_{Z_0}^2$ and $M_{Z'}^2/M_{Z_0}^2$:

$$\sin^2\theta_M = \frac{M_{Z_0}^2 - M_Z^2}{M_{Z'}^2 - M_Z^2}, \tag{2.5}$$

or

$$\tan^2\theta_M = \frac{M_{Z_0}^2 - M_Z^2}{M_{Z'}^2 - M_{Z_0}^2}. \tag{2.6}$$

Generally, for $M_{Z'}^2 \gg M_Z^2$, $\theta_M \sim M_Z^2/M_{Z'}$. This is only a general statement about the magnitude of the mixing angle, however: A quantitative prediction depends on details of the Higgs sector.

The physical Z boson, then, is a mixture of the Standard Model Z_0 and the Z'. This mixing has two effects. First, it changes the mass of the physical Z boson from the mass M_{Z_0} predicted by the Standard Model[1], and second, it changes the couplings of the Z from the Standard Model values to those values plus an admixture of the Z''s couplings.

The mass shift is immediately obtained from Eq. (2.5). For $\theta_M \ll 1$ and $M_{Z'}^2/M_Z^2 \gg 1$,

$$M_{Z_0}^2 - M_Z^2 = \theta_M^2 M_{Z'}^2, \tag{2.7}$$

or

$$M_{Z_0}^2 = M_Z^2\left(1 + \theta_M^2\frac{M_{Z'}^2}{M_Z^2}\right). \tag{2.8}$$

The Standard Model relation between the W and Z masses is in terms of M_{Z_0}, not M_Z. When expressed in terms of the physical Z mass, M_Z, this relation thus acquires a correction of $\mathcal{O}(\theta_M^2 M_{Z'}^2/M_Z^2)$. Since $\theta_M \sim M_Z^2/M_{Z'}$, these corrections are of $\mathcal{O}(\theta_M)$.

In fact, it turns out that this mass shift is not as sensitive a test as might be hoped. First, the uncertainty in M_W is large enough so that, even in the absence of any theoretical difficulties, $\theta_M^2 M_{Z'}^2/M_Z^2$ would have to be on the order of 1% to have any observable effect. Second, however, and more important, this shift has exactly the same form as other corrections to M_W/M_Z, and it is difficult to disentangle the Z''s contribution from the rest. Specifically [47], it is simply an additional term in the ρ parameter, which already, in the Standard Model, receives contributions from the t quark and the Higgs boson. This effect is unobservable [48] unless $\theta_M^2 M_{Z'}^2/M_Z^2 > 0.05$, a range that is already excluded by (model dependent) limits.

[1] In some renormalization schemes, the mass of the physical Z is taken as a defining parameter of the Standard Model—that is, other masses are predicted in terms of M_Z, rather than the other way around. In these schemes, what is changed is the mass of the W predicted in terms of M_Z.

Although this upper bound on the Z-Z' mixing angle is not as stringent as those obtained by considering the effect of mixing on the Z's couplings, it has the virtue of being model-independent: Unlike every other lower bound on $M_{Z'}$, or upper bound on θ_M, it requires no assumptions at all about the Z''s couplings.

The shift in Z couplings due to mixing with the Z' provides more stringent constraints, but does require assumptions about the Z''s couplings to fermions. If the Standard Model Z_0's coupling to some fermion f is g_{z_0}, and the pure Z''s coupling is $g_{z'_0}$, then the physical Z and Z' couple with strengths

$$g_z = \cos\theta_M g_{z_0} - \sin\theta_M g_{z'_0} \tag{2.9}$$

$$g_{z'} = \sin\theta_M g_{z_0} + \cos\theta_M g_{z'_0}. \tag{2.10}$$

As an extreme illustration of the model-dependence of any limit based on this mixing, consider the "sequential" model, where the Z' has the same couplings as the Standard Model Z. Clearly, this model is completely unconstrained by such limits.

Less pathological models, however, are subject to very strong constraints. Many observables measured at LEP depend on Z couplings; the only challenge is finding combinations of observables that are independent of other corrections to the Standard Model. Two particularly useful quantities [47] are

$$\tilde{\gamma}_e \equiv \gamma_e - \frac{2}{3}\xi \tag{2.11}$$

$$\tilde{\gamma}_\nu \equiv \gamma_\nu - \frac{2}{3}\xi, \tag{2.12}$$

where γ_e and γ_ν are the normalized e^+e^- and $\nu\bar{\nu}$ partial widths,

$$\gamma_e = \frac{9}{\alpha(M_Z)}\frac{\Gamma_{e^+e^-}}{M_Z} \tag{2.13}$$

$$\gamma_\nu = \frac{9}{2\alpha(M_Z)}\frac{\Gamma_{\nu\bar{\nu}}}{M_Z}, \tag{2.14}$$

and

$$\xi = \frac{M_W^2}{M_Z^2\cos^2\theta_w}. \tag{2.15}$$

These quantities have been measured at LEP. Comparing them to the values expected in various Z' models yields [49] a limit of $|\theta_M| < 0.01$ for most models. This can be combined with the limits on $\theta_M^2 M_{Z'}^2/M_Z^2$ to obtain a model-dependent lower bound on $M_{Z'}$, which, in most models, is 100 to 150 GeV [50].

2.2.2 Low-energy measurements

Other indirect limits can be derived from low-energy experiments. At low energies, parity-violating effects would be affected both by the shift in Z couplings due to mixing with the Z', and by exchange of virtual Z's. Note that effects due to virtual Z' exchange cannot be observed on the Z resonance. Observation of these effects requires

either energies much less than or much greater than M_Z; at present, of course, only the first is an option.

Analyses of atomic parity violation [51] provide model-dependent bounds on $M_{Z'}$ and θ_M. For most models, $|\theta_M|$ is constrained to be less than a few percent, and $M_{Z'}$ to be greater than 200 or 300 GeV. This is a region of parameter space already ruled out by combining the direct search at the Tevatron with the mixing experiments at LEP.

Marciano and Sirlin [52] have found another indirect constraint, based on radiative corrections to low-energy weak interactions—specifically, radiative corrections to the four-fermion charged current contact interaction. In any model where the Z' couples differently to quarks than it does to leptons, box diagrams involving a Z' have the effect of changing the relative strength of lepton and quark four-fermion operators. This relative strength is already parameterized by the elements of the Kobayashi-Maskawa matrix, and Marciano and Sirlin show that, if corrections from Z' exchange are considered to be corrections to the Kobayashi-Maskawa matrix, they have the effect of effect of destroying its unitarity relationship. In the first row of the Kobayashi-Maskawa matrix, $|V_{ub}|$ is known to be small (see Eq. (1.24)); $|V_{ud}|$ and $|V_{us}|$ come close enough to saturating unitarity so that the unitarity constraint can be used to limit the Z''s mass and couplings. The Z_χ of SO(10), for example (see Section 1.3.3), must have a mass greater than 260 GeV. This too, however, is a mass range already ruled out by direct search at the Tevatron. Note also that this calculation cannot constrain a Z', such as the Z_ψ of E_6 (see Section 1.3.4), that couples with equal strength to all quarks and leptons.

These methods are interesting, and provide nontrivial constraints, but they are dominated by theoretical error and there is little prospect for significant improvement in the near future. It is likely that the best constraints on $M_{Z'}$ and θ_M will continue to come from collider experiments.

2.3 Future prospects

Precision measurements at e^+e^- colliders, with $\sqrt{s} > M_Z$, are expected to yield new constraints on the Z' mass and coupling. These constraints would mainly be due to the interference of the γ, Z, and Z' propagators. At LEP, where measurements are made at M_Z, this interference is negligible, but it must be included at $\sqrt{s} > M_Z$. This is discussed in more detail, in the context of studying a Z' already known to exist, in Section 4.4.

These measurements can establish a model-dependent lower bound on $M_{Z'}$ of roughly two or three times the center of mass energy at which they are made. Limits from LEP 200, then, will probably not raise the lower bound on $M_{Z'}$ by more than 100 or 200 GeV. A high-energy e^+e^- collider, with $\sqrt{s} = 500$ GeV, will be able to rule out a higher range of Z' masses, but the lower bounds on $M_{Z'}$ established by indirect experiments at such a collider are expected to be lower than those established by direct search at the LHC. The e^+e^- limits are complementary, however, in that they apply to models where the Z' couples only to leptons.

Chapter 3

Measurements at hadron colliders

3.1 Z' production and discovery

3.1.1 The parton model

At a hadron collider, Z' production proceeds through the process $q\bar{q} \rightarrow Z'$. Quark and antiquark beams are impractical, however; a hadron collider uses proton or antiproton beams. The cross section for Z' production in pp or $p\bar{p}$ collisions is calculated using the parton model.

A high-energy hadronic collision can be thought of as a collision involving quarks and gluons (generically referred to as partons), illustrated in Fig. 3.1. The partons are constituents of the incoming hadrons, and it is assumed that a collision involves one parton from each hadron, rather than either hadron as a whole. The other constituents of the hadrons do not take part in the hard scattering, but comprise the underlying event. The fundamental assumption of the parton model is that even though the constituents of hadrons are strongly bound, those partons that participate in the hard scattering may be treated as free particles; formal justification for this assumption relies on the operator product expansion [54].

If the hadrons are labelled A and B, and their momenta are p_a and p_b, then the momenta of the partons are defined to be $x_a p_a$ and $x_a p_b$, where x_a and x_b, the momentum fractions, are dimensionless numbers between 0 and 1. The probability that a parton i in hadron A has a momentum fraction x_a is denoted $f_{i/A}(x_a)$, where i can refer to a gluon or to any flavor of quark or antiquark. The parton distribution functions are normalized by the requirement that the momenta carried by the hadron's constituents add up to the hadron's momentum, or

$$\sum_i \int_0^1 dx\, x f_i(x) = 1, \tag{3.1}$$

where the sum is over all species of partons. Requiring that the sum of the electric charges of the partons equals the hadron's charge yields another such sum rule.

A hadronic cross section, in the context of the parton model, is given as the incoherent sum of the partonic contributions, where each contribution is weighted by the parton distribution function f. Specifically, for a process that proceeds only through

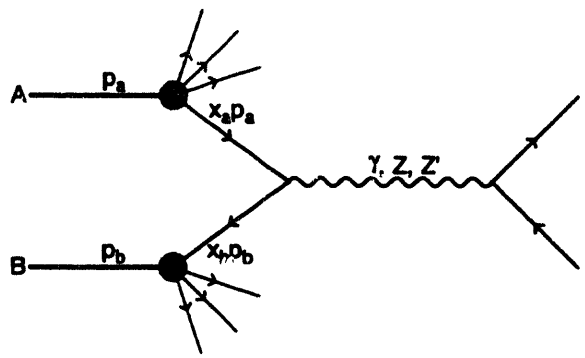

Figure 3.1: Parton model diagram of Z' production at a hadron collider. A Z' is produced by $q\bar{q}$ annihilation, where the quark and the antiquark are constituents of the initial-state hadrons. The other constituents of the initial-state particles, the underlying event, are shown schematically. Particles produced in the underlying event typically have small angles with respect to the incoming beams.

quark-antiquark annihilation, the total cross section is

$$\sigma(AB \to X) = \sum_q \int dx_a dx_b \left[f_{q/A}(x_a) f_{\bar{q}/B}(x_b) + f_{q/B}(x_b) f_{\bar{q}/A}(x_a) \right] \hat{\sigma}(q\bar{q} \to X), \quad (3.2)$$

where the sum is over all flavors of quarks, and where $\hat{\sigma}$ is the cross section for the reaction $q\bar{q} \to X$, *i.e.*, for the production of X by the annihilation of a free quark and a free antiquark with center-of-mass energy $\sqrt{\hat{s}}$, where $\hat{s} = 4x_a x_b p_a p_b$. The sum in the square brackets represents the fact that there are two possibilities for the origin of the partons: Either the quark can come from A and the antiquark from B, or the quark from B and the antiquark from A,

All of the parton distribution functions $f_i(x)$ fall to 0 as $x \to 1$. For the u and d valence quarks in a proton, $x f_{q/p}(x)$ peaks at about $x = 0.2$, while for gluons, all other quarks, and all antiquarks, $x f_{i/p}(x)$ peaks at $x = 0$. In other words, it is very unlikely that all of a proton's momentum, or even most, is carried by just one of its quarks or gluons. Most energetic parton-parton events at a hadron collider, then, take place at energies $\sqrt{\hat{s}}$ considerably lower than the center-of-mass energy of the two hadron beams.

Any calculation involving the parton model requires knowledge of the parton distribution functions $f_i(x)$. The parton distribution functions are typically extracted from fits to experiments such as deep inelastic scattering; these experiments are usually performed at relatively modest energies, so the parton distribution functions are not directly measured for very small values of x. The distribution functions for small x are obtained by extrapolation, sum rules, theoretical expectations about hadronic structure, and other methods. Similarly, due to higher-order QCD corrections [55], the parton distribution functions depend not only on x, but also on the energy, $\sqrt{\hat{s}}$, of the collision itself. Qualitatively, as $\hat{s}$ increases, the parton distribution functions become increasingly biased toward small values of x; this dependence is logarithmic in $\hat{s}$ For experiments at a different (usually higher) $\hat{s}$ than those used in the fit, the parton distribution functions must incorporate these corrections.

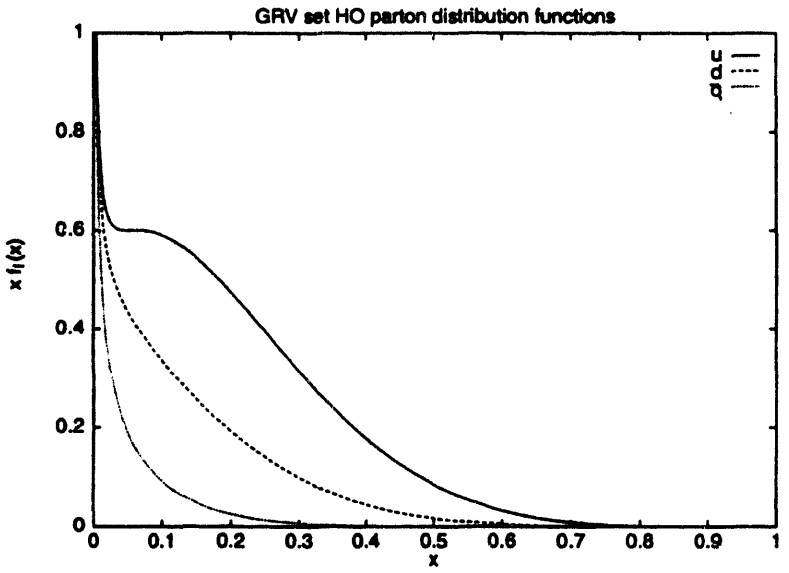

Figure 3.2: Graph of x times the parton distribution functions for u and d quarks and antiquarks in protons, using the GRV HO [61] set. The value of $\hat{s}$ used in this plot is 1 TeV, the scale relevant for Z' production at the LHC. The solid line is $xf_{u/p}(x)$, the dashed line is $xf_{d/p}(x)$, and the dotted line is either $xf_{\bar{u}/p}(x)$ or $xf_{\bar{d}/p}(x)$. In the GRV parton distribution functions, the distributions for $\bar{u}$ and $\bar{d}$ are equal. The curve peaks at $x = 0$ even for $f_{u/p}(x)$ and $f_{u/p}(x)$ because this graph includes all u and d quarks, not just the valence quarks.

Many different sets of parton distribution functions are in common use today, including EHLQ [56], Duke and Owens [57], HMRS [58], Morfin and Tung [59], DFLM [60], and GRV [61]. Each of these sets represents a different fit to experimental data and a different way of calculating the parton distribution function for values of x and $\hat{s}$ outside those that entered the fit. When performing a parton-level calculation, it is common to estimate the theoretical uncertainty due to the parton distribution functions as the range of predictions obtained when the choice of parton distribution functions is varied. As an example, the GRV (set HO) quark distribution functions are plotted in Fig. 3.2.

3.1.2 Production rates

If a Z' is discovered in the near future, discovery will almost certainly be at the CERN Large Hadron Collider (LHC), a proposed pp collider with a center of mass energy of 14 TeV[1] and a luminosity of 1.5×10^{34} cm^{-2} s^{-1}, or 150 fb^{-1}/yr. Specifically, discovery will be through the e^+e^- and $\mu^+\mu^-$ channels. In general the l^+l^- final state receives contributions from the γ, Z, and Z', but interference between the Z' and the two lighter bosons is negligible on the Z' resonance, so it suffices to consider only the Z'. The l^+l^- events arising from γ and Z can be treated as a background.

[1]The LHC was originally to have $\sqrt{s} = 17$ TeV, and most published studies of Z' production at the LHC assume that value. The change from 17 TeV to 14 TeV significantly worsens the possibilities for observation and study of a Z' at the LHC.

The cross section for $pp \to Z' \to l^+l^-$ can be estimated, in the context of the parton model, by approximating Z' production as a simple Breit-Wigner. The total cross section $\hat{\sigma}$ for $q\bar{q} \to Z' \to l^+l^-$ depends only on $\hat{s} \equiv x_a x_b s$, so the integration over the momentum fractions is particularly simple. Making the additional approximation that the proton contains only u and d quarks,

$$\sigma = \frac{12\pi^2}{M_{Z'}^2}\frac{1}{M_{Z'}}B(Z' \to l^+l^-) \times \frac{1}{9}\left[\tau\frac{d\mathcal{L}_u}{d\tau}\Gamma_{u\bar{u}} + \tau\frac{d\mathcal{L}_d}{d\tau}\Gamma_{d\bar{d}}\right], \tag{3.3}$$

where

$$\frac{d\mathcal{L}_q}{d\tau} = \int dx_a dx_b \delta(\tau - x_a x_b)\left[f_{q/p}(x_a)f_{\bar{q}/p}(x_b) + f_{q/p}(x_b)f_{\bar{q}/p}(x_a)\right], \tag{3.4}$$

$\Gamma_{u\bar{u}}$ and $\Gamma_{d\bar{d}}$ are the partial widths for $Z' \to u\bar{u}$ and $Z' \to d\bar{d}$, and and $\tau = M_{Z'}^2/s$. The factor of $1/9$ comes from the requirement that the quark and antiquark must have the same color in order to annihilate.

This expression can be rewritten as

$$\sigma = \frac{4\pi^2}{3}\frac{1}{M_{Z'}^2}B(e^+e^-)\left[\frac{\Gamma_{u\bar{u}}}{M_{Z'}} + R\frac{\Gamma_{d\bar{d}}}{M_{Z'}}\right]\tau\frac{d\mathcal{L}_u}{d\tau}, \tag{3.5}$$

where

$$R \equiv (d\mathcal{L}_d/d\tau)/(d\mathcal{L}_u/d\tau). \tag{3.6}$$

This expression is actually quite simple. In the ratio R, much of the theoretical uncertainty of the parton distributions cancels out, as does much of the energy dependence. In fact, R is typically a number of order $\frac{1}{2}$, the value one would naïvely expect from the observation that a proton in the static quark model has twice as many up quarks as down quarks. Eq. (3.5), then, consists of three factors: A model-independent overall factor that falls as $1/M_{Z'}^2$, a model-dependent combination of Z' coupling constants, and a mass-dependent factor that requires knowledge of the parton distribution functions.

With the branching ratio and widths of Section 1.4 (taking $m_t^2 \ll M_{Z'}^2$), Eq. (3.5) becomes

$$\sigma = \frac{\pi}{18}\frac{1}{M_{Z'}^2}\frac{(g_L^2 + g_e^2)\left(g_u^2 + g_Q^2 + R(g_d^2 + g_Q^2)\right)}{2g_L^2 + g_e^2 + 6g_Q^2 + 3g_u^2 + 3g_d^2}\tau\frac{d\mathcal{L}_u}{d\tau}, \tag{3.7}$$

or, in the case of SU(5)-invariant couplings,

$$\sigma = \frac{\pi}{90}\frac{\tilde{g}^2}{M_{Z'}^2}\frac{R + 2\cos^2\beta}{1 + \cos^2\beta}\tau\frac{d\mathcal{L}_u}{d\tau}. \tag{3.8}$$

The quantities $\tau d\mathcal{L}_u/d\tau$ and R can be obtained, for various choices of parton distribution functions, using the computer program PDFLIB [62]. These numbers are given in Table 3.1 for a range of Z' masses and a representative sample of parton distribution functions.

Table 3.1 and Eq. (3.8) together determine the cross section for Z' production as a function of $M_{Z'}$, $\tilde{g}$, and β. This cross section is plotted in Fig. 3.3 for several values of $M_{Z'}$, assuming that $\tilde{g}$, the Z' coupling constant, is equal to 0.15, a value typical of many models. The cross section for production of a 1 TeV Z' in $\sqrt{s} = 14$ TeV pp collisions

Table 3.1: Differential luminosity $d\mathcal{L}_u/d\tau$ and luminosity ratio R, defined in Eqs. (3.4) and (3.6), where $\tau = M_{Z'}^2/s$ and $s = (14\text{ TeV})^2$. The parton distribution functions are EHLQ 1 [56], DFLM [60], and GRV HO [61]. The Z' production cross section is on the order of $(\tau/M_{Z'}^2)d\mathcal{L}_u/d\tau$.

	EHLQ 1		DFLM		GRV	
$M_{Z'}$	$\tau d\mathcal{L}_u/d\tau$	R	$\tau d\mathcal{L}_u/d\tau$	R	$\tau d\mathcal{L}_u/d\tau$	R
1 TeV	5.25×10^{-1}	0.448	5.16×10^{-1}	0.490	5.75×10^{-1}	0.477
2 TeV	1.05×10^{-1}	0.366	9.87×10^{-2}	0.409	1.22×10^{-1}	0.375
3 TeV	2.36×10^{-2}	0.314	2.31×10^{-2}	0.365	2.86×10^{-2}	0.307
4 TeV	5.24×10^{-3}	0.273	5.68×10^{-3}	0.310	6.29×10^{-3}	0.258
5 TeV	1.06×10^{-3}	0.239	1.36×10^{-3}	0.268	1.23×10^{-3}	0.220
6 TeV	1.94×10^{-4}	0.210	3.02×10^{-4}	0.230	2.06×10^{-4}	0.190

is about 100–200 fb, which at the LHC will result in a production rate on the order of 25000 Z' events per year. Even though only a few percent of these events will have e^+e^- or $\mu^+\mu^-$ final states, this is a large enough production rate so there is no doubt that a 1 TeV Z' could be discovered at the LHC. A 2 TeV Z' is probably still observable, but 3 TeV is marginal at best, and a 4 TeV Z' is out of the question unless its couplings are much larger than those assumed for this calculation.

The leptons resulting from Z' decay are preferentially produced with a transverse momentum of $M_{Z'}/2$, as shown in Fig. 3.4; this effect is simply due to the change of variables from angular variables to the transverse momentum. As a result, it is possible to impose very stringent cuts on the leptonic transverse momentum without substantial loss of data.

The signature for a Z' candidate event at the LHC is exactly the same as at the Tevatron—an opposite-sign dilepton event where both leptons have high transverse momentum. The only difference is the scale: At the Tevatron, the transverse momentum cut is $p_\perp > 20$ GeV, but at the LHC, for $M_{Z'} \geq 1$ TeV, even a cut of 100 GeV rejects very few genuine $Z' \to l^+l^-$ events. The Z' is a narrow resonance; the Z' peak in the l^+l^- invariant mass spectrum will be quite striking if the Z' is light enough to be produced with sufficient statistics and if the detector's electromagnetic calorimeter has sufficient energy resolution to resolve the peak. Studies taking detector effects into account [63, 64, 65] suggests that it may be possible to observe a Z' as massive as 5 TeV; these studies reach such optimistic conclusions because they postulate much larger Z' couplings than the ones used for Fig. 3.3. For a 1 TeV Z', it may be possible to measure $M_{Z'}$ with a precision of 100 MeV, and $\Gamma_{Z'}$ with a precision of 200 MeV.

The maximum observable value of $M_{Z'}$ depends on the Z''s couplings to u and d quarks, but the most important limiting factor is the behavior of the parton distribution functions, which fall rapidly at large x. Production of a 5 TeV Z' at the LHC requires $x_1x_2 \sim 0.1$.

To lowest order, a Z' is produced with zero transverse momentum, but this is simply an artifact of the $\mathcal{O}(\alpha_s^0)$ calculation. The dominant production process for a Z' is

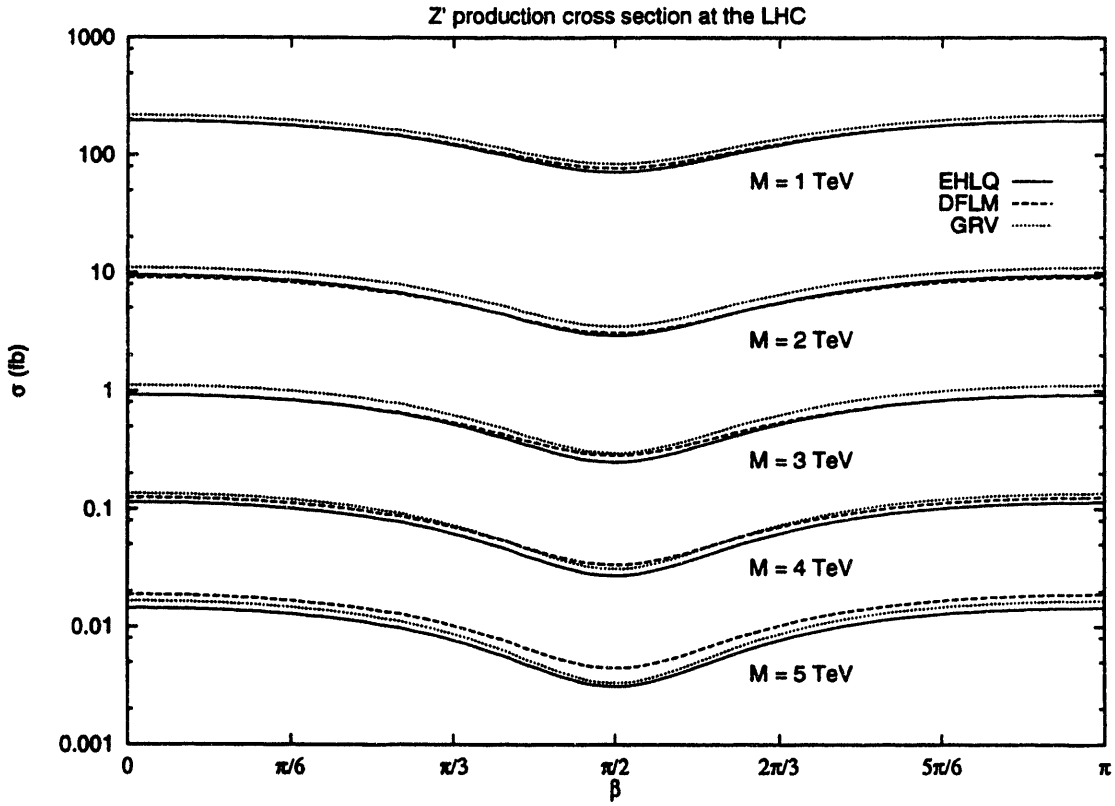

Figure 3.3: Production cross section for $pp \to Z'$ at $\sqrt{s} = 14$ TeV, calculated using Eq. (3.8) and the values in Table 3.1. The Z''s couplings are assumed to be invariant under SU(5), and β is the angle defined in Eq. (1.66). The overall coupling constant $\tilde{g}$ is taken to be 0.15. For each value of $M_{Z'}$, the calculation was performed using three different sets of parton distribution functions, EHLQ set 1 [56], drawn on this graph with solid lines, DFLM [60], drawn with dashed lines, and GRV [61], drawn with dotted lines.

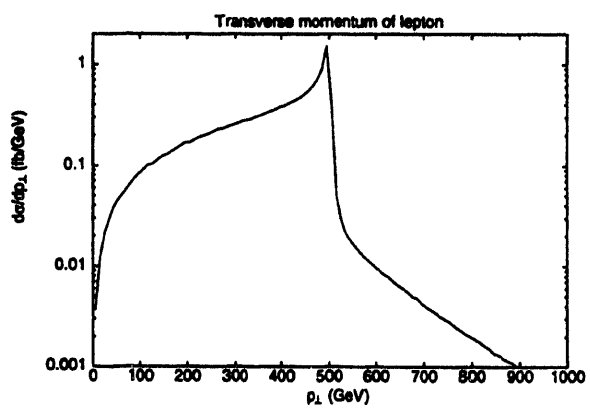

Figure 3.4: Transverse momentum spectrum for leptons produced in the reaction $pp \to Z' \to l^+l^-$, where $M_{Z'} = 1$ TeV. Note the peak at $p_\perp = M_{Z'}/2$, which comes from the Jacobian relating angular variables to transverse momenta.

quark-antiquark annihilation, which produces Z's with no transverse momentum. Higher order processes result in a Z' with nonzero transverse momentum, accompanied by one or more jets. The most important one-jet processes are $gq \to Z'q$ and $g\bar{q} \to Z'\bar{q}$; for two or more jets, many different partonic processes contribute. A Z' with finite transverse momentum, however, is no more difficult to observe than one with zero transverse momentum.

3.2 Hadronic decays of the Z'

It has been proposed [66] that, despite the enormous QCD background, it might be possible to observe the decay $Z' \to q\bar{q}$ at the LHC, and, even more optimistically, that it might be possible to distinguish $Z' \to b\bar{b}$ from $t\bar{t}$ [67]. This would be quite valuable, since measurement of the leptonic decay modes alone does not permit individual determination of the three quark coupling constants g_Q, g_u, and g_d, but only of the combination that appears in the Z' production rate.

Specifically, the proposal is to examine $d\sigma/dM_{jj}$, where M_{jj} is the invariant mass of the two jets from Z' decay. If the Z' has already been discovered in the dilepton channel, and its mass is known precisely, it might be possible to see a small increase in $d\sigma/dM_{jj}$ at $M_{jj} = M_{Z'}$.

Unfortunately, this would be an extraordinarily difficult measurement. At any hadron collider, the cross section for production of events with two or more jets is quite large: At the LHC, the cross section for dijet production with an invariant mass of 1 TeV is larger than the peak Z' cross section by a factor of at least 10^4. A set of aggressive cuts, relying mainly on the fact that the QCD dijet production cross section falls steeply as a function of the jet transverse momentum, while the transverse momentum of Z' decay products is typically on the order of $M_{Z'}/2$, can reduce this background. Even with the most optimistic possible assumptions about Z' production rates and the effects of cuts, however, direct calculation using the Monte Carlo program PAPAGENO [68] shows that the signal to background ratio at $M_{jj} = M_{Z'}$ is still at most 0.1.

An enhancement of 0.1 in the dijet cross section is not necessarily unobservable, but it is important to remember that this is the peak value of the enhancement, and that the Z' peak is quite narrow. Observation of $Z' \to q\bar{q}$ at the LHC requires a detector whose dijet mass resolution is $2\Gamma_{Z'}$ or better, an understanding of QCD background to a level much better than 10%, and high enough statistics in the region $M_{Z'} - 2\Gamma_{Z'} < M_{jj} < M_{Z'} + 2\Gamma_{Z'}$ to make a small excess statistically significant. None of these assumptions is particularly plausible.

For the remainder of this chapter, I will assume that a Z' can only be studied at the LHC through its decays to leptonic final states.

3.3 Forward-backward asymmetry

The forward-backward asymmetry has long been recognized as a useful means for studying a Z' produced in $p\bar{p}$ collisions [69]. It is also possible to define a non-zero

forward-backward asymmetry in a pp collider [36, 70], even though it is not immediately obvious how to define "forward" and "backward" in a collider where both beams consist of the same type of particle. The leptonic couplings of the Z' can be probed by measuring the forward-backward asymmetry, A_{FB}, in the e^+e^- and $\mu^+\mu^-$ modes.

Ideally one would like to define A_{FB} as the cross section for $0 < \theta < \frac{\pi}{2}$ minus the cross section for $\frac{\pi}{2} < \theta < \pi$, where θ is the angle between the l^- and the q momenta in the $q\bar{q}$ center of mass frame. Since we cannot know which proton contributed the q and which the $\bar{q}$, this does not define a measurable quantity. However, since the quark distribution function $xf_{q/p}(x)$ peaks at a higher value of the momentum fraction x than does the antiquark distribution $xf_{\bar{q}/p}(x)$, the Z''s will usually be produced with longitudinal momentum in the same direction as that of the quark. Making the approximation that the longitudinal direction of the Z' always tells us which beam contributed the quark, this allows a forward-backward asymmetry to be defined at a pp collider. This assumption is usually correct for Z's with large longitudinal momentum, but is frequently incorrect for Z's with small longitudinal momentum; the net result is that the measurable asymmetry is washed out, with the Z's produced nearly at rest providing no information.

More formally, if σ^F and σ^B are the forward and backward cross sections described above and y is the Z' rapidity, then

$$A_{FB} = \frac{\left[\int_0^{-(\ln\tau)/2} - \int_{(\ln\tau)/2}^0\right]\left[\frac{d\sigma^F}{dy} - \frac{d\sigma^B}{dy}\right]dy}{\left[\int_0^{-(\ln\tau)/2} + \int_{(\ln\tau)/2}^0\right]\left[\frac{d\sigma^F}{dy} + \frac{d\sigma^B}{dy}\right]dy}. \tag{3.9}$$

This can be related to the Z' couplings, using the unintegrated parton luminosity functions $G_q^{\pm}(y,\tau) \equiv q(x_a)\bar{q}(x_b) \pm q(x_b)\bar{q}(x_a)$, where $x_a = \sqrt{\tau}e^{+y}$ and $x_b = \sqrt{\tau}e^{-y}$. Then the asymmetry is predicted to be [36]

$$A_{FB} = \frac{3}{4}\frac{(g_L^l)^2 - (g_R^l)^2}{(g_L^l)^2 + (g_R^l)^2} \cdot \frac{\sum_q \left[(g_L^q)^2 - (g_R^q)^2\right] H_q^-}{\sum_q \left[(g_L^q)^2 + (g_R^q)^2\right] H_q^+}, \tag{3.10}$$

where the sum is over the quark flavors that contribute to Z' production, and where

$$H_q^{\pm} \equiv \left[\int_0^{-\frac{1}{2}\ln\tau} \pm \int_{\frac{1}{2}\ln\tau}^0\right] dy\, G_q^{\pm}. \tag{3.11}$$

Specializing to SU(5)-invariant couplings, and making the approximation that only u and d quarks and antiquarks are found in the proton,

$$A_{FB} = -\frac{3}{4}\cos^2 2\beta \cdot \frac{H_d^-}{H_d^+ + 2\cos^2\beta\, H_u^+}, \tag{3.12}$$

where only H_d^- appears in the numerator because a Z' with SU(5)-invariant couplings couples equally to left- and right-handed u quarks. The quantities $H_u^{\pm}$ and $H_d^{\pm}$ can easily be obtained by numerical integration of the parton distribution functions provided by

PDFLIB [62]. For a 1 TeV Z' at the LHC, and using the GRV [61] parton distribution functions, the results are

$$\begin{aligned} H_d^- &= 23.6 \\ H_d^+ &= 53.4 \\ H_u^- &= 71.9 \\ H_u^+ &= 112. \end{aligned} \tag{3.13}$$

Independent of the Z' model, A_{FB} will be reduced from its parton-level value because, for both u and d, $H_q^-/H_q^+ < 1$. In models with SU(5)-invariant couplings there is an additional suppression: Protons contain more u quarks than d quarks, but the u quark couplings of such a Z' do not contribute to its forward-backward asymmetry.

The forward-backward asymmetry, as calculated using Eq. (3.12), is shown in Fig. 3.5. The asymmetry attains its maximum absolute value at $\beta = \pi/2$, when the Z' doesn't couple to u quarks at all, but even this maximum value is rather small. Furthermore, Fig. 3.5 is only valid under the unrealistic assumption that all leptons from Z' decays, regardless of their pseudorapidities, can be used for the measurement of A_{FB}. This is particularly important because the events that contribute the most to A_{FB} are those where the Z' has substantial longitudinal momentum, and those are precisely the events where the Z''s leptonic decay products are likely to have so much longitudinal momentum that at least one of them falls outside the pseudorapidity coverage of the detector. A more realistic assumption is that the only usable events are those where both the l^+ and the l^- satisfy the requirement $|\eta| < \eta_{\max}$, where the value of $\eta_{\max}$ depends on the details of the detector. The maximum absolute value of A_{FB} will be reduced by about 40% even assuming $\eta_{\max} = 5$.

The statistical error in a measurement of A_{FB} is roughly $1/\sqrt{N}$, where N is the number of events used in the measurement. Assuming a sample of 25000 Z' events of which 10% decay into e^+e^- or $\mu^+\mu^-$, the statistical error will be approximately 2%. Since even the maximum possible value of A_{FB} is rather small, however, the relative error, $\delta A_{FB}/A_{FB}$, will be quite large. Note also that theoretical interpretation of a measurement of A_{FB} will be difficult. The forward-backward asymmetry is determined by a rather complicated combination of couplings to leptons, u quarks, and d quarks, and it depends on quantities, $H_u^\pm$ and $H_d^\pm$, that are obtained by integrating the parton distribution functions. Only the ratios of $H_u^\pm$ and $H_d^\pm$ enter into the expression for A_{FB}, so much of the theoretical uncertainty in the parton distribution functions will cancel out, but, as can be seen from the range of values for R in Table 3.1, some uncertainty exists even in ratios.

3.4 Tau polarization asymmetry

3.4.1 Definition of A_{pol}

Despite the unobserved neutrinos from τ decay, it is also possible to study the polarization asymmetry A_{pol}, that is, the asymmetry in $Z' \to \tau^+\tau^-$ between production

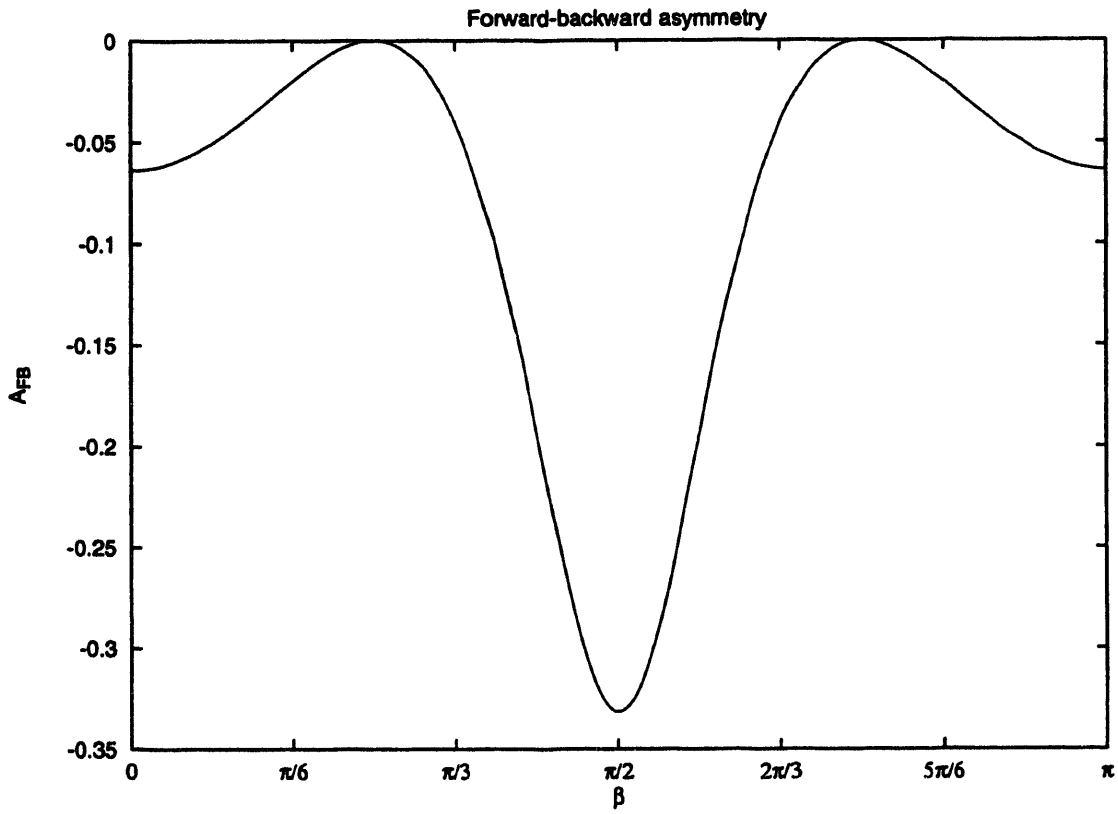

Figure 3.5: Forward-backward asymmetry A_{FB} in $pp \to Z' \to l^+l^-$, as a function of β, for a Z' with SU(5)-invariant couplings. The expression for A_{FB} as a function of β, Eq. (3.12), depends on quantities obtained by integrating parton distribution functions. This plot uses the GRV [61] parton distribution functions, and assumes $M_{Z'} = 1$ TeV and $\sqrt{s} = 14$ TeV. See text for the definition of A_{FB} at a pp collider.

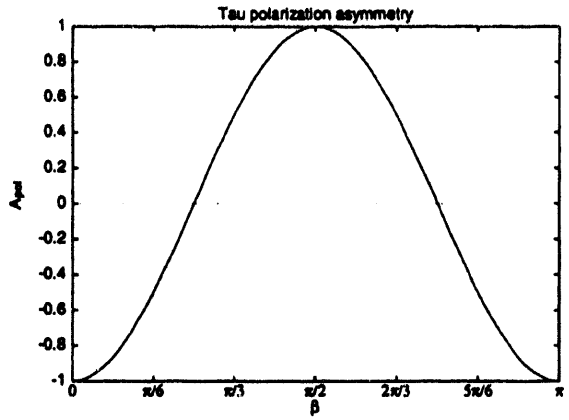

Figure 3.6: Polarization asymmetry in the decay $Z' \to \tau^+\tau^-$, for a Z' with SU(5)-invariant couplings. Note that $A_{\rm pol}$ may have any value within the range $(-1, 1)$, and that it depends strongly on β, as defined in Eq. (1.66). Even an imprecise measurement of $A_{\rm pol}$ provides useful information about β.

of left-handed and right-handed τ^- leptons [71]. If σ_L is the production cross section for τ_L^- and σ_R the production cross section for τ_R^-,

$$A_{\rm pol} = \frac{\sigma_L - \sigma_R}{\sigma_L + \sigma_R}. \tag{3.14}$$

The decay of the τ proceeds through the weak interaction, which violates parity. Left-handed and right-handed τs thus have different decay properties, and it is possible to distinguish them on a statistical basis. This method has been used to study Z couplings at LEP [72]. There are additional complications at a hadron collider, but they are not prohibitive.

In general, measurement of a polarization asymmetry for the production of some fermion f requires that f decay within the detector, that the decays of f_L and f_R be distinct, and that f's decays be both measurable and theoretically well understood. For the purpose of studying a Z' at a hadron collider, the only fermion f that meets these requirements is the τ.

Unlike A_{FB}, which depends on both the quark and lepton couplings, $A_{\rm pol}$ depends only on the Z''s couplings to the τ. Assuming universality, and using the notation of Section 1.4,

$$A_{\rm pol} = \frac{g_L^2 - g_e^2}{g_L^2 + g_e^2}. \tag{3.15}$$

The τ polarization asymmetry does not depend on the Z''s couplings to u or d quarks, or on the parton distribution functions, but only on g_e^2/g_L^2. For a Z' with SU(5)-invariant couplings,

$$A_{\rm pol}(\beta) = -\cos 2\beta. \tag{3.16}$$

This is shown in Fig. 3.6. Note that it depends strongly on β; even an imprecise measurement of $A_{\rm pol}$ provides a reasonably precise measurement of g_e^2/g_L^2.

3.4.2 Decays of the τ lepton

The matrix element for the decay $\tau^- \to \nu_\tau X^-$ is

$$\mathcal{M} = \frac{G_F}{\sqrt{2}} J^\mu_{(\tau)} J_\mu, \tag{3.17}$$

where

$$J^\mu_{(\tau)} = \bar{\nu}(\mathbf{p}_\nu)\gamma^\mu(1-\gamma_5)\tau(\mathbf{p}_\tau, s_\tau) \tag{3.18}$$

and

$$J^\mu = \langle X|J^\mu_{cc}|0\rangle. \tag{3.19}$$

When $X = e\bar{\nu}_e$ or $\mu\bar{\nu}_\mu$, the final state matrix element J^μ is completely calculable. Even for some simple hadronic states, however, J^μ can be determined up to an overall normalization. In fact, it turns out that these well-understood decays have a branching ratio [8] of about 80%.

The quantity that depends on the τ's polarization is the angular distribution of the τ's decay products in the τ's rest frame. For a relativistic τ, an equivalent quantity, more directly related to experimental measurements, is the distribution in x, the visible momentum fraction. The visible momentum fraction is defined as $x \equiv p_{\rm vis}/p_\tau$, where $p_{\rm vis}$ and p_τ are respectively the momenta of the visible decay products and the decaying τ, both measured in the lab frame. The visible decay products are defined to be all decay products except for neutrinos.

Tsai [73] discussed τ decays in detail more than 20 years ago, before the τ was even discovered, and expressions for the decay of a polarized τ in terms of the visible momentum fraction x have been obtained [74] for most simple decay modes.

The τ^- decays into $e^-\bar{\nu}_e\nu_\tau$ and $\mu^-\bar{\nu}_\mu\nu_\tau$ with the same branching ratio—about 17%. The calculation is identical to that for μ decay. There are no theoretical ambiguities, and

$$J^\mu = \bar{l}(\mathbf{p}_l)\gamma^\mu(1-\gamma_5)\nu(\mathbf{p}_\nu). \tag{3.20}$$

From this, it is straightforward to derive the normalized decay distributions for left- and right-handed τ^-s,

$$\left(\frac{1}{\Gamma}\frac{d\Gamma}{dx}\right)_L = \frac{4}{3}(1-x^3) \tag{3.21}$$

$$\left(\frac{1}{\Gamma}\frac{d\Gamma}{dx}\right)_R = 2(1-3x^2+2x^3). \tag{3.22}$$

These two decay distributions, unfortunately, have very little discriminating power; one way to understand this is that the polarization information contained in the angular distributions is diluted by the integral over the momenta of two neutrinos. Distinguishing Γ_L from Γ_R for leptonic decays will require very high statistics.

The τ^- decays into $\pi^-\nu_\tau$ about 11% of the time. The only possible Lorentz structure for J^μ in this case is

$$J^\mu \propto k^\mu, \tag{3.23}$$

where k is the momentum of the pion. Neglecting terms of $\mathcal{O}(m_\pi^2/m_\tau^2)$, this gives the very simple relations

$$\left(\frac{1}{\Gamma}\frac{d\Gamma}{dx}\right)_L = 2(1-x) \tag{3.24}$$

$$\left(\frac{1}{\Gamma}\frac{d\Gamma}{dx}\right)_R = 2x. \tag{3.25}$$

Some multi-hadronic decays are also calculable. The data are consistent with the assumption that the two- and three-π final states are dominated by single hadronic resonances [75], the most common of which are the vector decay, $\rho\nu_\tau$, and the axial vector decay, $a_1(1260)\nu_\tau$. If the ρ or a_1 is treated as a unit, and the pions are not distinguished, the Lorentz structure of J_μ is again completely determined up to a constant of proportionality:

$$J_\mu \propto \epsilon_\mu^* f(M^2), \tag{3.26}$$

where ϵ is the polarization vector, and M^2 the mass squared, of the resonance. In the approximation where the form factor f is taken to be constant, the normalized decay distributions are

$$\left(\frac{1}{\Gamma}\frac{d\Gamma}{dx}\right)_L = \frac{2}{2\zeta^3-3\zeta^2+1}\left[(1-2\zeta^2)-(1-2\zeta)x\right] \tag{3.27}$$

$$\left(\frac{1}{\Gamma}\frac{d\Gamma}{dx}\right)_R = \frac{2}{2\zeta^3-3\zeta^2+1}\left[(\zeta+(1-2\zeta)x)\right], \tag{3.28}$$

where $\zeta = M^2/m_\tau^2$, and kinematics require $\zeta \le x \le 1$.

Because both the ρ and the a_1 are wide resonances, it is inappropriate to treat ζ as a fixed parameter; it is, instead, necessary to convolve these distributions with the appropriate line shapes. Making the assumption that the ρ and a_1 are simple Breit-Wigner resonances with the measured masses and widths, the smeared distributions are shown in Figs. 3.7 and 3.8. The two distributions for the a_1 are so similar that this mode is unlikely to be useful, except as a trigger. The two distributions are more distinct in the case of ρ decay, but, unfortunately, it is difficult experimentally to distinguish the ρ's from the a_1's decay products. At the LHC, none of the τ's multihadronic decays are likely to be useful for measuring τ polarizations.

The τ_L^- and τ_R^- decay spectra are most distinct for the decay $\tau^- \to \pi^-\nu$. The observed spectrum dN/dx for $\tau \to \pi\nu$, where x is the visible momentum fraction, is the weighted sum of $(dN/dx)_L = 2(1-x)$ and $(dN/dx)_R = 2x$; a one-parameter fit determines the coefficient of this sum, hence the polarization asymmetry. Note that the background for $\tau \to \pi\nu$ is likely to be lower than for the other decay modes: There are very few plausible sources of high-energy isolated pions.

It is likely, then, that only the 20% of $\tau^+\tau^-$ events where at least one τ decays to $\pi\nu$ can be used for measurement of the polarization asymmetry. The other τ decay modes may still be useful, however, in distinguishing $\tau^+\tau^-$ events from background.

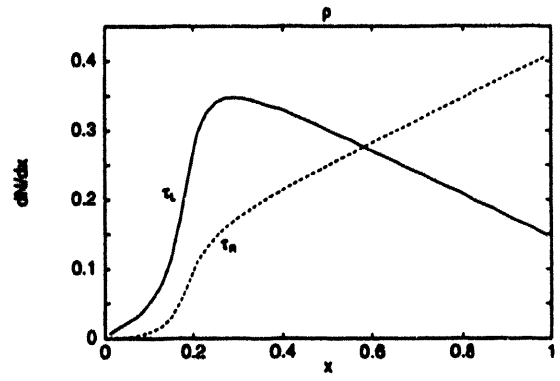

Figure 3.7: The decay distributions $\frac{1}{\Gamma}\frac{d\Gamma}{dx}$ for left- and right-handed τ^-s decaying into $\rho\nu_\tau$, normalized to the branching ratio of this decay mode. The distributions have been smeared to account for the finite width of the ρ. The solid line is the distribution for $\tau_L^- \rightarrow \rho^-\nu_\tau$, and the dashed line is the distribution for $\tau_R^- \rightarrow \rho^-\nu_\tau$.

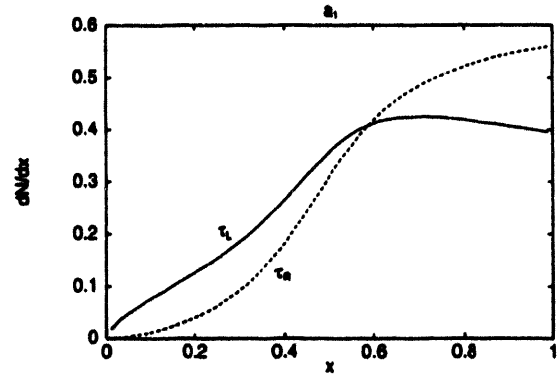

Figure 3.8: The decay distributions $\frac{1}{\Gamma}\frac{d\Gamma}{dx}$ for left- and right-handed τ^-s decaying into $a_1\nu_\tau$, normalized to the branching ratio of this decay mode. The distributions have been smeared to account for the finite width of the a_1. The solid line is the distribution for $\tau_L^- \rightarrow a_1^-\nu_\tau$, and the dashed line is the distribution for $\tau_R^- \rightarrow a_1^-\nu_\tau$.

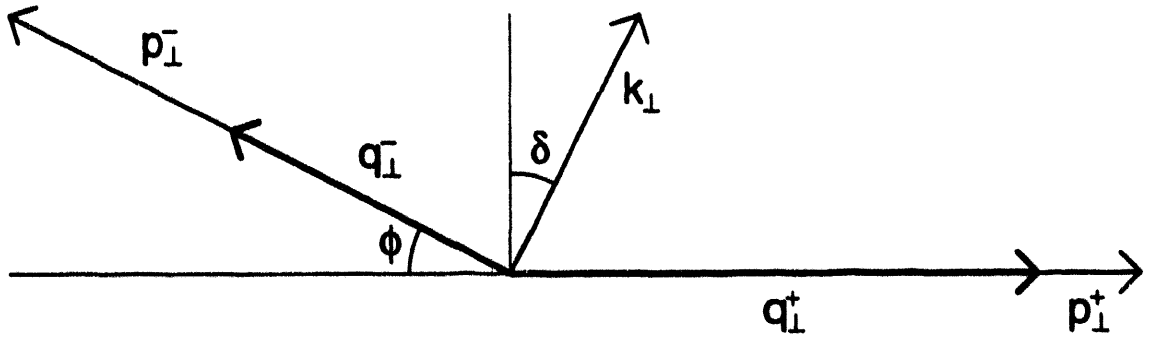

Figure 3.9: Diagram of a $Z' \to \tau^+\tau^-$ event. The transverse momenta of the τ^+ and the τ^- are $\mathbf{p}_\perp^\pm$, and $\mathbf{q}_\perp^\pm$ are the transverse momenta of the "visible" τ decay products—that is, all of the decay products other than the neutrinos. The visible momentum fraction, x, is defined by $p^\pm = x_\pm p^\pm$. The observable quantities are $\mathbf{q}_\perp^\pm$ and $\mathbf{k}_\perp$, where $\mathbf{k}_\perp$ is the transverse momentum of the Z'. The angle ϕ is constrained to lie in the range $0 \le \phi \le \pi$.

3.4.3 Reconstruction of τ momenta

The visible momentum fraction x is defined in terms of the τ's momentum and the momentum of its visible decay products. Because at least one of a τ's decay products is always a neutrino, the momentum of a τ is not a directly observable quantity. A $Z' \to \tau^+\tau^-$ event, however, is sufficiently constrained that is it possible to reconstruct the momenta of both τs.

For all but a small fraction ($\mathcal{O}(m_\tau/E_\tau)$) of events, a τ and its decay products are essentially collinear in a frame where its momentum is much greater than its mass. In such a frame,

$$q^\pm = x_\pm p^\pm, \tag{3.29}$$

where p is the momentum of the τ, q is the total momentum of all of the τ's decay products except for the neutrino, and x is the "visible" momentum fraction, that is, the fraction of the τ's momentum contained in decay products which are observable through tracking and calorimetry.

If a $\tau^+\tau^-$ pair is known to be the product of a Z' decay, it must satisfy two constraints. Since the width of the Z' is expected to be small compared to its mass, the invariant mass of the $\tau^+\tau^-$ system must equal $M_{Z'}$, assumed to be a known quantity. Similarly, measuring jets not part of the τ decay and demanding transverse momentum balance yields the transverse momentum of the Z'. These constraints, using the notation defined in Fig. 3.9, are

$$\left(\frac{1}{x_+}q^+ + \frac{1}{x_-}q^-\right)^2 = M_{Z'}^2 \tag{3.30}$$

$$\frac{1}{x_+}\mathbf{q}_\perp^+ + \frac{1}{x_-}\mathbf{q}_\perp^- = \mathbf{k}_\perp, \tag{3.31}$$

where $\mathbf{k}_\perp$ is the transverse momentum of the Z'. These equations uniquely determine x_+ and x_-.

For simplicity, first consider the special case where $\mathbf{k}_\perp = 0$. Eqs. (3.30) and (3.31) immediately yield

$$x_+ x_- = (2q^+ \cdot q^-)/M_{Z'}^2, \tag{3.32}$$

$$x_+/x_- = q_\perp^+/q_\perp^-. \tag{3.33}$$

In the case where $k_\perp \neq 0$, the situation is more complicated. There are three constraints but only two unknown parameters, and the problem is overdetermined. In principle, it would be possible to determine x_+ and x_- using any two of these equations (or some combination) and to use the remaining information as a consistency check. In the presence of experimental error, however, the most practical way to determine x_+ and x_- consistently is simply to make them part of the fit that determines experimental quantities. That is, $q^\pm$, $x_\pm$, and $\mathbf{k}_\perp$ are to be chosen such that χ^2 is minimized, subject to the constraints of Eqs. (3.30) and (3.31). It is cumbersome to express the results of this procedure in closed form, but there are no conceptual difficulties in performing it.

If the minimum value of χ^2 is unacceptably large for some event, or if it minimized for unphysical values of $x_\pm$, then the event can be rejected as inconsistent with $Z' \to \tau^+\tau^-$. A simpler consistency condition, which is useful for the study of background, can be obtained by noticing that if $k_\perp = 0$, the τs must be collinear; more generally, the degree of acollinearity yields a minimum value for $k_\perp$. If ϕ is the angle of acollinearity,

$$k_\perp \geq 2\sqrt{\frac{q_\perp^+ q_\perp^-}{x_+ x_-}} \sin\frac{\phi}{2}. \tag{3.34}$$

3.4.4 Background

Background is not a serious obstacle to discovery of the Z' at a hadron collider through its decay into e^+e^- and $\mu^+\mu^-$, or to the study of A_{FB} in those modes: The invariant mass of the e^+e^- system will stand out above any likely background. For the study of $\tau^+\tau^-$ pairs, however, this is no longer true. The τ^+ and τ^- themselves are unobservable, so an event must be identified as a $Z' \to \tau^+\tau^-$ event by some means other than its invariant mass.

As discussed in Sec. 3.1, the Z' decay products have a very high transverse momentum, peaking at $p_\perp = M_{Z'}/2$. The transverse momenta of the τs' decay products is less than this, but it is still possible to impose very stringent cuts on transverse momenta without rejecting a very large fraction of genuine $Z' \to \tau^+\tau^-$ events. The most serious backgrounds, after such cuts, are $t\bar{t}$ pairs, conventional Drell-Yan production of $\tau^+\tau^-$ pairs, and possibly jet misidentification.

There is no reliable way to estimate the rate of jet misidentification in advance of experiment; this rate depends both on parton fragmentation functions at very high energies, and on the tracking and calorimetry capabilities of LHC detectors. The QCD cross section for dijet production at a high-energy hadron collider, however, is enormous, and if any appreciable fraction of jets can mimic single isolated pions, measuring $A_{\rm pol}$ at the LHC may be impossible.

The cross section for production of $t\bar{t}$ at the LHC will be extremely large. Taking $m_t = 175$ GeV, direct calculation using PAPAGENO [68] and the EHLQ 1 parton distribution functions [56] shows it to be about 800 pb. Even after requiring that both t quarks decay to τ and imposing a $p_\perp$ cut of 100 GeV on both τs, the cross section is still 200 fb, which is on the same order as the production cross section for a 1 TeV Z'. After requiring that at least one τ have $p_\perp > 200$ GeV, the cross section is 50 fb. Further cuts are still necessary if the $Z' \to \tau^+\tau^-$ mode is to be useful.

It is likely, however, that these further cuts can be found. Top events differ from Z' events in three crucial ways. First, all $t\bar{t}$ events contain two b quarks, which, if b jets can be identified as such, may be used to discard these events. Second, the invariant mass of a t quark's decay products must be less than m_t; in particular, if a t decays into $b\tau\bar{\nu}_\tau$, then $M^2_{\tau b} < m_t^2 - M_W^2$, where $M_{\tau b}$ is the invariant mass of the τ and the b. For $m_t = 175$ GeV, this is 155 GeV. Third, the momenta of the τs' visible decay products in a genuine $Z' \to \tau^+\tau^-$ event must satisfy a consistency condition, Eq. (3.34), which, in general, will not be satisfied by the τs produced by the decay of a $t\bar{t}$ pair.

Tagging of b jets at hadron colliders through observation of a secondary vertex has already been demonstrated at the Tevatron; at the LHC, where the b quarks will be more energetic and their decay lengths greater, b tagging should be easier. Rejecting events with tagged b jets may [64] reduce $t\bar{t}$ background by up to a factor of 2. Similarly, the consistency condition of Eq. (3.34) will provide roughly another factor of 2 [71]. The effectiveness of the $M_{\tau b}$ cut depends on the detector's jet momentum resolution, and also on the jet multiplicity in Z' production at the LHC. If Z' events tend to have a high jet multiplicity then an overly aggressive $M_{\tau b}$ cut will reject genuine Z' events, because even a genuine $Z' \to \tau^+\tau^-$ event will be likely to have a jet such that $M_{\tau,\text{jet}}$ is fairly small.

Optimization of these cuts will have to wait until the properties of leptonic Z' decays have been studied in the e^+e^- and $\mu^+\mu^-$ channels, but it is plausible that these cuts, or others, can reduce the $t\bar{t}$ background sufficiently.

Drell-Yan events, finally, are events with a high-$p_\perp$ $\tau^+\tau^-$ pair produced by a virtual γ or Z; they are essentially the same process as $Z' \to \tau^+\tau^-$. The only kinematic distinction between $Z' \to \tau^+\tau^-$ events and conventional Drell-Yan events is the invariant mass of the τ pair, which is not an observable quantity.

Conventional Drell-Yan events are peaked at low transverse momentum, and a 100 GeV $p_\perp$ cut reduces their contribution to about 20% of the Z' cross section. The remaining Drell-Yan events have essentially the same kinematics as $Z' \to \tau^+\tau^-$ events. They are an irreducible background, and must be dealt with by subtracting the Drell-Yan cross section as measured in the e^+e^- and $\mu^+\mu^-$ channels.

3.4.5 Evaluation of discriminating power

If it actually is possible to obtain a clean sample of $Z' \to \tau^+\tau^-$ events where at least one τ decays to $\pi\nu$, then measuring the spectrum dN/dx corresponds to measuring the average τ polarization A_{pol}. The measured spectrum is a sum of the left-handed and

right-handed $\tau \to \pi\nu$ decay spectra, both of which are linear. Specifically,

$$\frac{dN}{dx} = \frac{1+A_{\rm pol}}{2}(2(1-x)) + \frac{1-A_{\rm pol}}{2}(2x) \tag{3.35}$$

$$= 1 + A_{\rm pol} - 2xA_{\rm pol}. \tag{3.36}$$

Generally, if a distribution $g(x)$ depends on a parameter c, the value of c can be extracted from the measured distribution by means of a maximum likelihood analysis. This analysis will have an uncertainty [76]

$$\Delta c = \frac{1}{\sqrt{N}}\left[\int dx\, \frac{1}{g}\left(\frac{dg}{dc}\right)^2\right]^{-1/2}. \tag{3.37}$$

Applying this to the case at hand,

$$\Delta A_{\rm pol} = \frac{1}{\sqrt{N}}\sqrt{2}A_{\rm pol}^{3/2}\left(\ln\frac{1+A_{\rm pol}}{1-A_{\rm pol}} - 2A_{\rm pol}\right)^{-1/2}. \tag{3.38}$$

For most values of $A_{\rm pol}$, $\Delta A_{\rm pol} \approx 1.5/\sqrt{N}$.

At the LHC, as discussed in Section 3.1.2, the rate for the production of a 1 TeV Z' is on the order of 25000 per year. Assuming that the branching ratio to $\tau^+\tau^-$ is 5%, that in 20% of $\tau^+\tau^-$ events at least one τ will decay to a pion, and that, because of cuts, only half of these events will be usable, this leaves only about 120 events for this measurement. The error in $A_{\rm pol}$, then, will be 15%.

This is significantly worse than the precision with which A_{FB} can be measured, but $A_{\rm pol}$ is inherently a more sensitive test of Z' couplings. The forward-backward asymmetry is restricted to the range $(-0.3, 0)$, while the polarization asymmetry can attain any value between -1 and 1. Both measurements will be needed in order to measure the Z' couplings to both quarks and leptons.

3.5 Rare Z' decay modes

The Z-Z' mixing angle, θ_M, is already known to be small; the upper bounds, obtained from measurements at LEP, are discussed in Section 2.2.1. If a Z' is discovered, θ_M may be determined by measuring the branching ratio for rare Z' decays that can only proceed if θ_M is nonzero.

One particularly useful rare decay mode is $Z' \to W^+W^-$ [77]. This decay would be forbidden if there were no Z-Z' mixing, since the W's couplings are just those of an SU(2) gauge boson. For finite Z-Z' mixing, however, the Z' has an admixture of Z couplings, so this decay proceeds via the trilinear ZWW term in Eq. (1.11), which, in turn, is due to the trilinear SU(2) gauge boson self-interaction found in a pure Yang-Mills theory.

The decay $Z' \to W^+W^-$ is suppressed by a factor of θ_M^2, but it is enhanced by a factor of $M_{Z'}^4/M_W^4$ due to interactions between the longitudinal components of the

gauge bosons, and the branching ratios may, for θ_M sufficiently large, be large enough to be observable.

The background for this mode is substantial: The production cross section at the LHC for W^+W^- pairs, calculated using PAPAGENO [68], is almost 50 pb. In most $Z' \to W^+W^-$ events, however, the W^+ and W^- have very high transverse momenta, while the transverse momentum of W^+W^- pairs from direct electroweak production peaks at small values. A 200 GeV $p_\perp$ cut on the transverse momentum of both members of the W pair reduces the background by a factor of about 70. The W^+W^- pairs from Z' decay have other distinctive kinematic properties as well, and several studies [78] have concluded that they can probably be distinguished from the background due to electroweak W^+W^- pair production, at least in the channel where both Ws decay leptonically.

Unfortunately, these studies were all performed at a time when it was assumed that the t quark was lighter than the W; we now know that $m_t > M_W$. A t quark decays to bW with essentially probability 1, so $t\bar{t}$ is another source of W^+W^- pairs. In fact, since $t\bar{t}$ pairs are produced by QCD, this is the dominant source of W^+W^- pairs: As discussed in Section 3.4.4, the production cross section for $t\bar{t}$ pairs is more than ten times that for direct electroweak W^+W^- pair production. Although it is possible to reduce this background somewhat by b tagging, it is unlikely that it could be reduced sufficiently so that the rare decay $Z' \to W^+W^-$ could be observed.

The rare decay $Z' \to l^\pm \nu_l W^\mp$ may be observable at the LHC [79, 80] despite the $t\bar{t}$ background, but this decay is less interesting theoretically. It results from an ordinary $Z' \to l^+l^-$ event where one of the leptons produces a $W^\pm$ by final-state bremsstrahlung and turns into a ν_l. Because the W couples only to the left-handed component of the charged lepton, this branching ratio is an indirect measurement of the l^+l^- polarizations, and thus, like A_{pol}, provides information about g_e^2/g_L^2. It does not, however, provide any information about θ_M.

Chapter 4

Study of a Z' at future lepton colliders

4.1 Production of Z' bosons in e^+e^- collision

4.1.1 Corrections to the cross section

To first approximation, the line shape for the Z' production cross section is a simple Breit-Wigner:

$$\sigma(e^+e^- \to Z') = \frac{12\pi}{s} B(Z' \to e^+e^-) \frac{\Gamma^2/4}{\left(\sqrt{s} - M_{Z'}\right)^2 + \Gamma^2/4}. \tag{4.1}$$

Several corrections, however, render this a poor approximation.

The most important correction is the essentially classical phenomenon of initial-state radiation of photons from the incident beams. Although this is a purely electromagnetic effect, and is thus suppressed by a factor of α, it is nonetheless significant because it is enhanced by a factor of $\ln(M_{Z'}^2/m_e^2)$, representing the presence of two very different energy scales. Using the formalism of Kuraev and Fadin [81], it is possible to sum all orders of initial-state radiation by performing a single integral:

$$\sigma(s) = t \int_0^{\sqrt{s}/2} dk \left[\frac{1}{k} \left(1 + \frac{3t}{4}\right) \left(\frac{2k}{\sqrt{s}}\right)^t - \frac{2}{\sqrt{s}} \left(1 - \frac{k}{\sqrt{s}}\right) \right] \sigma_0 \left[\left(\sqrt{s} - k\right)^2 \right], \tag{4.2}$$

where

$$t = \frac{2\alpha}{\pi} \left(\ln\left(\frac{M_{Z'}^2}{m_e^2}\right) - 1 \right), \tag{4.3}$$

and where σ_0 is the cross section in the absence of initial-state radiation. For a Z' of mass 500 GeV, $t \approx 0.13$.

The first term in the integral is the result of summing all orders of soft photon emission, while the second is due to single-photon hard bremsstrahlung, and turns out to be negligible when σ_0 is sharply peaked. When σ_0 is a Breit-Wigner, in fact, it is possible

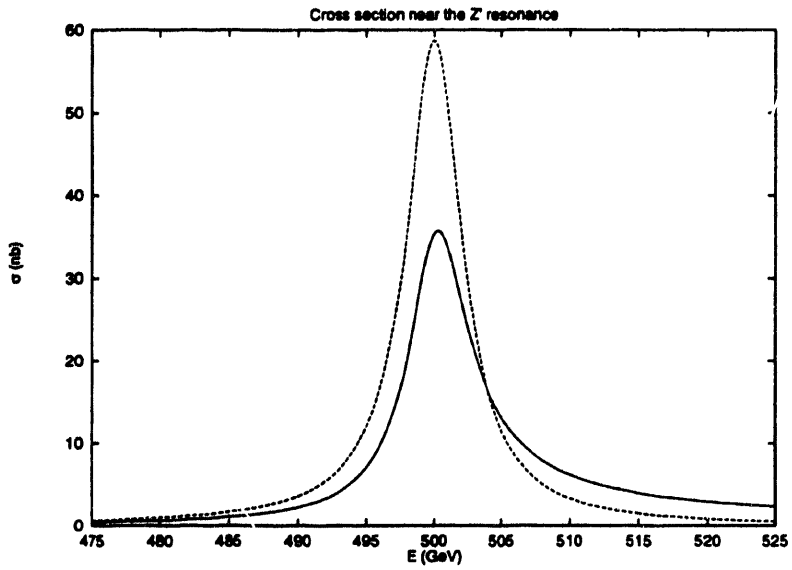

Figure 4.1: Cross section for e^+e^- production of a Z' near resonance, setting $B(Z' \to e^+e^-) = 1$. The solid line includes the effects of initial-state radiation, and the dashed line is an unmodified Breit-Wigner. The Z' is taken to have a mass of 500 GeV, and a width of 5 GeV.

to do the integral analytically, yielding [82]

$$\sigma(s) = \left(1 + \frac{3t}{4}\right)\left(\frac{\Gamma_{Z'}}{\sqrt{s}}\right)^t \Phi\left(2\frac{\sqrt{s} - M_{Z'}}{\Gamma}\right)\sigma_0(M^2_{Z'}), \tag{4.4}$$

where

$$\Phi(\lambda) \equiv \frac{\pi t}{\sin \pi t}(1+\lambda^2)^{(t-1)/2} \sin\left[(1-t)\cos^{-1}\frac{-\lambda}{\sqrt{1+\lambda^2}}\right]. \tag{4.5}$$

This effect is familiar from studies at the Z resonance, where it leads to a 26% reduction in the maximum value of the cross section. In the case of the Z', where t is larger and where, in most models, Γ/M is smaller, this effect is even more significant. The effect of initial-state radiation is shown in Fig. 4.1.

What is actually observed, however, is not the cross section σ, but rather an effective cross section obtained by convolving σ with a collider's energy distribution. At future e^+e^- colliders, this distinction is expected to be significant: At high energies and luminosities, when an electron and a positron bunch collide, the electromagnetic field from one bunch causes the particles in the other bunch to radiate. This effect, known as "beamstrahlung" [83], causes a broadening of the effective beam energy spectrum. In extreme cases, beamstrahlung can lead to the sort of broad-band distribution function more familiar in hadron colliders than in e^+e^- colliders, but most modern designs for high-energy linear e^+e^- colliders yield a relatively narrow spectrum, where almost all particles have an energy close to the nominal energy of the machine.

The beamstrahlung spectrum depends on two parameters, the effective "beamstrahlung parameter" Υ_{eff}, a dimensionless measure of the beam's average magnetic field, and σ_z, the length of a bunch in the lab frame. If a beam's energy spectrum, in the

absence of beamstrahlung, is a sharp delta function at E', then the approximate effect of beamstrahlung is to modify this to [84]

$$\psi_{E'}(E) = \frac{1}{N_c}\left((1-e^{-N_c})\delta(E'-E) + \frac{e^{-\eta(E/E')}}{E'-E}\bar{h}\left(\eta(E/E')\right)\right), \tag{4.6}$$

where

$$\eta(x) \equiv \frac{2}{3\Upsilon_{eff}}\left[\frac{1}{x}-1\right], \tag{4.7}$$

$$\bar{h}(\eta) \equiv \sum_{n=1}^{\infty}\frac{\gamma(n+1,N_c)}{n!\Gamma(n/3)}\eta^{n/3}, \tag{4.8}$$

the classical number of photons N_c radiated per particle in traversing an opposing bunch is given by

$$N_c = \frac{5}{2}\alpha^2\frac{\sigma_z}{r_e}\frac{m_e}{E'}\Upsilon_{eff}, \tag{4.9}$$

and m_e and r_e are the electron mass and the classical electron radius. The actual energy spectrum is time dependent: The energy spectrum of a bunch is modified during its traversal of the opposing bunch. The expression in Eq. (4.6) is a time average, defined by

$$\psi(E) = \frac{2}{L}\int_0^{L/2} dt\,\psi(E,t), \tag{4.10}$$

where L is the length of each bunch. If the longitudinal beam profile is gaussian, the effective bunch length is $L = 2\sqrt{3}\sigma_z$.

Although Eq. (4.6) is strictly valid only for $\Upsilon_{eff} \ll 1$, it provides a reasonable approximation to the gross features of the beamstrahlung spectrum even for $\Upsilon_{eff} \sim 1$ [85]. A fully realistic prediction would, in any case, require detailed machine-dependent calculations that take into account the measured beam shape and linac energy spread.

A beam's electromagnetic field varies depending on the transverse position within the beam; properly, it is necessary to perform an integral over the transverse (x-y) plane. The parameter Υ_{eff} is an effective field strength resulting from such an integral [84], and has the value

$$\Upsilon_{eff} \approx \frac{5}{6}\frac{E_0}{m_e}\frac{r_e^2 N}{\alpha\sigma_z(\sigma_x+\sigma_y)}, \tag{4.11}$$

where E_0 is the nominal beam energy, N is the number of particles per bunch, and σ_x and σ_y are the widths of the beam in the transverse plane. Eq. 4.11 relies on the assumption that the beam shape is gaussian in both x and y, but it is not necessary to assume that $\sigma_x = \sigma_y$.

Even in the absence of beamstrahlung, of course, the beam's energy spectrum is not a sharp delta function, but has a finite spread. The details of this spread vary from machine to machine; naïvely, however, it suffices to model it as a gaussian,

$$\rho_{E_0}(E) = \frac{1}{\delta\sqrt{2\pi}}e^{-(E-E_0)^2/2\delta^2}, \tag{4.12}$$

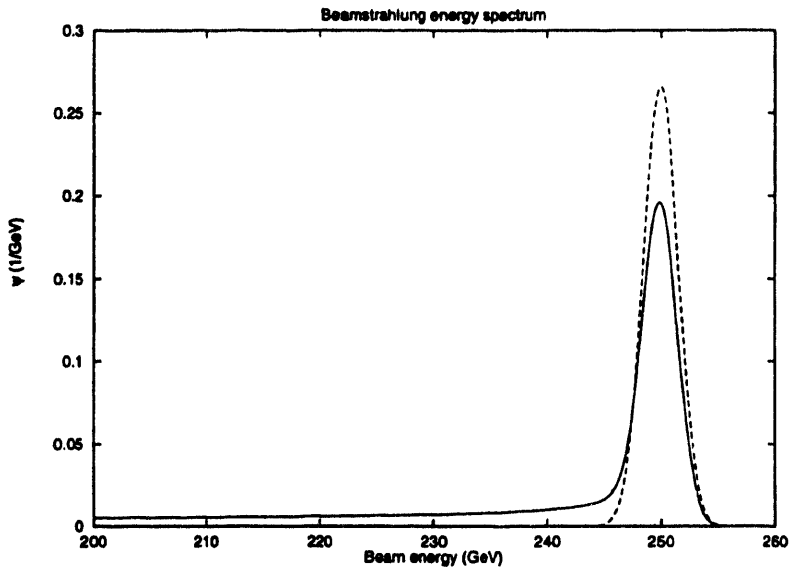

Figure 4.2: Energy spectrum of a beam at an e^+e^- collider, averaged over its traversal of the opposing beam. The nominal energy of the beam is 250 GeV, the beamstrahlung parameter Υ_{eff} is 0.1, and the linac energy spread is 0.6%. The solid line in the graph includes both beamstrahlung and the linac energy spread, while the dashed line includes only the linac energy spread.

where E_0 is the machine's nominal energy, and δ^2 is its variance. This is to be convolved with the beamstrahlung spectrum. That is, the observed beam energy spectrum is

$$\tilde{\psi}_{E_0}(E) = \int_E^\infty dE' \rho_{E_0}(E') \psi_{E'}(E). \tag{4.13}$$

This integral can be performed explicitly, yielding

$$\begin{aligned} \tilde{\psi}_{E_0}(E) \;=\; & \frac{1}{N_c}\left(1 - e^{-N_c}\right) \frac{1}{\sqrt{2\pi}\delta} e^{-(E-E_0)^2/2\delta^2} \\ & + \frac{1}{N_c}\frac{1}{\sqrt{2\pi}\delta} \exp\left[-\tfrac{1}{4}\left(\frac{E-E_0}{\delta}\right)^2 + \frac{1}{3\Upsilon_{eff}}\frac{E_0-E}{E} + \frac{1}{9\Upsilon_{eff}^2}\frac{E_0-E}{E}\frac{\delta^2}{E^2}\right] \\ & \times \sum_{n=1}^{\infty} \frac{\gamma(n+1, N_c)}{n!} \left(\frac{2\delta}{3\Upsilon_{eff}E}\right)^{n/3} D_{-n/3}\left(\frac{E-E_0}{\delta} + \frac{2\delta}{3\Upsilon_{eff}E}\right), \end{aligned} \tag{4.14}$$

where $D_\nu(x)$ is the parabolic cylinder function. This function is shown in Fig. 4.2. The collider design parameters used for this calculation, and for the calculation shown in Fig. 4.3, are discussed in Section 4.1.2.

Each beam loses energy through beamstrahlung. For $\Upsilon_{eff} \ll 1$, a good approximation [84] is that only the electron or the positron, but not both, loses a significant amount of energy. For $\Upsilon_{eff} \sim 1$ (the regime relevant at very high energy e^+e^- colliders) this approximation breaks down: Even for $\Upsilon \approx 0.1$, neglecting the case where both particles lose energy changes the spectrum by roughly 10%.

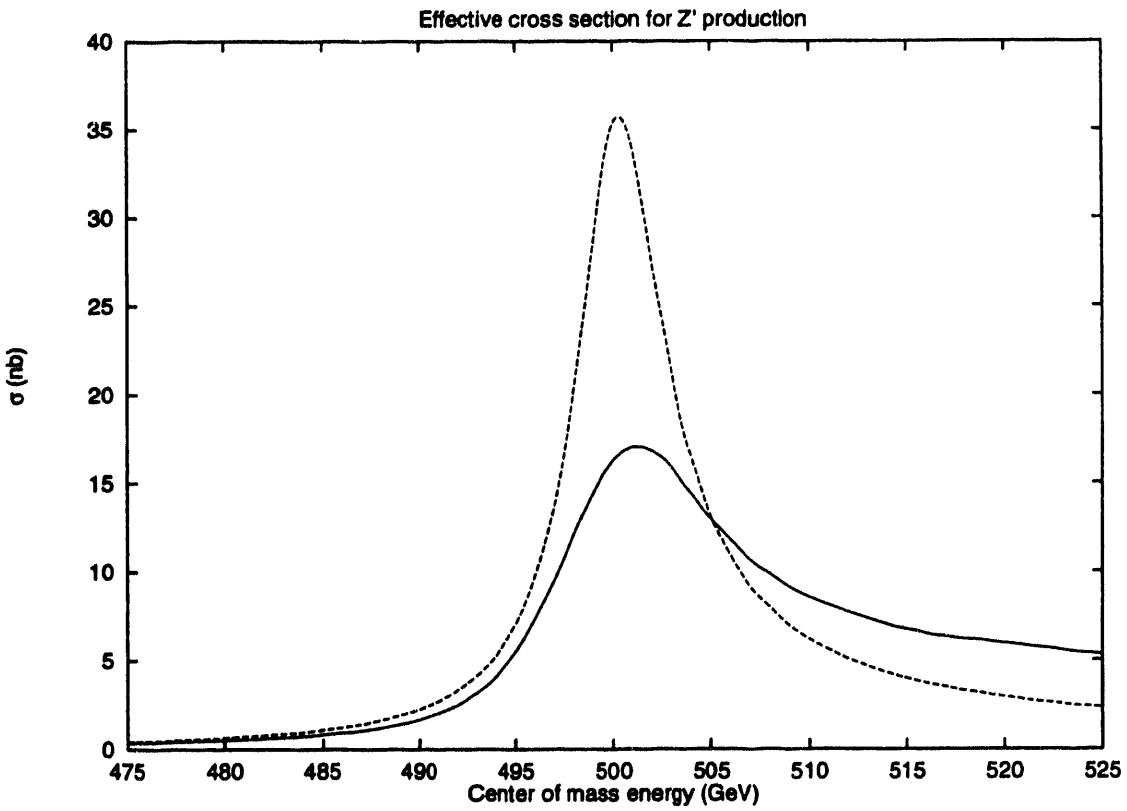

Figure 4.3: Effective cross section for Z' production at an e^+e^- collider, setting $B(Z' \to e^+e^-) = 1$. The Z''s mass and width are, respectively, 500 GeV and 5 GeV. The machine's beamstrahlung parameter Υ_{eff} is taken to be 0.1, and its linac energy spread to be 0.6%. The solid curve includes the effects of initial-state radiation, linac energy spread, and beamstrahlung, as given by Eq. (4.15). The dashed curve includes only the effect of initial-state radiation.

The observed cross section, the result of convolving the physical cross section with the beamstrahlung spectrum for each beam, is

$$\sigma_{\rm eff}(s) = \int\int dE_1 dE_2 \tilde{\psi}_{\sqrt{s}/2}(E_1)\tilde{\psi}_{\sqrt{s}/2}(E_2)\sigma(4E_1E_2). \qquad (4.15)$$

This integral must be performed numerically.

The effective cross section near resonance for $e^+e^- \to Z'$, including initial-state radiation, linac energy spread, and beamstrahlung, is shown in Fig. 4.3, again setting $B(e^+e^-) = 1$, and again assuming $M_{Z'} = 500$ GeV and $\Gamma_{Z'} = 5$ GeV. As might be expected, the major effects of linac energy spread and beamstrahlung are to reduce the maximum cross section and to increase the width of the peak. The maximum is also shifted by about 500 MeV, and the cross section in the tail above the peak is increased. This tail represents events in which a high-energy electron or positron loses just enough energy so that it falls on the resonance.

The main practical importance of these results for the purpose of studying a Z' is the reduction in the total number of Z' events that can be observed by running the

collider on resonance. The combined effects of initial-state radiation, beamstrahlung, and linac energy spread are quite dramatic: After including all of these effects the peak cross section is only 17 nb, compared to 59 nb for the maximum value of the pure Breit-Wigner. This is a reduction by more than a factor of three.

4.1.2 Collider parameters

Production rates of a Z' can only be calculated in the context of a specific accelerator design. It is likely that a high-energy e^+e^- collider will be built, partly to study gauge interactions at high energies and partly to study $t\bar{t}$ physics [86]; generically, such a collider is referred to as the "Next Linear Collider," or NLC. Its actual design parameters, however, are quite uncertain. There have been many different proposals for a high-energy e^+e^- collider [87, 88, 89], and it is likely that by the time the NLC is built, and more thought has been given to practical engineering questions, the design will be different than any currently being discussed.

Note that one difficult design issue is the minimization of beamstrahlung while maintaining high luminosity: Many of the machine parameters that affect the luminosity, such as the number of particles per bunch and the beam shape in the transverse plane, also affect the beamstrahlung parameter Υ_{eff}. As has been seen above, beamstrahlung can dramatically reduce the usable luminosity, and a high-luminosity collider is of no use if much of the beam energy spectrum lies in a region of no physical interest.

Note, further, that the luminosity-beamstrahlung tradeoff depends to a great extent on the physics for which the machine is designed. For the study of resonant phenomena, such as Z' physics, only that part of the energy spectrum in a rather narrow range is useful, so reduction of beamstrahlung, even at the cost of reduced luminosity, can boost the event rate. For the study of continuum phenomena, however, this is not true.

An NLC built after the discovery of a Z', and designed with Z' physics in mind, would probably be a very different machine from the NLC designs discussed today. These designs are based on the assumption that there are no resonant phenomena at $\sqrt{s} = 500$ GeV, and that cross sections will be very small; they are thus designed to have extraordinarily large luminosities. As discussed in Section 4.1.3, however, the event rate for Z' production at such a collider would be large enough so as to make statistical error negligible. The dominant errors would be systematic, and a broad-band spectrum would contribute to that systematic error. For the purpose of studying the Z' resonance, it would almost certainly be preferable to choose a design that sacrifices some of this luminosity in exchange for a cleaner beam energy spectrum.

Rather than design my own NLC, however, I will assume design parameters typical of proposed NLC designs. These designs usually feature a high bunch rate, a beam with a very small spot size, and a beam shape that is flat in the transverse plane—that is, one where σ_x/σ_y is a large number. In some designs, in fact, $\sigma_x/\sigma_y > 100$. I assume already in Section 4.1.1, and elsewhere, the following collider parameters:

$$\mathcal{L} = 1.4 \times 10^{33}\ \mathrm{cm}^{-2}\mathrm{s}^{-1} \tag{4.16}$$

$$\sqrt{s} = 500\ \mathrm{GeV} \tag{4.17}$$

$$\sigma_x = 612 \text{ nm} \quad (4.18)$$
$$\sigma_y = 3.4 \text{ nm} \quad (4.19)$$
$$\sigma_z = 110\ \mu\text{m} \quad (4.20)$$
$$N = 1.67 \times 10^{10} \quad (4.21)$$
$$\Upsilon_{eff} = 0.11 \quad (4.22)$$
$$\delta = 0.6\%, \quad (4.23)$$

where the beam shape is assumed to be gaussian in each dimension, with lab-frame widths σ_x, σ_y, and σ_z and with N particles per bunch, and where Υ_{eff} and δ, as discussed in Section 4.1.1, are the effective beamstrahlung parameter and the spread in the linac energy. None of these values is either the largest or the smallest that have been proposed.

4.1.3 Event rates

The cross sections plotted in Figs. 4.1 and 4.3 take $B(e^+e^-) = 1$. The actual branching ratio for this mode is

$$B(e^+e^-) = \frac{1}{3}\frac{g_e^2 + g_L^2}{2g_L^2 + g_e^2 + 3g_d^2 + g_u^2(2+y) + g_Q^2(5+y) + 6\tilde{y}g_Q g_u}, \quad (4.24)$$

where $x \equiv m_t^2/M_{Z'}^2$, $y = (1-x)\sqrt{1-4x}$, $\tilde{y} = x\sqrt{1-4x}$, and the couplings are those defined in Section 1.4. Specializing to SU(5)-invariant couplings, this becomes

$$B(e^+e^-) = \frac{1}{3}\left[\frac{1}{5 + \cos^2\beta\,(3 + 2y - 6\tilde{y})}\right], \quad (4.25)$$

or, when $m_t^2/M_{Z'}^2$ can be neglected,

$$B(e^+e^-) = \frac{1}{15}\left(\frac{1}{1+\cos^2\beta}\right). \quad (4.26)$$

As shown in Fig. 4.4, including the mass of the top can have a sizeable effect.

Typically, $B(e^+e^-)$ lies in the range 0.03–0.07. The observed production cross section, then, using the maximum value from Fig. 4.3, is 0.5–1.2 nb. Despite the degradation of the peak, this cross section is still quite large. If the ambitious NLC luminosity of Eq. (4.16) can be achieved, Z' production will be copious, with a rate comparable to that of Z production at LEP. A year's running should, for any reasonable assumptions about Z' couplings, provide a sample of at least a million Z' events. This is a sufficient statistical sample for high-precisions studies.

4.2 Measurement of the Z' width and branching ratios

4.2.1 Measurement of $M_{Z'}$ and $\Gamma_{Z'}$

As seen in Fig. 4.3, the observed Z' line shape at the NLC will be significantly distorted. The cross section's maximum value is at a value about 1 GeV higher than $M_{Z'}$,

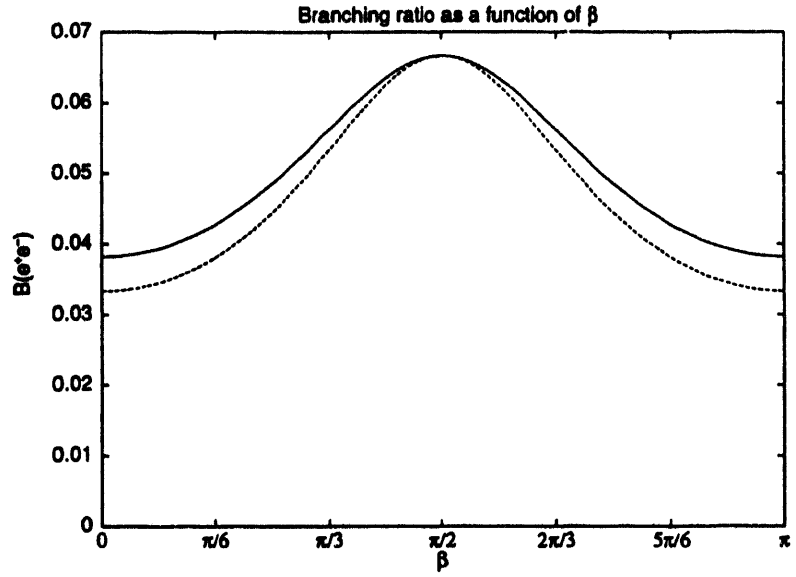

Figure 4.4: Branching ratio $B(Z' \to e^+e^-)$. The solid curve is for $m_t = 175$ GeV and $M_{Z'} = 500$ GeV, and the dashed curve is for $m_t^2 \ll M_{Z'}^2$. The two curves are equal for $\beta = \pi/2$ because the Z' does not couple to t quarks at all at that value of β.

and the width of the peak is greater than $\Gamma_{Z'}$. Extraction of $M_{Z'}$ and $\Gamma_{Z'}$, then, will be more complicated than simply fitting a Breit-Wigner to the measured line shape.

This is familiar from LEP measurements of M_Z and Γ_Z [90], where the Z line shape is distorted by initial-state radiation. The same methods used at LEP can be applied at the NLC—that is, running the accelerator at several energies in the vicinity of $M_{Z'}$ and comparing the measured line shape to the line shape predicted by a Monte Carlo program that includes initial-state radiation, linac energy spread, beamstrahlung, and detector resolution. As at LEP, the statistical error in this measurement is likely to be negligible; the dominant systematic error will probably be the prediction of the beamstrahlung spectrum.

An alternative method, not possible at LEP, takes advantage of the relatively broad energy distribution of the NLC. If the accelerator is run at a single, fixed energy, the spread in the actual collision energy is sufficient to cover the entire Z' peak. A detector with sufficiently precise energy resolution can reconstruct the invariant mass of leptonic Z' events, and measure the invariant mass spectrum. The necessary precision is high, but not inconceivably so. In most realistic models, $\Gamma_{Z'}/M_{Z'} \sim 1\%$. Resolving a 5 GeV peak in the $e^+e^- \to \mu^+\mu^-$ channel requires an electromagnetic calorimeter with energy resolution of a few GeV or better.

Both methods rely on a detailed understanding of the beamstrahlung spectrum, but they use that information in somewhat different ways. Consistency between these two methods can be used to verify that the Monte Carlo program is predicting beamstrahlung correctly.

4.2.2 Heavy-quark flavor tagging

The Z''s branching ratio into e^+e^- or $\mu^+\mu^-$ is given in Eqs. (4.24–4.26), and is plotted, for the special case of SU(5)-invariant couplings, in Fig. 4.4. It is also possible [67] to measure the branching ratios into up- and down-type quarks.

There is no reliable way of differentiating jets from up, down, and strange quarks, but, for t and b quarks, it is quite practical. At the NLC, b quarks will be very distinctive: A b quark with energy 250 GeV has a decay length of more than 2 cm. This large decay length, and a beam with a very small spot size, should make it easy to see secondary vertices. Although c quarks and τ leptons also exhibit secondary vertices, they do not present a serious background problem. Using the known multiplicity of b decays, and possibly also the presence of a c in the decay products, it should be possible to distinguish $b\bar{b}$ events from $c\bar{c}$ and $\tau^+\tau^-$ events with high reliability.

Top quark events will be even more distinctive: A t quark decays to a b and a W with a branching ratio of essentially one. The signature for a $t\bar{t}$ event at the NLC, then, is a $b\bar{b}$ pair and the decay products of two Ws. These decay products could either be two $l\bar{\nu}_l$ pairs, an $l\bar{\nu}_l$ pair and two jets, or four jets. None of those three signatures is likely to be mimicked by any significant background. It is possible to reduce the background still further by requiring that the kinematics of the ostensible W decay products be consistent with the hypothesis that they result from W decay.

Using the same notation as for $B(e^+e^-)$, the branching ratios to $b\bar{b}$ and $t\bar{t}$ are

$$B(b\bar{b}) = \frac{g_d^2 + g_Q^2}{2g_L^2 + g_e^2 + 3g_d^2 + g_Q^2(5+y) + g_u^2(2+y) + 6\tilde{y}g_Q g_u} \tag{4.27}$$

$$B(t\bar{t}) = \frac{y\left(g_u^2 + g_Q^2\right) + 6\tilde{y}g_Q g_u}{2g_L^2 + g_e^2 + 3g_d^2 + g_Q^2(5+y) + g_u^2(2+y) + 6\tilde{y}g_Q g_u}, \tag{4.28}$$

or, if $m_t^2 \ll M_{Z'}^2$,

$$B(b\bar{b}) = \frac{g_d^2 + g_Q^2}{2g_L^2 + g_e^2 + 3g_d^2 + 3g_u^2 + 6g_Q^2} \tag{4.29}$$

$$B(t\bar{t}) = \frac{g_u^2 + g_Q^2}{2g_L^2 + g_e^2 + 3g_d^2 + 3g_u^2 + 6g_Q^2}. \tag{4.30}$$

Measurement of $B(b\bar{b})$, $B(t\bar{t})$, and $B(e^+e^-)$ is a simple matter of counting, so the statistical error for each of these measurements is roughly $1/\sqrt{N}$, where N is the number of events in each mode. At the NLC, a sample of at least a million Z' events should be obtainable, but, assuming only 10^5 events, the statistical errors in the e^+e^- and in the heavy-quark modes should be on the order of 1.5% and 1% respectively. The dominant sources of systematic error will probably be uncertainty in the detector's acceptance and in its heavy-quark identification efficiency.

These two measurements, when combined with the total width $\Gamma_{Z'}$ (shown in Eq. (1.68) and, for SU(5)-invariant couplings, in Fig. 1.2), determine $g_d^2 + g_Q^2$ and $g_u^2 + g_Q^2$. These data are still insufficient to determine all three quark couplings, but that

determination only requires one additional independent measurement. One of the quark asymmetries, such as the $b\bar{b}$ or $t\bar{t}$ forward-backward asymmetry, would be an obvious choice.

Similarly, the e^+e^- partial width depends on $g_e^2 + g_L^2$. A measurement of g_e^2/g_L^2, such as the e^+e^- forward-backward asymmetry, or the τ polarization asymmetry, then allows the determination of g_e^2 and g_L^2.

Note the importance of the assumption that $b\bar{b}$ and $t\bar{t}$ events can be identified. Heavy-quark flavor tagging allows the measurement of the magnitudes of all five Z' gauge coupling constants; without it, however, only a combination of g_u^2, g_d^2, and g_Q^2 can be measured.

4.3 Asymmetries

Generally, the quantity determined by measuring an asymmetry is the difference between the right-handed and left-handed couplings to some fermion. Specifically, define

$$A^f = \frac{\left(g_L^f\right)^2 - \left(g_R^f\right)^2}{\left(g_L^f\right)^2 + \left(g_R^f\right)^2}. \tag{4.31}$$

The fermion f may be a lepton, an up-type quark, or a down-type quark, so this defines three quantities, A^e, A^U, and A^D. Measurement of A^U and A^D will require the ability to tag heavy flavors, as discussed in Section 4.2.2.

4.3.1 Forward-backward asymmetries

On resonance, the forward-backward asymmetry for $e^+e^- \to Z' \to f\bar{f}$ is given by

$$A_{FB}^f = \frac{3}{4} A^e A^f. \tag{4.32}$$

This equation assumes that the final-state fermions are massless, and thus that the different helicity amplitudes do not interfere; if the final-state fermions are t quarks, A^t must be be generalized to

$$A^t = \sqrt{1-4x} \cdot \frac{g_Q^2 - g_u^2}{(1-x)\left[g_Q^2 + g_u^2\right] + 6x g_Q g_u}. \tag{4.33}$$

where $x = m_t^2/M_{Z'}^2$. If $M_{Z'}$ is sufficiently small, this correction can result in a sizeable decrease in A_{FB}. Note also that it depends on the relative signs of g_Q and g_u, rather than just on their magnitudes. As is discussed below, however, this potential sensitivity to the sign is not useful in SU(5)-invariant models.

Off resonance, interference terms become important, and the variation of A_{FB} with energy can, in principle, be used to determine not only the magnitude, but also the sign of the Z' couplings. For energies within a few tens of GeV of $M_{Z'}$, however, A_{FB}

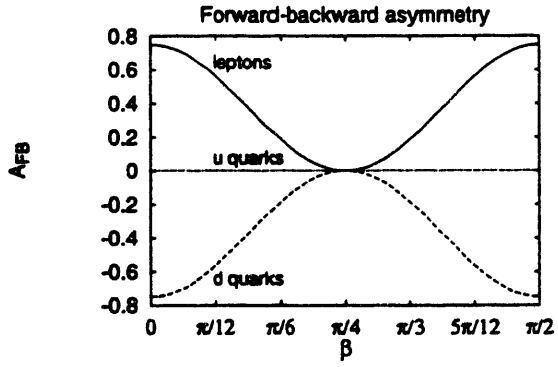

Figure 4.5: Graph of forward-backward asymmetry in $e^+e^- \to Z' \to f\bar{f}$. The couplings of the Z' are assumed to be invariant under SU(5), and β, defined in Eq. (1.66), determines the relative strength of couplings to fermions in the $\mathbf{5}^*$ and $\mathbf{10}$ representations of SU(5). The solid line is for the case where the final-state fermions are charged leptons, the dashed line for down-type quarks, and the dotted line for up-type quarks.

typically changes only by a few percent. This is fortunate: If A_{FB} varied quickly, then any effect would be likely to be smeared out by beamstrahlung.

If the Z' has SU(5)-invariant couplings, as discussed in Section 1.4, then for any final-state fermion f, A_{FB}^f depends only on the parameter β defined in Eq. (1.66). This dependence is shown in Fig. 4.5. Explicitly,

$$A_{FB}^E = \frac{3}{4}\cos^2 2\beta, \tag{4.34}$$

$$A_{FB}^D = -\frac{3}{4}\cos^2 2\beta, \tag{4.35}$$

$$A_{FB}^U = 0. \tag{4.36}$$

It is a general result in models with SU(5)-invariant couplings that A^U and A_{FB}^U are necessarily zero, because the left- and right-handed up-type quarks appear in the same representation of SU(5),

When interference terms are included A_{FB}^U is no longer exactly zero, but is still small. The full expression for A_{FB} is somewhat cumbersome, and depends not only on the ratios of the Z' couplings to fermions, but also on their magnitude relative to the γ and Z couplings. Fig. 4.6 shows A_{FB}^t as a function of energy for a Z' with SU(5)-invariant couplings, assuming $\tilde{g} = g_Z$, $M_{Z'} = 500$ GeV, and $m_t = 145$ GeV. Although it is possible in principle to measure A_{FB}^U at some energy other than $\sqrt{s} = M_{Z'}$, Fig. 4.6 shows that A_{FB}^U is unmeasurably small except at energies so far off resonance that there will be too few events for a precise measurement. It can thus be taken as a definite prediction of all models with SU(5)-invariant Z' gauge couplings that $A_{FB}^U = 0$.

Even with very high statistics, the effects described in Section 4.1.1 would make measurement of an energy-dependent asymmetry very challenging: Any sample of events would probe Z' couplings not at any one energy, but at a range of energies, and if taken above $M_{Z'}$, would be heavily contaminated by on-resonance events. Making this mea-

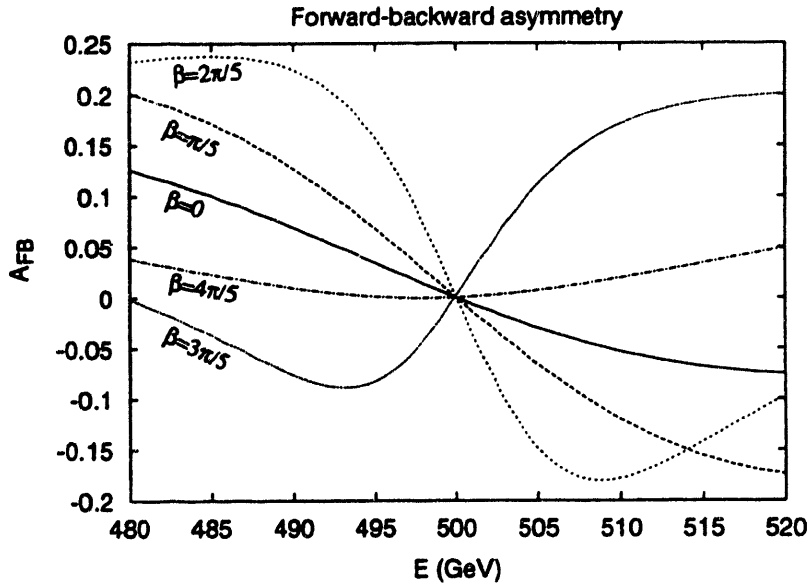

Figure 4.6: Graph of forward-backward asymmetry in $e^+e^- \to Z' \to t\bar{t}$ as a function of energy, for $M_{Z'} = 500$ GeV and $\Gamma_{Z'} = 10$ GeV. The Z' couplings are assumed to be invariant under SU(5), and $\tilde{\mathbf{g}}$, defined in Eq. (1.66), is assumed to be 0.15. The five curves refer to five different values of the parameter β, also defined in Eq. (1.66). The Z' width, $\Gamma_{Z'}$, is given by Eq. (1.69), and, for these values of $M_{Z'}$ and $\tilde{\mathbf{g}}$, varies between 2 and 4 GeV.

surement would require a precise understanding of the beamstrahlung spectrum in order to understand at exactly which energies A_{FB}^U is actually being measured.

At a hadron collider a Z' is usually produced with a sizeable longitudinal momentum, so its decay products are often nearly collinear with the incoming beams. Additionally, detector coverage of pseudorapidity is usually limited to fairly small values of η, so a substantial fraction of events are unusable. At an e^+e^- collider, however, Z's produced on resonance are produced at rest, thus yielding roughly isotropic decay distributions. Essentially all events should be usable for the purpose of measuring A_{FB}.

Measuring the forward-backward asymmetry in some mode involves measuring two quantities, N_F and N_B; their statistical uncertainties δN_F and δN_B are $\sqrt{N_F}$ and $\sqrt{N_B}$, or, if N is the total number of events in this mode, roughly $\sqrt{N/2}$. The statistical error of A_{FB} is

$$\delta A_{FB} = \sqrt{\left(\delta N_F \frac{\partial A_{FB}}{\partial N_F}\right)^2 + \left(\delta N_B \frac{\partial A_{FB}}{\partial N_B}\right)^2}, \tag{4.37}$$

or roughly $1/\sqrt{N}$. With a sample of 5000 events in each mode, this is about a 1.5% statistical error. Most systematic errors cancel out in the ratio, so the actual error in this measurement will probably not be much larger than Eq. (4.37).

4.3.2 Polarization asymmetries

In addition to the left-right asymmetry, for certain final-state fermions it is also possible to measure the polarization asymmetry, *i.e.*, the asymmetry between the production of right-handed and left-handed particles in the final state. Specifically, if σ_L is defined to be the cross section for production of left-handed particles and σ_R the cross section for production of right-handed particles, the polarization asymmetry is defined to be

$$A_{\rm pol} = \frac{\sigma_L - \sigma_R}{\sigma_L + \sigma_R}. \tag{4.38}$$

Measurement of $A_{\rm pol}$ requires that the final-state fermions be unstable, that they have well-understood decays, and that the decays of left-handed and right-handed particles be substantially different. The only particles that meet these requirements are τ leptons. In the future, t quarks [91] may also be suitable candidates, but not enough is known at present about the extent to which polarization is affected when the t quarks or, more likely, their decay products, hadronize.

Unlike A_{FB}, which depends both on the Z' couplings to the initial-state electrons and to the final-state fermions, $A_{\rm pol}$ depends only on the couplings of the final-state fermions: In the notation of Eq. (4.31),

$$A^\tau_{\rm pol} = A^\tau. \tag{4.39}$$

For the special case of SU(5)-invariant couplings,

$$A^\tau_{\rm pol} = -\cos 2\beta. \tag{4.40}$$

For the Z^0, $A^\tau_{\rm pol}$ has been measured at LEP [72]; as discussed in Section 3.4, it is potentially also valuable as a diagnostic tool for studying a Z' at hadron colliders.

The relevant quantities, at both lepton and hadron colliders, are dN_L/dx and dN_R/dx, the normalized decay spectra for left- and right-handed τs. The measured decay spectrum, dN/dx, can be fitted to a linear combination of dN_L/dx and dN_R/dx, and this fit directly determines $A^\tau_{\rm pol}$: If

$$\frac{dN}{dx} = c_L \frac{dN_L}{dx} + c_R \frac{dN_R}{dx}, \tag{4.41}$$

then

$$A^\tau_{\rm pol} = \frac{c_L - c_R}{c_L + c_R}. \tag{4.42}$$

Although measurement of $A^\tau_{\rm pol}$ at a hadron collider would be a very challenging experiment, essentially none of the difficulties involved in this measurement apply to Z' studies at an e^+e^- collider. The two main difficulties at a hadron collider are that it is necessary to find the decay products of a $\tau^+\tau^-$ pair above all possible backgrounds (chiefly QCD jets and $t\bar{t}$ pairs), and that the kinematics of $Z' \to \tau^+\tau^-$ events at hadron colliders, in which the Z''s longitudinal momentum is unknown, and in which the Z' is often produced with substantial transverse momentum, make it difficult to reconstruct the momentum of the τ^+ and τ^-.

Neither of these presents a problem at an e^+e^- collider. Reconstruction of the τs' momenta is trivial, since the Z' is produced at rest in the lab frame: Both the τ^+ and the τ^- always have a momentum of $M_{Z'}/2$, so determination of x_+ and x_- is a simple matter of measuring the momenta of the τ decay products. Background, similarly, is negligible.

The reason that background is a serious problem at a hadron collider is that, while the invariant mass of the $\tau^+\tau^-$ pair is equal to $M_{Z'}$, the invariant mass of the τs' visible decay products is reduced by a factor of $\sqrt{x_+x_-}$, and there are many other processes that can result in an event with an invariant mass of $\sqrt{x_+x_-}M_{Z'}$. At an e^+e^- collider with $\sqrt{s} = M_{Z'}$ there are no such processes: Essentially all events have an invariant mass of $M_{Z'}$, so the only events that could conceivably mimic $\tau^+\tau^-$ events are other events where unstable particles are produced at the Z' resonance and then decay. It is almost impossible, however, that $b\bar{b}$, $c\bar{c}$, or $t\bar{t}$ decays could be mistaken for $\tau^+\tau^-$ decays: The vast majority of τ decays are one-prong, while heavy quark decays have a high multiplicity.

One possible source of low-invariant mass events is pair production of e^+e^- or $\mu^+\mu^-$, in conjunction with a high-energy bremsstrahlung photon. This is not a resonant process, however, so such events will be rare. Moreover, bremsstrahlung is strongly peaked in the beam direction, so these events will always have a very small missing transverse momentum and can be rejected by a simple cut.

The statistical error in $A_{\rm pol}$ is roughly $1.5/\sqrt{N}$, where N is the number of $\tau^+\tau^-$ events used in the measurement. Assuming a sample of 5000 $\tau^+\tau^-$ events, of which 20% decay into channels that are sufficiently well understood to be used in this measurement, this error is about 5%. This is significantly larger than the error in A_{FB}, but $A_{\rm pol}$ is more sensitive than is A_{FB} to variations in A_e, which is the actual quantity of interest. Assuming universality, A_{FB} is proportional to A_e^2, while $A_{\rm pol}$ is equal to A_e. If A_e is small, $A_{\rm pol}$ will provide a better measurement than A_{FB} despite the larger statistical error.

Finally, it is possible to combine A_{LR} and $A_{\rm pol}$, *i.e.*, to measure the forward-backward asymmetry separately for left-handed and right-handed τs. This simply involves fitting the τ decay spectra separately for forward and backward events, and yields the results

$$A_{FB}^{\tau_L} = -A_{FB}^{\tau_R} = \frac{3}{4}A^e. \tag{4.43}$$

Except as a test of universality, this measurement is redundant: If e and τ couplings are equal, it provides the same information as $A_{\rm pol}^{\tau}$, but with less precision.

4.3.3 Polarized beams

If one of the initial beams is partially longitudinally polarized (there is no advantage to polarizing both, because the cross section for production of a $J = 1^{--}$ resonance by a relativistic e^+e^- pair vanishes when the electron and the positron have the same helicity), it will be possible to measure yet another polarization asymmetry, A_{LR}. This is defined as the cross section for Z' production by a left-handed e^- minus the cross section for production by a right-handed e^-, divided by the sum of the cross sections. That is,

$$A_{LR} \equiv \frac{\sigma_L - \sigma_R}{\sigma_L + \sigma_R}. \tag{4.44}$$

The value of this asymmetry is

$$A_{LR} = \frac{g_L^2 - g_e^2}{g_L^2 + g_e^2}. \tag{4.45}$$

Measurement of A_{LR} is straightforward: Counting the number of events for each polarization.

Note that, except as a test of universality, A_{LR} and $A_{\rm pol}$ are redundant: Both of these methods provide direct measurements of g_u^2/g_Q^2. If, however, it is possible to obtain a sufficiently high degree of polarization, then A_{LR} can be measured more precisely than $A_{\rm pol}$.

4.4 Study of a Z' below resonance

Although the possibility is not ruled out by present search limits, it is perhaps overly optimistic to hope that a new gauge boson will be found with a mass sufficiently low for it to be the subject of on-resonance studies at the NLC. This section discusses the possibility that a Z' will be discovered at the LHC with a mass higher than the NLC's maximum value of $\sqrt{s}$. If the Z' has a mass less than a few TeV its couplings can still be measured at the NLC, but only through virtual Z' exchange. Several detailed studies of this case [40, 92] have been performed.

In fact, even if a Z' is sufficiently light that it can be produced at an e^+e^- collider, studies of it at energies far below its mass would still be valuable: All of the measurements discussed up to this point deal only with the magnitudes of the Z's couplings, but studies below the resonance are able to determine their signs as well [40, 92, 93].

At the NLC, with $\sqrt{s} < M_{Z'}$, the effect of Z-Z' mixing on Z couplings will be no greater than the same effect at LEP. Since mixing is already known to be small and NLC measurements will be less precise than those at LEP because of the lower statistics associated with running off-resonance, mixing may safely be neglected. The Z' will affect observables at the NLC simply though interference between the γ, Z, and Z' propagators.

In general, an event at the NLC is of the form $e^+e^- \to f\bar{f}$. The three Feynman diagrams that contribute to this reaction are shown in Fig. 4.7, and the matrix element takes the form

$$\mathcal{M} = \mathcal{M}_\gamma + \mathcal{M}_Z + \mathcal{M}_{Z'}. \tag{4.46}$$

Observable quantities depend on $|\mathcal{M}|^2$. The largest contribution from the Z' comes from the interference between the γ and Z' propagators, but none of the terms in this product may be neglected.

The quantities that can be measured at the NLC are the production rates and asymmetries discussed in Sections. 4.2 and 4.3, specifically $\sigma(e^+e^- \to f\bar{f})$, $A_{\rm pol}^f$, and, if one beam can be polarized, A_{LR}^f. The identifiable final-state fermions are e, μ, τ, c, b, and t. I assume, as before, that only the τ can be used in the measurement of $A_{\rm pol}$. It is possible, however, that t polarization asymmetry might also be measurable.

Off resonance, the tree-level cross section $\sigma(e^+e^- \to f\bar{f})$ is

$$\sigma(f\bar{f}) = \frac{1}{48\pi s}\left(F_{LL}^f + F_{RR}^f + F_{LR}^f + F_{RL}^f\right), \tag{4.47}$$

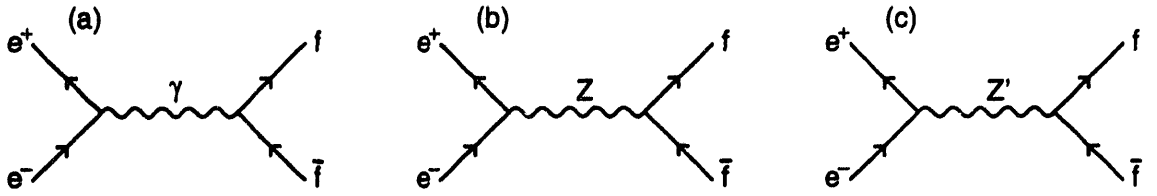

Figure 4.7: Feynman diagrams for $e^+e^- \to f\bar{f}$, for the case where $M_Z < \sqrt{s} < M_{Z'}$. On resonance only diagram (c) contributes, but off resonance all three are important, and interference between the diagrams must be included. The interference terms depend on the signs, not just the magnitudes, of the Z' couplings. If the final-state fermions are electrons, interference from t-channel gauge boson exchange must also be included.

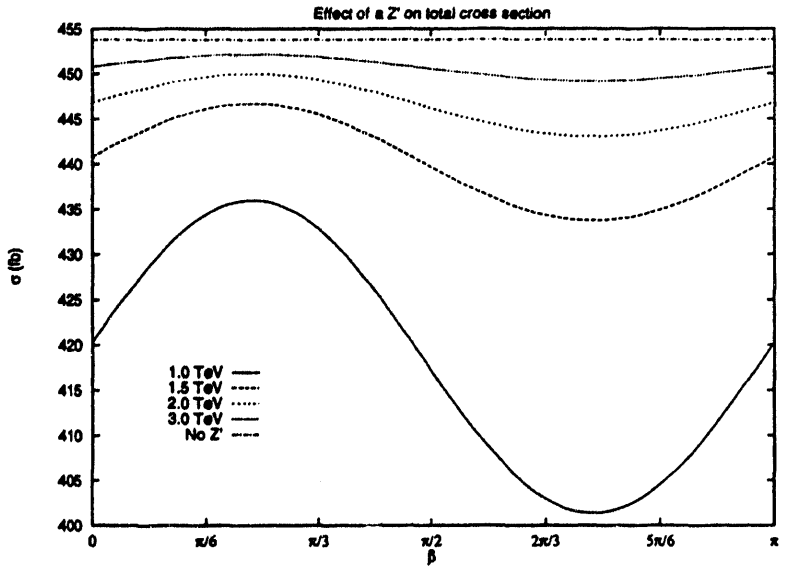

Figure 4.8: Cross section for $\sigma(e^+e^- \to \mu^+\mu^-)$ at $\sqrt{s} = 500$ GeV as a function of β, assuming a Z' with SU(5)-invariant couplings whose overall coupling strength $\tilde{g}$ is equal to 0.2. The cross section is plotted for $M_{Z'} = 1$ TeV, $M_{Z'} = 1.5$ TeV, $M_{Z'} = 2$ TeV, $M_{Z'} = 3$ TeV, and $M_{Z'} = \infty$.

where the individual helicity terms are

$$F_{ij}^f = \left(e^2 Q_{EM}^{e,i} Q_{EM}^{f,j} + g_Z^{e,i} g_Z^{f,j} \frac{s}{s - M_Z^2} + g_{Z'}^{e,i} g_{Z'}^{f,j} \frac{s}{s - M_{Z'}^2} \right)^2 . \tag{4.48}$$

This expression assumes that the final-state fermions are not electrons, and that their masses can be neglected. In the case of quarks, it must be multiplied by a color factor of 3. Fig. 4.8 shows $\sigma(e^+e^- \to \mu^+\mu^-)$ at 500 GeV (below $M_{Z'}$) as a function of β for four different values of $M_{Z'}$, for SU(5)-invariant Z' couplings and $\tilde{g} = 0.2$. The Z' contribution to σ falls as $1/M_{Z'}^2$, so, while a 1 TeV Z' has a very substantial effect, a 2 TeV Z' results in a cross section that is scarcely distinguishible from the Standard Model value.

The Standard Model prediction at $\sqrt{s} = 500$ GeV is $\sigma(e^+e^- \to \mu^+\mu^-) \approx 450$ fb. An e^+e^- collider with the parameters described in Section 4.1.2 has an integrated luminosity (for one year of running) of about 10 fb^{-1}. With 5000 $\mu^+\mu^-$ pairs $\sigma(\mu^+\mu^-)$ can be

measured with a statistical error of about 1.4%, or about 6 fb. As can be seen in Fig. 4.8, this means that the effect of a 1 TeV Z' on $\sigma(e^+e^- \to \mu^+\mu^-)$ will be quite clear, and it will even be possible to obtain nontrivial information about β. The effect of a 2 TeV Z' will, however, be difficult to tell from a statistical fluctuation in the Standard Model cross section, and a 3 TeV Z' will be essentially invisible. As always, the effect is larger if the Z' has larger couplings than those assumed here.

Note that this cross section is not individually sensitive either to the Z' gauge coupling constant or to $M_{Z'}$, but only to the two in combination. This is a general feature of experiments at $\sqrt{s} < M_{Z'}$: None of the measurements discussed in this section can determine $M_{Z'}$. For $M_{Z'} \gg \sqrt{s}$, the Z' coupling is essentially a contact interaction; increasing $M_{Z'}$ has the same effect as decreasing its coupling strength.

Using the same notation as in Eq. (4.47) and making the same assumptions, the forward-backward asymmetry for $e^+e^- \to f\bar{f}$ is

$$\frac{3}{4} \cdot \frac{F^f_{LL} + F^f_{RR} - F^f_{LL} - F^f_{RR}}{F^f_{LL} + F^f_{RR} + F^f_{LL} + F^f_{RR}}. \tag{4.49}$$

Expressions for the other observables are equally straightforward.

Del Aguila and Cvetič [40] have analyzed the precision to which Z' coupling constants can be measured at the NLC, assuming $M_{Z'} = 1$ TeV. Assuming polarization of the initial e^- beam, they find that the parameters P^l_V, P^q_L, P^u_R, and P^d_R, defined in Eqs. (1.61–1.64) can be determined to 10–20%, the exact degree of uncertainty depending on the central values of the parameters.

This analysis does not include the effects of initial-state radiation or beamstrahlung, but far off resonance, where no quantities are varying rapidly with respect to energy, these effects should be less important than at $\sqrt{s} = M_{Z'}$. Since the quantities being measured are small deviations from Standard Model predictions, however, it is important that all Standard Model effects at $\sqrt{s} = 500$ GeV be understood in as much detail as possible.

4.5 Conclusions

If a Z' is discovered at the LHC, experiments there will be able to determine the its mass, width, and the magnitude of all of its couplings except those to quarks. These couplings must be measured at an e^+e^- collider.

Combining results obtained at the NLC with those obtained at the LHC, all of the parameters described in Section 1.4 may be determined. An e^+e^- collider at $\sqrt{s} = M_{Z'}$, with low beamstrahlung and relatively low luminosity, would allow high-precision measurement of all Z' parameters. Even if it proves impossible to build such a machine all of these parameters can still be obtained, to a reasonable degree of precision, from the combination of LHC measurements and off-resonance measurements at the NLC.

Bibliography

[1] C. N. Yang and R. L. Mills, Phys. Rev. **96**, 191 (1954). M. Gell-Mann and S. L. Glashow, Ann. Phys. (NY) **15**, 437 (1961).

[2] G. 't Hooft, Nucl. Phys. **B33**, 173 (1971). G. 't Hooft, Nucl. Phys. **B35**, 167 (1971).

[3] S. L. Glashow, Nucl. Phys. **22**, 579 (1961). S. Weinberg, Phys. Rev. Lett. **19**, 1264 (1967). A. Salam, In *Elementary particle physics: Nobel Symp. No. 8*, ed. N. Svartholm. Stockholm, 1968.

[4] Y. Nambu, Phys. Rev. Lett. **4**, 380 (1960). P. W. Higgs, Phys. Rev. Lett. **13**, 508 (1964). T. W. B. Kibble, Phys. Rev. **155**, 1554 (1967).

[5] L. D. Faddeev and V. N. Popov, Phys. Lett. **B25**, 29 (1967).

[6] S. Weinberg, Phys. Rev. **D7**, 1068 (1973).

[7] N. Cabibbo, Phys. Rev. Lett. **10**, 531 (1963). M. Kobayashi and T. Maskawa, Prog. Theor. Phys. **49**, 652 (1973).

[8] Particle Data Group, Phys. Rev. **D45**, part II, 1 (1992).

[9] S. R. Sharpe, "Recent Progress in Lattice QCD," Plenary talk given at the Meeting of the Division of Particles and Fields of the American Physical Society, Fermilab, November 1992. M. Creutz, "Lattice Gauge Theory—Present Status." In *Hadron 93: The Biennial Conference on Hadron Spectroscopy,* Como, Italy, June 1993.

[10] See, for example, H. Georgi, *Weak Interactions and Modern Particle Theory,* Benjamin/Cummings, Menlo Park, 1984.

[11] See, for example, L. Rolandi, "Precision Tests of the Electroweak Interaction," *Talk given at the XXVI ICHEP,* October 1992.

[12] D. J. Gross and R. Jackiw, Phys. Rev. **D6**, 477 (1972).

[13] CDF Collaboration, F. Abe *et al.*, "Evidence for Top Quark Production in $\bar{p}p$ Collisions at $\sqrt{s} = 1.8$ TeV", FERMILAB-PUB-94/097-E, 1994 (unpublished).

[14] K. F. Smith *et al.*, Phys. Lett. **B234**, 191 (1990).

[15] V. Baluni, Phys. Rev. **D19**, 2227 (1979). R. J. Crewther, P. Di Vecchia, G. Veneziano, and E. Witten, Phys. Lett. **B88**, 123 (1979).

[16] D. J. E. Callaway, Phys. Rep. **167**, 243 (1988), and references therein.

[17] M. Lindner, Z. Phys. **C31**, 295 (1986).

[18] R. D. Peccei and H. Quinn, Phys. Rev. Lett. **38**, 1440 (1977). R. D. Peccei and H. Quinn, Phys. Rev. **D16**, 1791 (1977).

[19] F. Wilczek and A. Zee, Phys. Rev. Lett. **42**, 421 (1979). C. L. Ong, Phys. Rev. **D19**, 2738 (1979). R. Foot, G. C. Joshi, H. Lew, and R. R. Volkas, Phys. Lett. **B226**, 318 (1989).

[20] S. Weinberg, Phys. Rev. **D19**, 1277 (1979). L. Susskind, Phys. Rev. **D20**, 2619 (1979).

[21] D. Volkov and V. P. Akulov, JETP Lett. **16**, 438 (1972). J. Wess and B. Zumino, Nucl. Phys. **B70**, 39 (1974). J. Wess and B. Zumino, Phys. Lett. **B49**, 52 (1974).

[22] H. E. Haber and G. L. Kane, Phys. Rep. **117**, 75 (1985), and references therein.

[23] J. C. Pati and A. Salam, Phys. Rev. **D10**, 275 (1974). R. N. Mohapatra and J. C. Pati, Phys. Rev. **D11**, 566 (1975). R. N. Mohapatra and G. Senjanovic, Phys. Rev. **D12**, 1502 (1975).

[24] R. N. Mohapatra, *Unification and Supersymmetry: The Frontiers of Quark-Lepton Physics*, Second Edition, Springer-Verlag, New York, 1992.

[25] I. Z. Rothstein, Nucl. Phys. **B358**, 181 (1991).

[26] R. N. Mohapatra and G. Senjanovic, Phys. Rev. Lett. **44**, 912 (1980). R. N. Mohapatra and G. Senjanovic, Phys. Rev. **D21**, 165 (1981).

[27] D. J. Gross and F. Wilczek, Phys. Rev. Lett. **30**, 1343 (1973). H. D. Politzer, Phys. Rev. Lett. **30**, 1346 (1973).

[28] L. Hall, Nucl. Phys. **B178**, 75 (1981). D. R. T. Jones, Phys. Rev. **D25**, 581 (1982).

[29] H. Arason *et al.*, Phys. Rev. **D46**, 3945 (1992).

[30] H. Georgi and S. L. Glashow, Phys. Rev. Lett. **32**, 438 (1974).

[31] H. Georgi, H. Quinn, S. Weinberg, Phys. Rev. Lett. **32**, 451 (1974). A. J. Buras, J. Ellis, M. K. Gaillard, and D. V. Nanopoulos, Nucl. Phys. **B135**, 66 (1978).

[32] U. Amaldi, W. de Boer, and H. Fürstenau, Phys. Lett. **B260**, 447 (1991).

[33] H. Fritzsch and P. Minkowski, Ann. Phys. **93**, 193 (1975). H. Georgi, in *Particles and Fields '74*, American Institute of Physics conference proceedings, Particles and fields subseries, no. 10, ed. C. E. Carlson, AIP, New York, 1975.

[34] R. W. Robinett and J. L. Rosner, Phys. Rev. **D25**, 3036 (1982).

[35] D. London and J. L. Rosner, Phys. Rev. **D34**, 1530 (1986).

[36] V. Barger, N. G. Deshpande, J. L. Rosner, K. Whisnant, Phys. Rev. **D35**, 2893 (1987).

[37] P. Langacker and M. Luo, Phys. Rev. **D45**, 278 (1992). A. Chiappinelli, Phys. Lett. **B263**, 287 (1991).

[38] E. Nardi, Phys. Rev. **D48**, 1240 (1993).

[39] F. del Aguila, M. Cvetič, P. Langacker, Phys. Rev. **D48**, R969 (1993).

[40] F. del Aguila and M. Cvetič, "Diagnostic power of future colliders for Z' couplings to quarks and leptons: e^+e^- versus pp colliders," UG-FT-33/93 and UPR-590-T, 1993 (unpublished).

[41] CDF Collaboration, F. Abe *et al.*, Phys. Rev. Lett. **67**, 2418 (1991). CDF Collaboration, F. Abe *et al.*, Phys. Rev. Lett. **68**, 1463 (1992). CDF Collaboration, F. Abe *et al.*, "A search for new gauge bosons in $\bar{p}p$ collisions at $\sqrt{s} = 1.8$ TeV in the dielectron decay mode", FERMILAB-CONF-93-211-E, 1993. Submitted to 16th International Symposium on Lepton and Photon Interactions, Ithaca, NY, 10-15 Aug 1993.

[42] D0 Collaboration, A. Taketani *et al.*, "Lepton charge asymmetry from W decay and search for new gauge bosons at D0", FERMILAB-CONF-94-017-E, 1994 (unpublished). Presented at 9th Topical Workshop on Proton-Antiproton Collider Physics, Tsukuba, Japan, October 1993.

[43] UA1 Collaboration, C. Albajar *et al.*, A. Phys. **C44**, 15 (1989).

[44] S. Grunendahl, in Proceedings of the Vancouver Meeting, Particles and Fields '91, Vancouver, Canada, August 1991.

[45] CDF Collaboration, F. Abe *et al.*, Phys. Rev. **D48**, 998 (1993).

[46] T. G. Rizzo, Phys. Rev. **D48**, 4470 (1993).

[47] A. Leike, S. Riemann, and T. Riemann, Phys. Lett. **B291**, 187 (1992). A. Djouadi, *et al.*, Nucl. Phys. **B349**, 48 (1991). C. Verzegnassi, "Phenomenology of one extra neutral Z," LAPP-TH-322/90. Presented at the First International Triangle Workshop CERN-IHEP-JINR, Dubna, October 1990.

[48] S. Riemann, "Search for Z'," DESY-92-143. In *Proceedings of the XV International Warsaw Meeting on Elementary Particle Physics,* Kazimierz, Poland, April 1992.

[49] G. Altarelli, *et al.*, "Extended gauge models and precision electroweak data," Phys. Lett. **B318**, 139 (1993). F. del Aguila, W. Hollik, J. Moreno, M. Quirós, Nucl. Phys. **B372**, 3 (1992).

[50] L3 Collaboration, O. Adriani, *et al.*, "Search for a Z' at the Z resonance, CERN-PPE-93-44, 1993 (unpublished).

[51] K. T. Mahanthappa and P. H. Mohapatra, Phys. Rev. **D43**, 3093 (1991), and erratum, Phys. Rev. **D44**, 1616 (1991). P. Langacker, Phys. Lett. **B256**, 277 (1991).

[52] W. J. Marciano and A. Sirlin, Phys. Rev. **D35**, 1672 (1987).

[53] A. Leike, "Model independent Z' constraints at future e^+e^- colliders," DESY-91-154, 1993 (unpublished).

[54] K. Wilson, Phys. Rev. **179**, 1499 (1969).

[55] G. Altarelli, Phys. Rep. **81**, 1 (1982), and references therein.

[56] E. Eichten, I. Hinchliffe, K. Lane, C. Quigg, Rev. Mod. Phys. **56**, 579 (1984), and erratum, Rev. Mod. Phys. **58**, 1056 (1984).

[57] D. W. Duke and J. F. Owens, Phys. Rev. **D27**, 508 (1984).

[58] P. Harriman *et al.*, Phys. Rev. **D42**, 798 (1990).

[59] J. Morfin and W. Tung, Z. Phys. **C52**, 13 (1991).

[60] M. Diemoz *at al*, Z. Phys. **C39**, 21 (1988).

[61] M. Glück, E. Reya, A. Vogt, Phys. Lett. **306B**, 391 (1993). M. Glück, E. Reya, A. Vogt, Z. Phys. **C53**, 127 (1992).

[62] H. Plothow-Besch, Comp. Phys. Comm. **75**, 396 (1993). H. Plothow-Besch, "PDFLIB: Nucleon, Pion and Photon Parton Density Functions and α_s Calculations," User's Manual—Version 4.0, W5051 PDFLIB, CERN-PPE, 1993 (unpublished).

[63] Solenoidal Detector Collaboration, "Letter of Intent," SDC-90-00151, 1990.

[64] I. Hinchliffe, M. D. Shapiro, "Z' production with SDC," SSC-SDC-90-00115, 1990 (unpublished).

[65] P. Chiappetta *et al.*, in Proceedings of the Large Hadron Collider Workshop, Aachen, Germany, 1990.

[66] A. Henriques and L. Poggioli, ATLAS Collaboration Note PHYS-NO-010, 1992 (unpublished).

[67] P. K. Mohapatra, Mod. Phys. Lett. **A8**, 771 (1993).

[68] I. Hinchliffe, personal communication. To obtain a copy of PAPAGENO, send mail to **hinchliffe@theorm.lbl.gov**.

[69] See, for example, P. Langacker, R. Robinett, J. L. Rosner, Phys. Rev. **D30**, 1470 (1984).

[70] F. del Aguila, M. Quirós, F. Zwirner, Nucl. Phys. **B287**, 419 (1987).

[71] J. D. Anderson, M. H. Austern, R. N. Cahn, Phys. Rev. Lett. **69**, 25 (1992). J. D. Anderson, M. H. Austern, R. N. Cahn, Phys. Rev. **D46**, 290 (1992).

[72] ALEPH Collaboration, Z. Phys. **C59**, 369 (1993). OPAL Collaboration, Phys. Lett. **B266**, 201 (1991). DELPHI Collaboration, Z. Phys. **C55**, 555 (1992). L3 Collaboration, Phys. Lett. **B294**, 466 (1992).

[73] Y.-S. Tsai, Phys. Rev. **D4**, 2821 (1971).

[74] K. Hagiwara, A. D. Martin, and D. Zeppenfeld, Phys. Lett. **B235**, 198 (1990). Y. Hara, "Complete tau polarization measurements at LEP and SLC," UTHEP-208, 1990 (unpublished).

[75] CELLO Collaboration, H. J. Behrend, *et al.*, Z. Phys. **C46**, 537 (1990).

[76] See, for example, J. Orear, "Notes on Statistics for Physicists," UCRL-8417, 1958 (unpublished).

[77] F. del Aguila, M. Quirós, F. Zwirner, Nucl. Phys. **B284**, 530 (1987). P. Kalyniak and M. Sundaresan, Phys. Rev. **D35**, 75 (1987).

[78] F. del Aguila, L. Ammetler, R. Field, and L. Garrido, Phys. Lett. **B221**, 408 (1989). N. Deshpande, J. Grifols, A. Méndez, Phys. Lett. **B208**, 141 (1988).

[79] M. Cvetič and P. Langacker, Phys. Rev. **D46**, 14 (1992).

[80] J. L. Hewett and T. G. Rizzo, Phys. Rev. **D47**, 4981 (1993). F. del Aguila, B. Alles, L. Ametller, A. Grau, Phys. Rev. **D48**, 425 (1993).

[81] E. A. Kuraev and V. S. Fadin, Yad. Fiz. **41**, 733 (1985).

[82] R. N. Cahn, Phys. Rev. **D36**, 2666 (1987).

[83] M. Jacob, T. T. Wu, G. Zobernig, Z. Phys. **C53**, 497 (1992). M. Bell and J. S. Bell, Part. Accl. **24**, 1 (1988). R. Blankenbecler and S. D. Drell, Phys. Rev. **D36**, 277 (1987). M. Jacob and T. T. Wu, Phys. Lett. **B197**, 253 (1987).

[84] T. Barklow, P. Chen, and W. Kozanecki, "Beamstrahlung spectra in next generation linear colliders." In P. Zerwas, ed., e^+e^- *Collisions at 500 GeV: The Physics Potential*, p. 845. Proceedings of the ECFA Workshop on Physics with Linear Colliders, Hamburg, September 1991.

[85] P. Chen, Phys. Rev. **D46**, 1186 (1992).

[86] K. Fuji, T. Matsui, and Y. Sumino, "Physics at $t\bar{t}$ threshold in e^+e^- collisions," KEK Preprint 93-125, 1993 (unpublished). R. N. Cahn and J. D. Jackson, "Prospects for studying the $t\bar{t}$ threshold at a linear collider," LBL-35344. Presented at QUARKS: The Third Generation, Santa Barbara, California, April 1994.

[87] JLC Group, KEK Report 92-16, 1992 (unpublished).

[88] W. A. Barletta *et al.*, "Linear Colliders." In Proceedings of of the 1990 DPF Summer Study on High Energy Physics, Snowmass, Colorado, 1990.

[89] R. B. Palmer, Ann. Rev. Nucl. Part. Sci. **40**, 529 (1990).

[90] ALEPH Collaboration, D. Buskulic *et al.*, Z. Phys. **C60**, 71 (1993). OPAL Collaboration, P. D. Acton *et al.*, Z. Phys. **C58**, 219 (1993). DELPHI Collaboration, P. Abreu *et al.*, "Measurements of the line shape of the Z^0 and determination of electroweak parameters from its hadronic and leptonic decays," CERN-PPE-94-08, 1994 (unpublished). L3 Collaboration, O. Adriani *et al.*, Phys. Rep. **236**, 1 (1993).

[91] J. H. Kuhn, Nucl. Phys. **B237**, 77 (1984). A. Czarnecki, M. Jezabek, J. H. Kuhn, Nucl. Phys. **B351**, 70 (1991). C. P. Yuan, Phys. Rev. **D45**, 782 (1992). R. H. Dalitz and G. R. Goldstein, Phys. Rev. **D45**, 1531 (1992). R. Arens and L. M. Sehgal, Nucl Phys. **B393**, 46 (1993).

[92] A. Djouadi, A. Leike, T. Riemann, D. Schaile, C. Verzegnassi, Z. Phys. **C56**, 289 (1992).

[93] J. L. Hewett, "Extended gauge sectors at linear colliders," ANL-HEP-CP-93-68. Presented at the Workshop on Physics and Experiments with Linear e^+e^- Colliders, Waikoloa, Hawaii, April 1993.

DATE
FILMED
10/14/94
END